

SEDIMENTARY GEOLOGY OF THE ORDOVICIAN COOL CREEK  
FORMATION AS IT IS EXPOSED IN THE WICHITA  
MOUNTAINS OF SOUTHWESTERN OKLAHOMA

By

DEBORAH ANN RAGLAND

Bachelor of Science

Oklahoma State University

Stillwater, Oklahoma

1981

Submitted to the Faculty of the Graduate College  
of the Oklahoma State University  
in partial fulfillment of the requirements  
for the Degree of  
MASTER OF SCIENCE  
December, 1983

Thesis  
1983  
R143s  
cop. 2



SEDIMENTARY GEOLOGY OF THE ORDOVICIAN COOL CREEK  
FORMATION AS IT IS EXPOSED IN THE WICHITA  
MOUNTAINS OF SOUTHWESTERN OKLAHOMA

*R. Nowell Donovan*

Thesis Advisor

*Stanley C. Finney*

*L. Simpson*

*Noraman A. Decker*

Dean of Graduate College

## PREFACE

The purpose of this thesis is to describe the sedimentology, sedimentary petrology, and stratigraphy of the Ordovician Cool Creek Formation as it is seen in the Slick Hills of Southwestern Oklahoma. The study includes field descriptions as well as analysis of samples in the laboratory using the petrographic microscope. A complete section of outcrop was measured in Blue Creek Canyon with supplementary sections measured in other areas of the Slick Hills and at Turner Falls in the Arbuckle Mountains, South Central Oklahoma.

I would like to express my sincerest thanks to my thesis advisor, Dr. R. Nowell Donovan, for his guidance, support, and especially his patience throughout this endeavor. I would also like to thank my committee members, Dr. Stanley Finney and Dr. Carol Simpson, for their assistance and advice on the final manuscript. A note of thanks is also extended to Dr. Steve Culver who was an original member of my committee before his move to another university.

I would also like to extend my appreciation to the Amoco Oil Company for their support in 1981-82 in the form of the Amoco Foundation Fellowship; to Dr. John W. Skinner for his support during 1982-83 in the form of the Skinner Foundation Fellowship; and to the Oklahoma Geological Survey for their honorarium in 1983 to help defray expenses incurred in the study.

A very special thanks is given to Mr. and Mrs. Charlie Oliver

and Mr. Kimbell of the Kimbell Ranch in the Slick Hills for so graciously allowing me to trek the entire extent of their land during my study. Thanks also to the other ranchers and land owners on whose land I studied outcrop.

My thanks also to Kelly Cloyd and Mary Rafalowski for cutting rocks and preparing endless thin sections. Also to Dave McConnell and Tom Ferraro for discussions about the Cool Creek Formation and geology in general, and to Weldon Beauchamp for supplying information on locations of good outcrop.

And, of course, very special thanks to my husband, Tommy, and my daughter, Tracie, for their sacrifices as I gave total concentration to graduate work instead of my family. They gave up their vacations in order to join me in the field during the heat of summer and ended up backpacking countless pounds of rock samples from the "area." Without their help and support I could not have completed this thesis.

TABLE OF CONTENTS

Chapter	Page
I. INTRODUCTION . . . . .	1
Purpose . . . . .	1
Location of Study . . . . .	1
Method of Study . . . . .	3
II. PREVIOUS INVESTIGATIONS . . . . .	6
III. LITHOLOGIC DESCRIPTION OF THE COOL CREEK FORMATION . . . . .	8
Introduction . . . . .	8
The Algal Boundstone Lithotype . . . . .	9
Classification of Boundstones . . . . .	9
Algal Mats . . . . .	9
Algal Mounds . . . . .	11
Algal Reefs . . . . .	25
Bioherms . . . . .	25
Encrusting Stromatolites . . . . .	27
The Micrite Lithotype . . . . .	31
The Intraformational Conglomerate Lithotype . . . . .	35
The Intraformational Breccia Lithotype . . . . .	37
The Oolitic Limestone Lithotype . . . . .	37
The Peloidal Limestone Lithotype . . . . .	44
Quartz-Rich Sandstone . . . . .	48
The Chert Lithotype . . . . .	51
Dolostone . . . . .	63
Body Fossils . . . . .	69
IV. ENVIRONMENTAL ANALYSIS OF THE COOL CREEK FORMATION . . . . .	72
Introduction . . . . .	72
The Paleoenvironment During the Early Ordovician . . . . .	72
The Algal Environment . . . . .	74
Intraformational Conglomerates . . . . .	85
Other Environmental Indicators . . . . .	91
Introduction . . . . .	91
Micrite . . . . .	91
Oolitic Lithologies . . . . .	94
Quartz Sand Lithologies . . . . .	94
Dolomite and Vanished Evaporites . . . . .	99

Chapter	Page
Bedded Chert . . . . .	102
Overview of the Cool Creek Environment . . . . .	104
Process Rates: Past Versus Present . . . . .	104
Preservation Versus Destruction . . . . .	105
Subsidence . . . . .	106
Cycles . . . . .	109
V.    DIAGENESIS OF THE COOL CREEK FORMATION . . . . .	114
Introduction . . . . .	114
Physical Diagenesis . . . . .	114
Chemical Diagenesis . . . . .	115
Dissolution and Reprecipitation . . . . .	115
Replacement . . . . .	122
Silica and Replaced Evaporites . . . . .	125
Conversion of Aragonite to Calcite . . . . .	130
Later Secondary Dolomite . . . . .	132
Authigenic Feldspars . . . . .	134
Aggrading Neomorphism . . . . .	137
Paragenesis . . . . .	139
VI.   SUMMARY AND CONCLUSIONS . . . . .	141
BIBLIOGRAPHY . . . . .	145
APPENDICES . . . . .	151
APPENDIX A - LOG OF THE COOL CREEK FORMATION AS EXPOSED IN BLUE CREEK CANYON . . . . .	152
APPENDIX B - SUBSIDENCE RATES IN OKLAHOMA DURING THE PALEOZOIC . . . . .	159
APPENDIX C - ANALYSIS OF REPRESENTATIVE THIN SECTIONS FROM THE COOL CREEK FORMATION . . . . .	167

LIST OF TABLES

Table	Page
I. Eccentricity Calculations for Algal Mounds on the Oliver Syncline . . . . .	19
II. Local Environments of Algal Boundstones . . . . .	77
III. Depositional Arrangements of IFC Clasts . . . . .	87



LIST OF FIGURES

Figure	Page
1. Maps Showing the Location of Blue Creek Canyon and Primary Measured Section . . . . .	2
2. Photograph in Blue Creek Canyon Showing Lateral Continuity of Individual Beds. . . . .	4
3. Algal Mat, Smooth Profile . . . . .	10
4. Algal Mat, Crinkly Profile . . . . .	10
5. Calcite Spar-Filled Tubules in Algal Mat Laminae . . . . .	12
6. Calcite Spar-Filled Gas Fenestrae in Algae . . . . .	12
7. Algal Mounds, LLH-C . . . . .	13
8. Algal Mound Morphologies . . . . .	14
9. LLH-C Stromatolites (a) Overlying Thrombolite Mounds (b) That Have Been Cut by a Channel Infilled with Small Scale Cross-Bedded Silty Micrite(c) . . . . .	15
10. LLH-S Algal Mounds . . . . .	17
11. LLH-C Algal Mounds, "Biscuit-Shaped" . . . . .	17
12. Plan View of Algal Mounds Outcropping on the Oliver Syncline . . . . .	18
13. Thrombolite Mound Showing Typical Clotted Appearance . . . . .	20
14. Gradational Change from Thrombolitic Texture (a), to Medium-Sized Intermediate Texture (b), to Stromatolitic Texture (c) . . . . .	21
15. Partially Silicified "Sunburst" Thrombolite Mounds . . . . .	23
16. Silica Spar-Filled Tubules in Thrombolitic Texture . . . . .	23
17. Calcite Spar-Filled Tubules Perpendicular to Stromatolite Laminae . . . . .	24

Figure	Page
18. Compactional Draping of Laminated Lime Mudstone and IFC's (a), Against a Bioherm (b) . . . . .	26
19. Penecontemporaneous Deformation of a Miniherm (a), Showing a Dislodged Fragment of the Algal Colony (b) . . .	28
20. Stromatolite and Thrombolite Morphologies in Algal Reefs and Bioherms . . . . .	29
21. Encrusting Stromatolites . . . . .	30
22. Bioturbated Micrite . . . . .	32
23. Subaqueous Shrinkage Cracks . . . . .	33
24. Subaerial Mudcracks . . . . .	34
25. Authigenic Feldspar in Micrite Matrix . . . . .	34
26. IFC Bed Showing Erosive Base and Gradational Upper Contact . . . . .	36
27. Algal Fragments Comprising IFC Clasts . . . . .	36
28. IFC Containing Imbricately Packed, Rounded Chert Pebbles . . . . .	38
29. Imbricately Packed IFC Clasts . . . . .	39
30. Vertically Packed IFC Clasts . . . . .	39
31. Collapse Breccias . . . . .	40
32. Stratigraphic Logs Measured at Turner Falls, Arbuckle Mountains, Southern Oklahoma . . . . .	41
33. Concentric Ooids; Most Have Detrital Quartz Nuclei . . . . .	45
34. Radial Ooid with Micrite Nucleus . . . . .	45
35. Oosparite . . . . .	46
36. Spastoliths, Probably Caused by Compaction . . . . .	46
37. Partially Silicified Ooids Cemented by Siliceous Spar . . .	47
38. Ooids with Nuclei Replaced by Large Crystals of Non-Ferroan Dolomite . . . . .	47
39. Subaqueous Shrinkage Crack Filled with Pelsparite . . . . .	49

Figure	Page
40. Small and Medium Scale Cross-Bedding in Quartz-Rich Sandy Limestone . . . . .	49
41. Sand in Troughs of Asymmetric Ripple Marks . . . . .	50
42. Photomicrograph of a Typical Quartz-Rich Limestone . . . . .	50
43. Rare Polycrystalline Quartz Grain in Quartz-Rich Limestone . . . . .	52
44. Chert Nodules Along a Bedding Plane Surface . . . . .	52
45. "Honeycomb" Texture Produced by Partially Silicified Oolitic Unit . . . . .	53
46. Silicified Core of an Algal Mound . . . . .	53
47. Bedded Chert . . . . .	55
48. Chert Pebble Breccia . . . . .	55
49. Multiple Generations of Syntaxial Quartz Overgrowths on a Detrital Quartz Grain that Forms the Nucleus of an Ooid . . . . .	56
50. Megaquartz as Pore-Filling Cement . . . . .	56
51. Rare Euhedral Quartz Crystals Replacing Calcite Spar . . . . .	57
52. Microquartz Replacing the Interior of an Echinoid Fragment . . . . .	57
53. Completely Silica-Replaced Ooids Showing Little or No Compactional Deformation . . . . .	59
54. Chalcedonite Filling in a Fossil Mold . . . . .	59
55. Zebraic Chalcedony Filling In Pore Space . . . . .	60
56. Spherulitic Chalcedony Replacing Calcite Spar Cement . . . . .	60
57. Evaporite Pseudomorph Molds in a Microcrystalline Chert Nodule . . . . .	61
58. Evaporite Pseudomorphs in Microcrystalline Chert . . . . .	62
59. IFC Clast Replaced by Microcrystalline Chert . . . . .	64
60. Sabkha Sequence . . . . .	65

Figure	Page
61. Secondary Dolomite Crystals Replacing Micrite in a Sandy IFC . . . . .	68
62. Interlocking Mosaic of Zoned Secondary Dolomite Crystals . .	68
63. Gastropod, <u>Lecanospira</u> (?) . . . . .	70
64. Masses of Sponge Remains on Bedding Surface . . . . .	70
65. Trilobite Fragment . . . . .	71
66. Trilobite Hash Associated with an IFC . . . . .	71
67. Paleoposition of North America during the Early Ordovician . . . . .	73
68. Interpretation of Environmental Relationships between Algal Types and Depth of Water . . . . .	76
69. Diagrammatic Representation of the Cyclic Growth of Stromatolitic Laminae . . . . .	79
70. Subaerial Mudcracks Formed on an Algal Surface . . . . .	80
71. Diagrammatic Representation of Algal Dome Formation . . . .	83
72. Interpretation of Environmental Relationship between IFC Morphology and Water Turbulence . . . . .	90
73. Block Diagram Illustrating the Transport of Quartz Sands from the Continent to the Shallow Marine Environment . . . . .	96
74. Stratigraphic Correlation of the Time Equivalent Cool Creek, Gorman, and Roubidoux Formations . . . . .	97
75. Log of the McKenzie Hill Formation-Cool Creek Formation Contact Showing Increase in Grain Size Up Section . . . .	100
76. Phase Diagram Showing the Relationships between Calcium Carbonate or Silica Concentration Versus pH . . . . .	103
77. Diagrammatic Representation of the Theorized Subsidence of the Anadarko Basin . . . . .	108
78. General Stratigraphic Log of the Formations Outcropping in the Slick Hills . . . . .	112
79. Summary of Silica Diagenesis in the Cool Creek Formation . .	116

Figure	Page
80. Diagram Illustrating the Silica Type Produced as a Function of Environment and Silica Concentration . . . . .	117
81. Illustration of an Example of Continuous and Discontinuous Cementation in an Oolitic Grainstone . . . . .	121
82. Diagrammatic Representation of the 1:1 Replacement of Calcite by Silica . . . . .	123
83. Discrete Chert Nodules and Chert Pseudolayer . . . . .	126
84. Chert Nodule Distorting Micrite Laminae Through Growth . . .	126
85. Fibrous Chalcedony . . . . .	128
86. Silica Nodule after Anhydrite . . . . .	128
87. Authigenic Feldspars . . . . .	135
88. Detrital Plagioclase with an Overgrowth of Feldspar . . . .	135
89. Qualitative Analysis of Authigenic Feldspar Crystal . . . .	136
90. Aggrading Neomorphism . . . . .	138
91. Summary of the Paragenetic Sequence of Events . . . . .	140

## CHAPTER I

### INTRODUCTION

#### Purpose

The purpose of this thesis is to describe the sedimentary geology of the Cool Creek Formation as it is developed in the Slick Hills of Southwestern Oklahoma.

The Lower Ordovician Cool Creek Formation outcrops in complete stratigraphic sequences in only two areas in Oklahoma: The Arbuckle Mountains of South Central Oklahoma and the Slick Hills to the north of the Wichita Mountains of Southwestern Oklahoma. Stratigraphic sections of the Cool Creek have been measured and described in both areas (Barthelman, 1968; Brookby, 1969; St. John and Eby, 1978), but no sedimentological study has yet been published for the Wichita Mountains area. The purpose of this thesis, therefore, is to provide such a study.

#### Location of Study

The principal section, measured in the Slick Hills, is located in Blue Creek Canyon, Township 4 North, Range 13 West, Comanche County, Oklahoma (Figure 1, Appendix A).

Although smooth in general profile, in detail the topography is rugged and exposure is good (from 20% to 70% rock). However, most

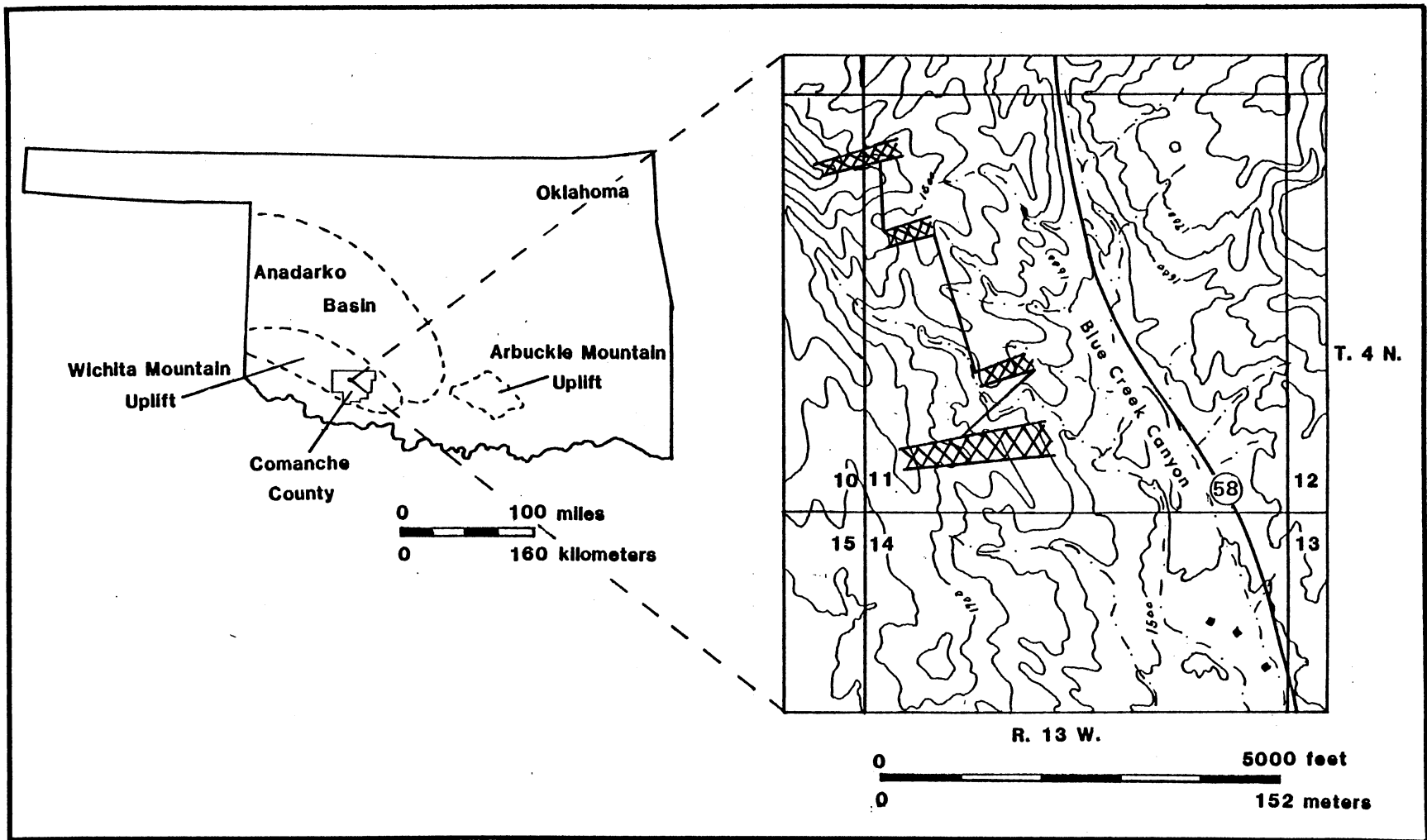


Figure 1. Maps Showing the Location of Blue Creek Canyon and Primary Measured Section (Shaded Areas).  
Lateral Shifts are Shown by Connecting Solid Lines

of the exposure is obscured by a thin coat of caliche and is of low quality for detailed sedimentological study. Some good quality exposures occur in water-worn stream valleys.

The hills have been extensively folded and faulted (Donovan, 1982; McConnell, 1983; Beauchamp, 1983). The dip of the beds ranges from nearly horizontal to vertical creating a variety of attitudes of exposure.

#### Method of Study

One complete section was measured in Blue Creek Canyon and supplementary sections were examined throughout the Slick Hills. Covered ground and tectonic deformation were the two main obstacles to measurement. However, the lateral continuity of the beds within the Formation is excellent and little difficulty was encountered when a movement along strike was necessary (Figure 2). In the measured section the dip of the beds ranged from  $16^{\circ}$  to  $52^{\circ}$  with the best exposures on the more steeply dipping beds.

Gross measurements were made using a Jacob's staff equipped with a Brunton Compass. More detailed measurements were made with a tape measure and millimeter ruler. The section was described in the field and distinctive lithologies recognized. Representative samples were collected for further study.

Initial laboratory study involved the slabbing and etching of hand samples. As all lithologies in the section are predominantly calcium carbonate, the slabs were first etched in dilute hydrochloric acid and then stained with alizarine red and potassium ferrocyanide to differentiate ferroan and non-ferroan varieties of calcite and



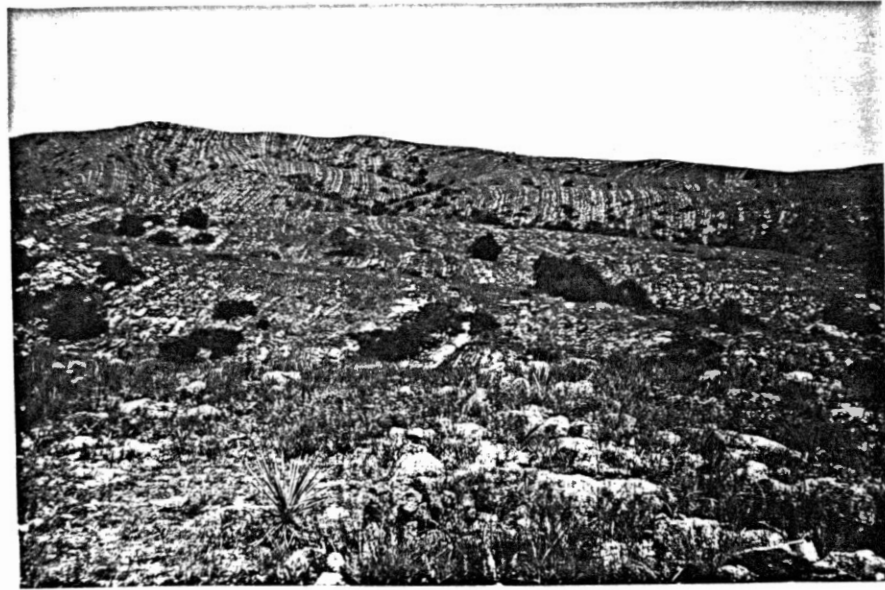


Figure 2. Photograph in Blue Creek Canyon Showing  
Lateral Continuity of Individual Beds

dolomite (Leeder, 1982). Acetate peels were then made in order to study selected carbonate textures.

The final step in the analysis of the Formation was the study and description of thin sections. At least one section was made of each distinctive lithology. The thin sections were stained to test for dolomite and ferrous iron (as above), as well as for feldspar using sodium cobaltinitrite.

## CHAPTER II

### PREVIOUS INVESTIGATIONS

The Cool Creek Formation was first described in the Slick Hills as an undifferentiated part of the Arbuckle Group by Decker and Merritt (1928). Decker (1939) subdivided the Arbuckle Group into the McKenzie Hill, Cool Creek, Kindblade, and West Spring Creek Formations. His very brief description of the Cool Creek Formation outcrop as seen on the Kindblade Ranch included a recognition of the more obvious sedimentological units: Algal zones and oolitic cherts.

Ham (1956) described the Cool Creek Formation as "probably the most distinctive lithologic unit of the Arbuckle Group." His measured section on the Kindblade Ranch was 1100 feet thick and, in addition to algal beds and cherts, Ham recognized quartz sands, intraformational conglomerates, and dolomite. Ham was the first worker to identify specific fossils that could be used as stratigraphic markers, that is, the gastropod Lecanospira and the brachiopod Diaphelasma oklahomense. Ham also specifically designated the lower boundary of the Cool Creek as a bed containing substantial amounts of quartz sand.

Harlton (1963) measured 979 feet of Cool Creek Formation at Ragged Mountain. In 1964, he correlated the Cool Creek to other areas in the South Central United States. His petrologic description differentiated between the various types of cherts within the

Formation.

Barthelman (1968) and Brookby (1969) described sections of the Cool Creek as part of their studies of the Ordovician outcrops in the Unap Mountain-Saddle Mountain area and Richards Spur-Kindblade Ranch areas of the Slick Hills respectively. Brookby's section measured 1100 feet; Barthelman's Unap Mountain-Saddle Mountain section was incomplete. Petrographic studies were not conducted.

St. John and Eby (1978) were the first to do detailed petrologic and petrographic studies of the Cool Creek Formation. However, their samples were collected from Interstate Highway 35 and Turner Falls outcrops in the Arbuckle Mountains. Their paper included an interpretation of the depositional environment and a description of evaporite pseudomorphs and collapse breccias.

Donovan (1982) conducted petrologic and petrographic studies on the Cool Creek lithologies in Blue Creek Canyon. He was able to distinguish between the several different morphologies of stromatolites and suggested a possible aeolian source for the quartz sand fraction of the Formation.

## CHAPTER III

### LITHOLOGIC DESCRIPTION OF THE COOL CREEK FORMATION

#### Introduction

Most of the Cool Creek Formation is composed of carbonate, predominantly limestone with minor dolomite. The third major constituent is silica found either as primary detrital quartz or as secondary cements and replacements.

The following lithotypes and related features have been recognized in the field:

1. Algal Boundstone
2. Micrite
3. Intraformational Conglomerate
4. Intraformational Breccia
5. Oolitic Limestone
6. Peloidal Limestone
7. Quartz-rich Sandstone
8. Chert
9. Dolostone
10. Body Fossils

## The Algal Boundstone Lithotype

### Classification of Boundstones

Several classification schemes have been devised in order to facilitate the study of algal buildups. Nelson et al. (1962), provided a scheme for classifying the gross external forms of the boundstones. Logan et al. (1964), developed a classification of the morphology of the structures that comprise the boundstones. Hoffman (1969) established a comprehensive system for describing the third order of boundstone construction, that is, the detailed morphology of stromatolites.

No system on its own has proven adequate to describe the algal buildups in the Slick Hills. Therefore, a combination of these three systems (with necessary modifications by the author) has been used.

Algal boundstones of various types are abundant in the Cool Creek Formation; they probably constitute more than half the Formation. The following forms have been recognized: algal mats, algal mounds, algal reefs, bioherms, and encrusting stromatolites.

### Algal Mats

Algal mats are composed of nearly flat to undulatory cryptalgal laminae (Figure 3). The wavelength of the laminar undulations is much greater than the vertical height of the mat. Individual laminae are up to 5 cm (2 in) but most are less than 3 mm (0.1 in) thick. The profile of the mat can be smooth (Figure 3) or, more rarely, crinkly (Figure 4). The average wavelength between undulations on the mats with smooth profiles is approximately 1 m (3 ft). Crinkly



Figure 3. Algal Mat, Smooth Profile



Figure 4. Algal Mat, Crinkly Profile

algal mats generally have smaller wavelengths averaging 25 cm (10 in).

The laminae of the mats consist of alternating layers of lithified algae, precipitated calcium carbonate, and trapped detritus. As seen in thin section, micrite comprises more than 85% of the mat (Figure 5). Growth lines are indistinct making it difficult to differentiate between the lithified algae and the chemically deposited carbonate. A few spar-filled filament tubules are the primary indicators of the algal origin of the mat (Figure 5). Calcite and silica filled fenestrae (birds-eye structures) are found throughout the boundstones and are often the most prominent microstructures in algal mats (Figure 6).

Detritus, seen as quartz silt, fossil fragments (mainly trilobites, gastropods, and echinoids), and pellets constitute approximately 10% of the mat. Minor mineral constituents include dolomite, hematite, and pyrite.

#### Algal Mounds

Algal mounds are dome shaped structures with circular to elliptical outlines in plan view (Aitken, 1967) (Figure 7). They are built by algal growth, entrapment of sediment, and deposition of sediment between algal members. Distances between mound apices can be as little as 5 cm (2 in) or as great as several meters. The smallest mounds are made up of closely linked hemispheroidal stromatolites, LLH-C (Logan et al., 1964) (Figure 8). As an example, a particularly persistent layer of LLH-C mounds occurs 15 m (50 ft) above the base of the Formation (Figure 9). The unit is only 15 cm (6 in) thick, but can be traced laterally for several kilometers.



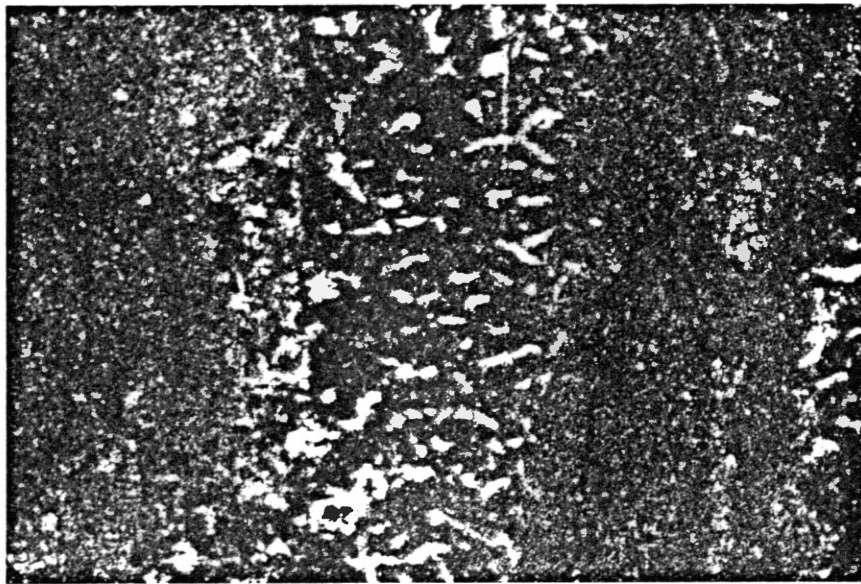


Figure 5. Calcite Spar-Filled Tubules in Algal Mat Laminae. Tubules are Perpendicular to Laminae (X40, Crossed Nicols)

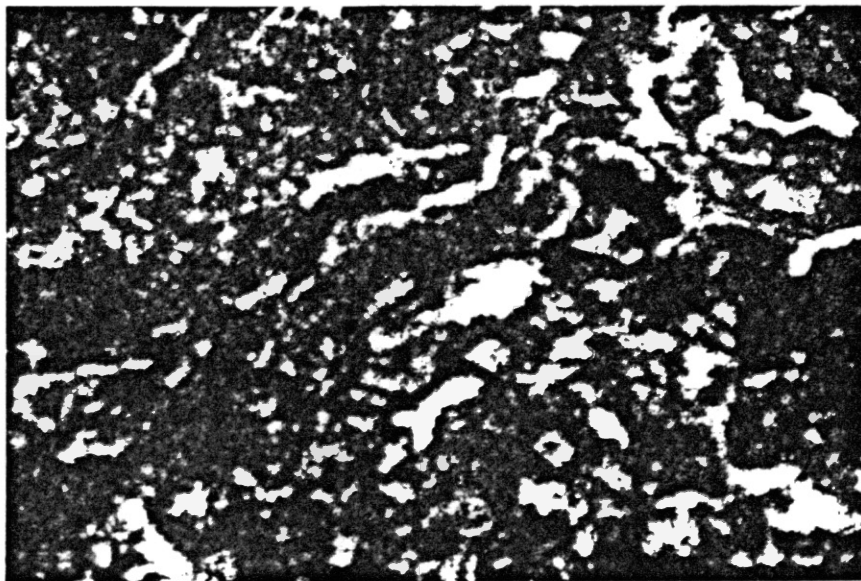


Figure 6. Calcite Spar-Filled Gas Fenestrae in Algae (X40, Ordinary Light)

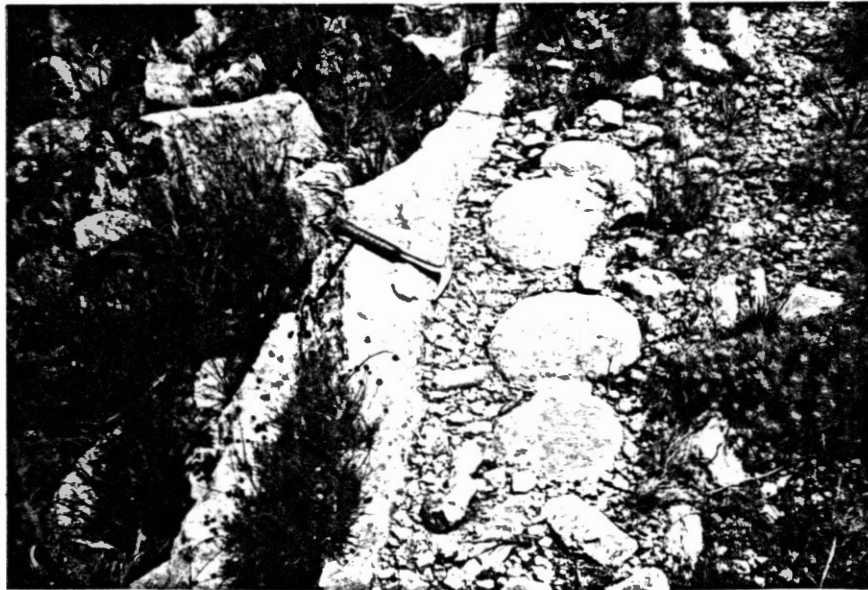


Figure 7. Algal Mounds, LLH-C. Mounds Appear Circular  
Due to Unusual Weathering; Beds are  
Actually Dipping West (Right on Photo)

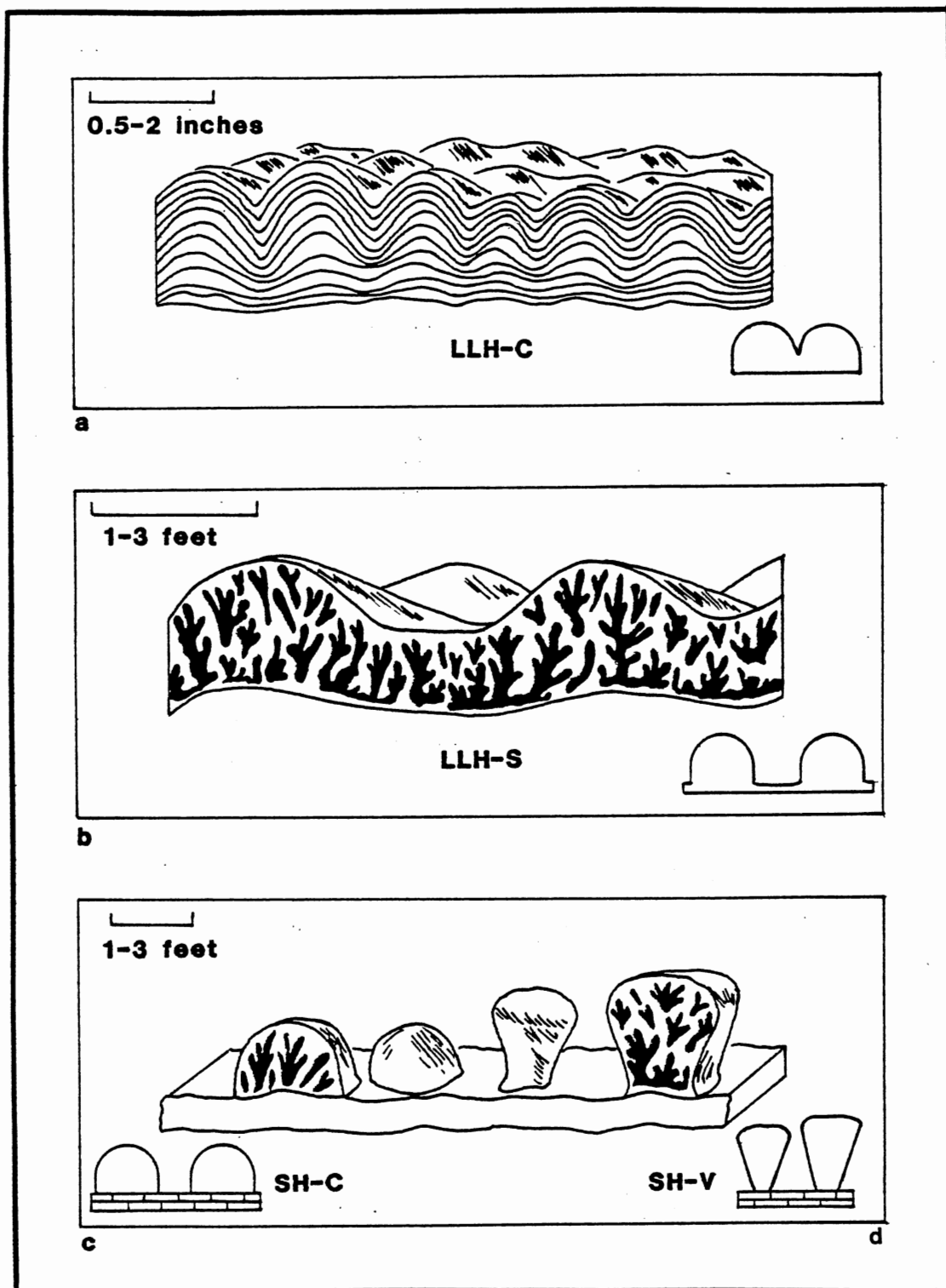


Figure 8. Algal Mound Morphologies (Terms from Logan et al., 1964):  
 (a) LLH-C, Laterally Linked Hemispheroids, Close;  
 (b) LLH-S, Laterally Linked Hemispheroids, Spaced,  
 (c) SH-C, Stacked Hemispheroids, Constant Radius;  
 (d) SH-V, Stacked Hemispheroids, Variable Radius.

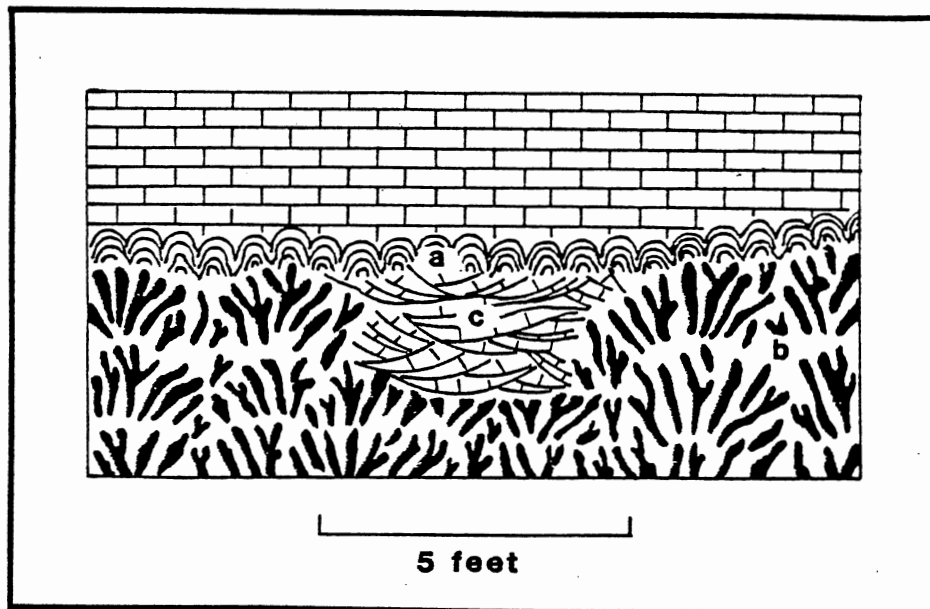


Figure 9. LLH-C Stromatolites (a) Overlying Thrombolite Mounds (b) That Have Been Cut by a Channel Infilled with Small Scale Cross-Bedded Silty Micrite (c). (Located 14 m (45 ft) Above Base of Section Measured in Blue Creek Canyon)

Larger mounds, in which the diameters of the heads are greater than 15 cm (6 in), are made up of hemispheroids that are laterally linked with algal colonies that are either spaced but connected (LLH-S) or free standing with their bases on substrata that are not algal (SH-C and SH-V) (Logan et al., 1964) (Figure 8). The mounds may consist of one large colony or several smaller colonies grouped together (Figure 10); they are usually circular to elliptical in plan outline, but a variety of shapes has been observed. Near the top of the Formation some "biscuit-shaped" groups are present (Figure 11). Bedding is not prominent in any of the mound morphologies.

An especially well exposed grouping of algal mounds is located on the Oliver Syncline (Figure 12, Table I). The horizontal attitude of the beds has allowed the erosion of the intermound sediments with resulting exhumation of the mounds. The resulting outcrop gives an insight into the appearance of the colonies at the time of their deposition.

The primary constituents of the algal mound colonies are stromatolites and thrombolites. Whereas stromatolites are "cryptalgal bodies characterized by non-planar lamination" in cross-profile (Aitken, 1967), thrombolites are characterized by their lack of lamination and the clotted appearance they give to a colony (Pratt and James, 1982) (Figure 13). Exact ratios of thrombolite to stromatolite composition in the mounds are impossible to determine because of the caliche and lichen encrustation on most exposures. However, in well-exposed areas mounds are seen to be composed not only of thrombolites and stromatolites, but also of stages intermediate between the two end members (Figure 14). The environmental significance of these



Figure 10. LLH-S Algal Mounds. Large Mound on Left is One Colony; Several Smaller Mounds Comprise Large Colony on Right

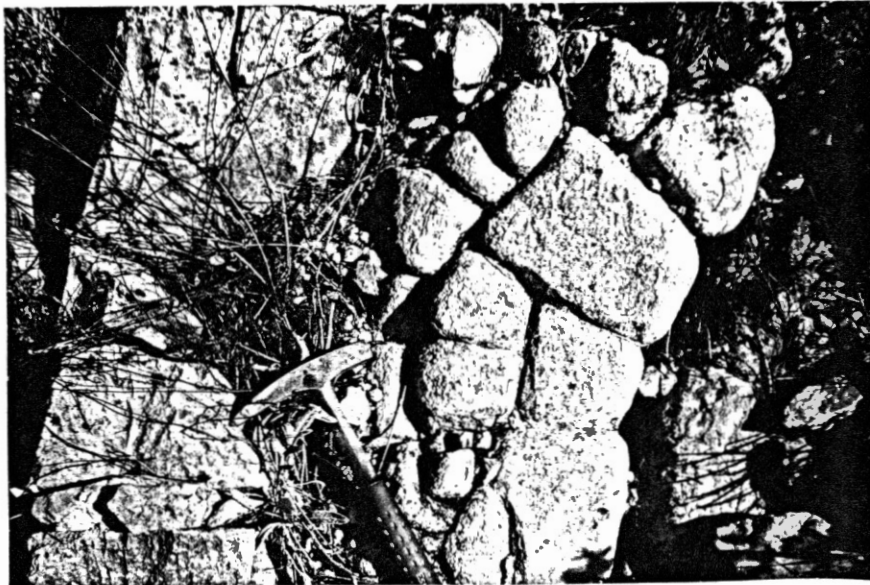


Figure 11. LLH-C Algal Mounds, "Biscuit-Shaped"

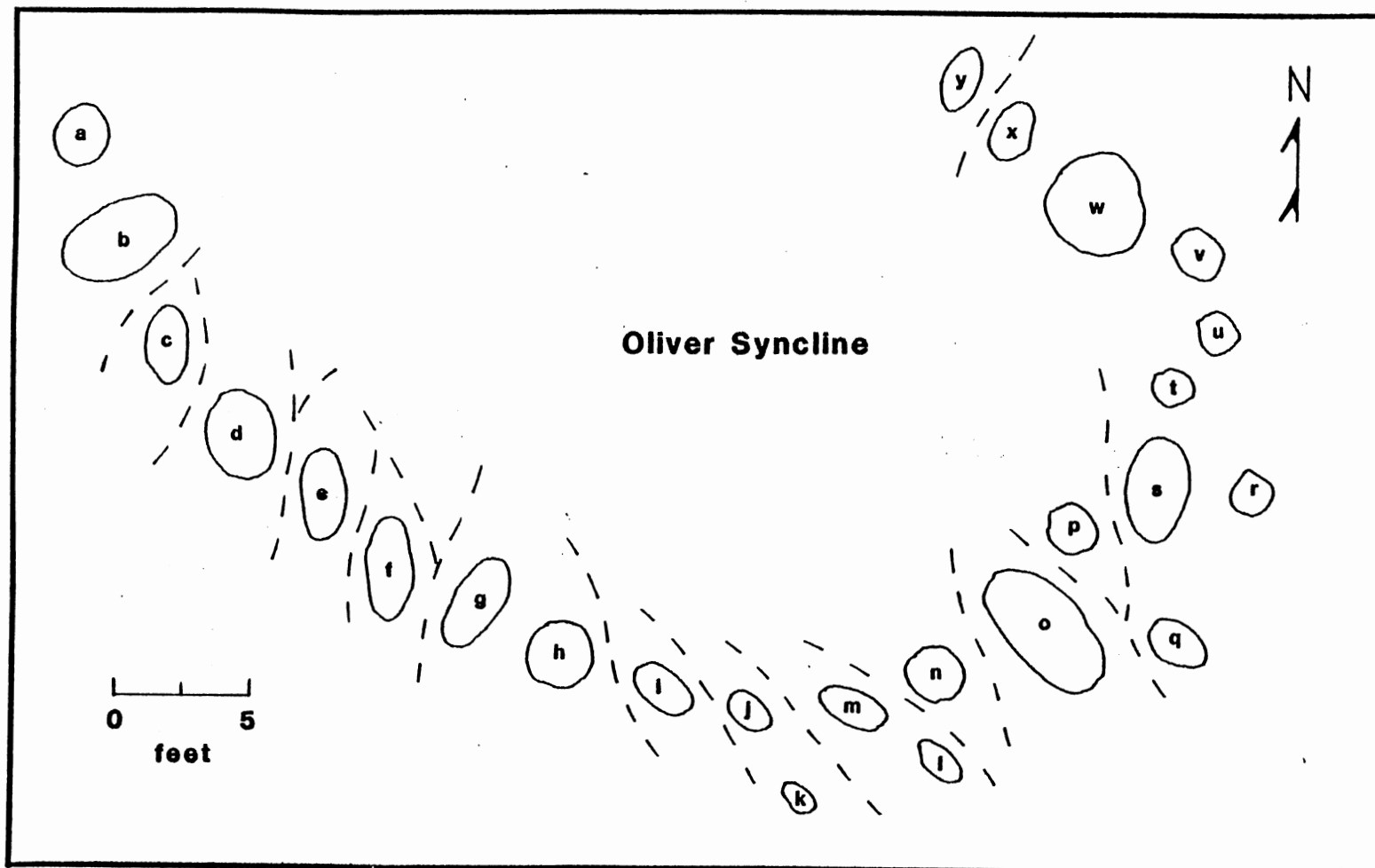


Figure 12. Plan View of Algal Mounds Outcropping on the Oliver Syncline (Sec. 10, T. 4 N., R. 13 W.). Dashed Lines Represent Possible Tidal Channels

TABLE I

## ECCENTRICITY CALCULATIONS FOR ALGAL MOUNDS ON THE OLIVER SYNCLINE

MOUND	$2a_1$	$2b_1$	$a_1$	$b_1$	$\sqrt{a_1^2 - b_1^2} = c_1$	$c_1/a_1 = e$
a	24	20	12.0	10.0	6.63	0.5525
b	35	25	17.5	12.5	12.25	0.7000
c	25	16	12.5	8.0	9.60	0.7680
d	28	23	14.0	11.5	7.98	0.5700
e	27	17	13.5	8.5	10.49	0.7770
f	31	17	15.5	8.5	12.96	0.8361
g	30	16	15.0	8.0	12.69	0.8460
h	20	20	10.0	10.0	0.0	0.0
i	21	14	10.5	7.0	7.83	0.7457
j	15	12	7.5	6.0	4.50	0.6000
k	13	11	6.5	5.5	3.46	0.5323
l	16	11	8.0	5.5	5.81	0.7263
m	20	12	10.0	6.0	8.00	0.8000
n	14	14	7.0	7.0	0.0	0.0
o	40	24	20.0	12.0	16.00	0.8000
p	18	13	9.0	6.5	6.22	0.6911
q	17	14	8.5	7.0	4.82	0.5671
r	13	13	6.5	6.5	0.0	0.0
s	30	23	15.0	11.5	9.63	0.6420
t	13	11	6.5	5.5	3.46	0.5323
u	14	14	7.0	7.0	0.0	0.0
v	15	15	7.5	7.5	0.0	0.0
w	30	30	15.0	15.0	0.0	0.0
x	19	17	9.5	8.5	4.24	0.4463
y	18	14	9.0	7.0	5.66	0.6289

$a_1$  = semi-major axis, measured in inches.

$b_1$  = semi-minor axis, measured in inches.

$c_1$  = half distance between foci, measured in inches.

$e$  = eccentricity, where  $e = 0$  is a circle,  
 $e = 1$  is a straight line.



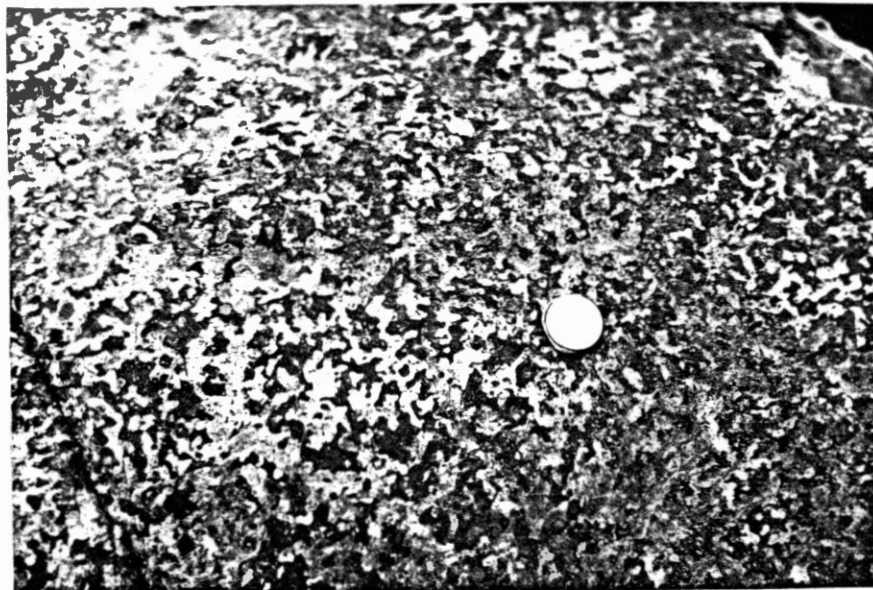


Figure 13. Thrombolite Mound Showing Typical Clotted Appearance

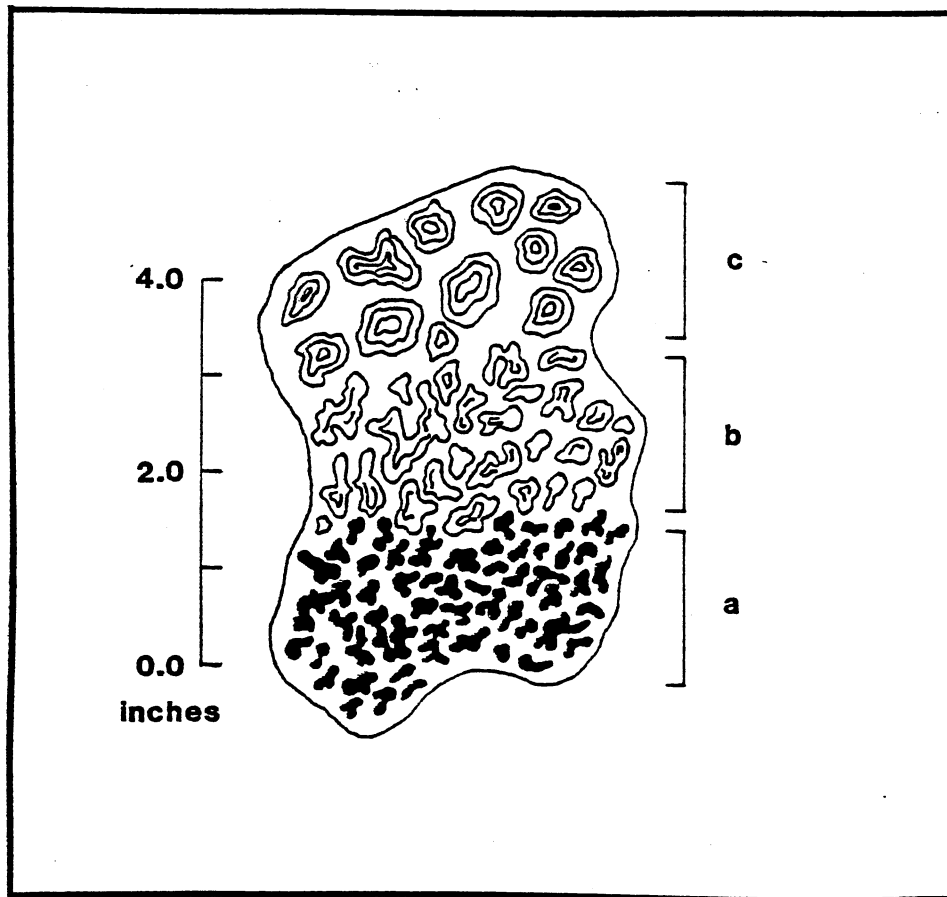


Figure 14. Gradational Change from Thrombolitic Texture (a), to Medium-Sized Intermediate Texture (b), to Stromatolitic Texture (c). Plan View Drawn from Etched Hand Sample

three stages will be discussed in Chapter 4.

Thrombolites are generally smaller than most stromatolite forms with diameters of individual members measuring less than 12 mm (0.5 in). They occur in dendritic and columnar groups; the overall morphology of the colonies is radial, forming a "sunburst" profile (Figure 15).

In thin section, thrombolites are characterized by a disrupted appearance (Figure 16). The major constituent is micrite with random spar-filled fenestrae. An occasional lamination is present resulting from the deposition of clasts or pellets. Detritus makes up less than 1% of thrombolites.

Intermediate algal forms show partial internal laminations and thus, have a slightly less clotted appearance than true thrombolites. The diameters of the members are slightly larger than the thrombolites, from 12 to 25 mm (0.5 to 1 in). Their morphologies are both dendritic and columnar.

Branching stromatolites are the third constituent of algal mounds. Within the mounds they are both digitate and dendritic with diameters in excess of 12 mm (0.5 in). The construction of their internal forms is variable, but all consist of a series of roughly parallel laminae. The laminae are very apparent in thin section, with spacing variable, but usually less than 1 mm (0.04 in) (Figure 17). Spar- and silica-filled filament molds are more abundant (or better preserved) than those in algal mats and are oriented perpendicular to the laminae. Pellets, fossil fragments, and detrital quartz silt make up less than 20% of the stromatolites. Spar-filled fenestrae are present (as in all algal structures studied). Inter-member areas are filled primarily with calcium carbonate and detritus

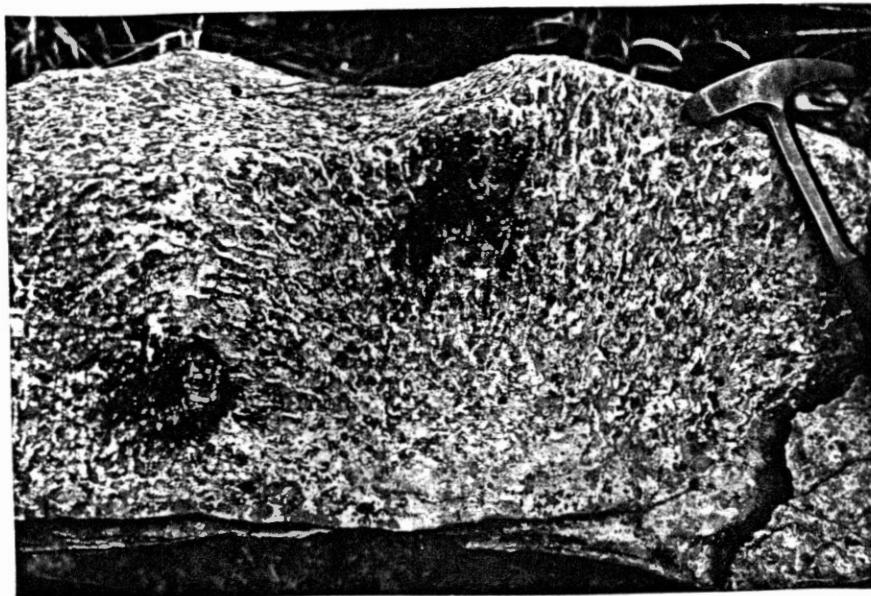


Figure 15. Partially Silicified "Sunburst" Thrombolite Mounds

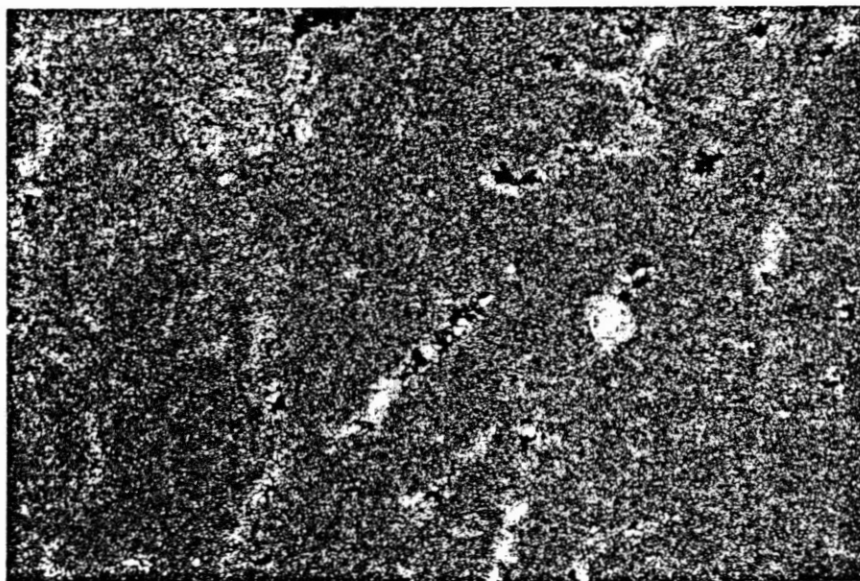


Figure 16. Silica Spar-Filled Tubules in Thrombolitic Texture (X40, Crossed Nicols)

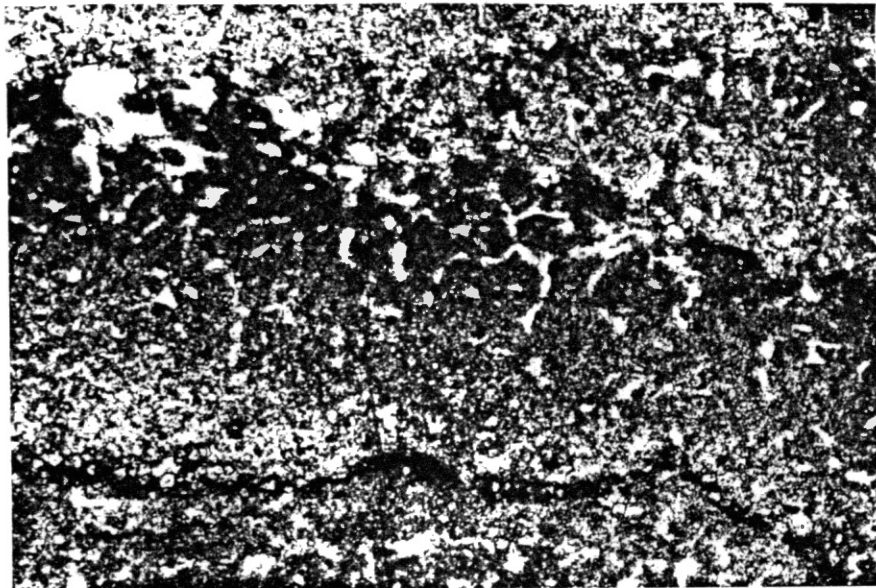


Figure 17. Calcite Spar-Filled Tubules Perpendicular to Stromatolite Laminae (X40, Crossed Nicols)

in the form of pellets, intraclasts, detrital quartz silt and sand, and fossil fragments.

### Algal Reefs

Reefs, which comprise a substantial part of the Formation, are buildups of sediment-binding organisms, in this case, algae (Nelson et al., 1962). The reefs are rigid structures that were built up from the sea floor and formed "wave-resistant mounds, platforms, or linear masses" (Cloud, in Nelson et al., 1962). They form extensive tabular outcrops that are unbedded and persist laterally for many meters in the Formation (Figure 2).

The constituents of algal reefs will be discussed in the section on bioherms.

### Bioherms

Bioherms and miniherms form the lateral termini of algal reefs. A bioherm is more than 2 m (6 ft) high and terminates against some lithotype other than the algal lithotype.

A bioherm 100 m (340 ft) above the base of the Formation consists of 6 m (20 ft) of algal mound which can be traced laterally for over a kilometer. The bioherm terminates abruptly against laminated mudstones and intraformational conglomerates which show compactional draping around the end of the bioherm (Figure 18).

Miniherms are more common than bioherms. They are usually less than 2 m (6 ft) high, passing laterally into mudstones and intraformational conglomerates in a similar fashion to bioherms. Evidence of some penecontemporaneous deformation of miniherms exists in a

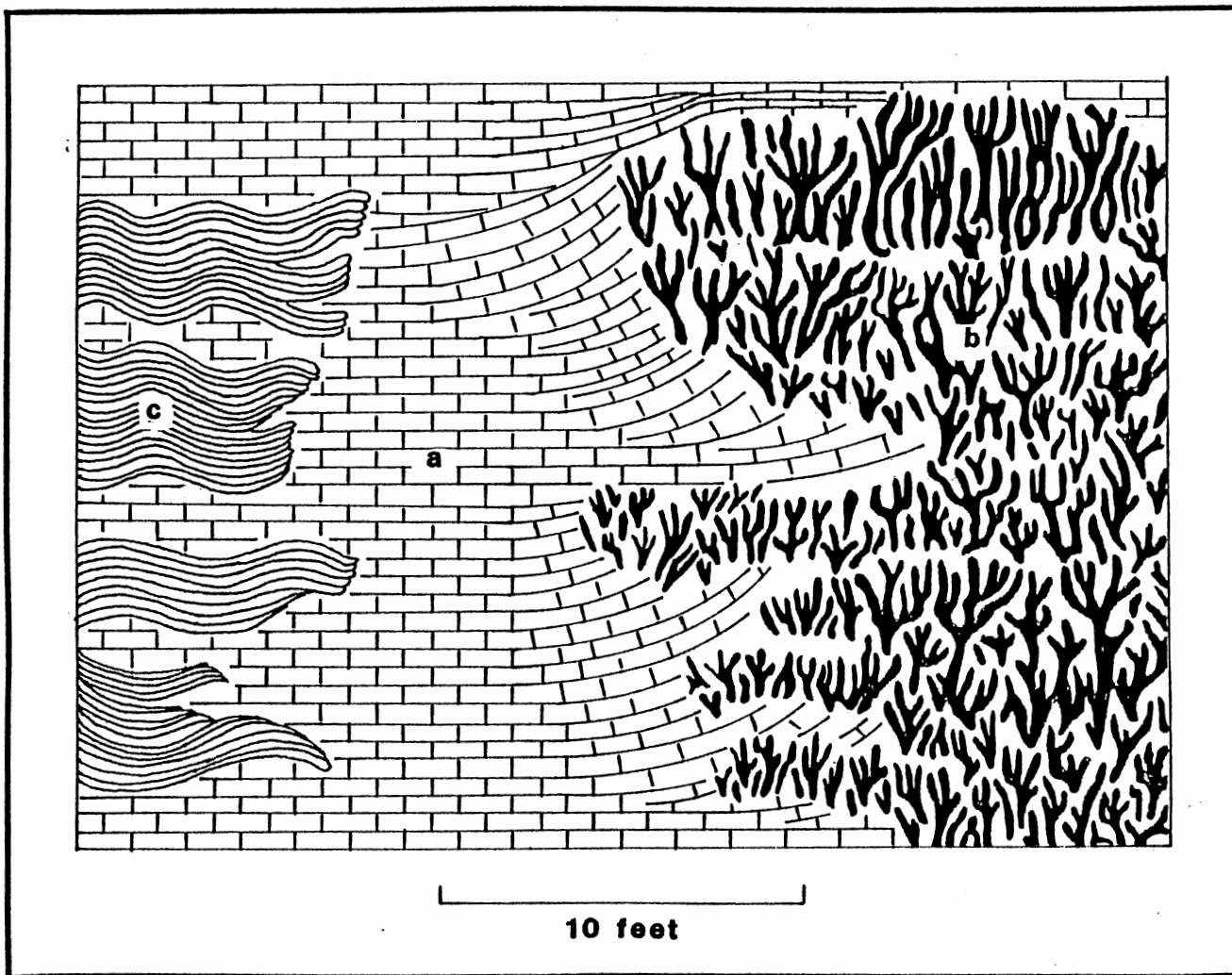


Figure 18. Compactional Draping of Laminated Lime Mudstone and IFC's (a),  
Against a Bioherm (b); (c) Algal Mat Interbedded with Micrite and  
IFC's

horizon 130 m (433 ft) above the base of the Formation (Figure 19).

Algal reefs and bioherms contain the most variety of stromatolite and thrombolite types (Figure 20). Columnar forms are cylindrical, terete, and turbinate ranging in diameter from 12 mm (0.5 in) to 200 mm (8 in). Branching forms, which are generally narrower (diameters less than 10 cm (4 in)), are dendritic, digitate, and coalescing. Thrombolites are dendritic and columnar with diameters generally less than 12 mm (0.5 in).

Thin section study of stromatolites and thrombolites in algal reefs and bioherms shows similar structures to those present in algal mounds. The principal difference is the larger size of both stromatolites and the clasts associated with them. In the larger individuals the laminae can be thicker ranging from 1 to 3 mm (0.04 to 0.010 in). Detrital clasts infilling the areas between individual stromatolites and thrombolites can be several centimeters in length and detrital quartz sizes range from fine to coarse grained.

#### Encrusting Stromatolites

Encrusting stromatolites are found throughout the Formation coating a variety of lithotypes. Usually, they initiate on micrite layers that have some minor relief. The algae begins growth as a stratiform crust. This crust may continue as parallel laminae or may pass upward into columnar and branching forms (Figure 21). Total thickness of the encrusting algae is usually less than 15 cm (6 in); lateral persistence may be several meters to several tens of meters.



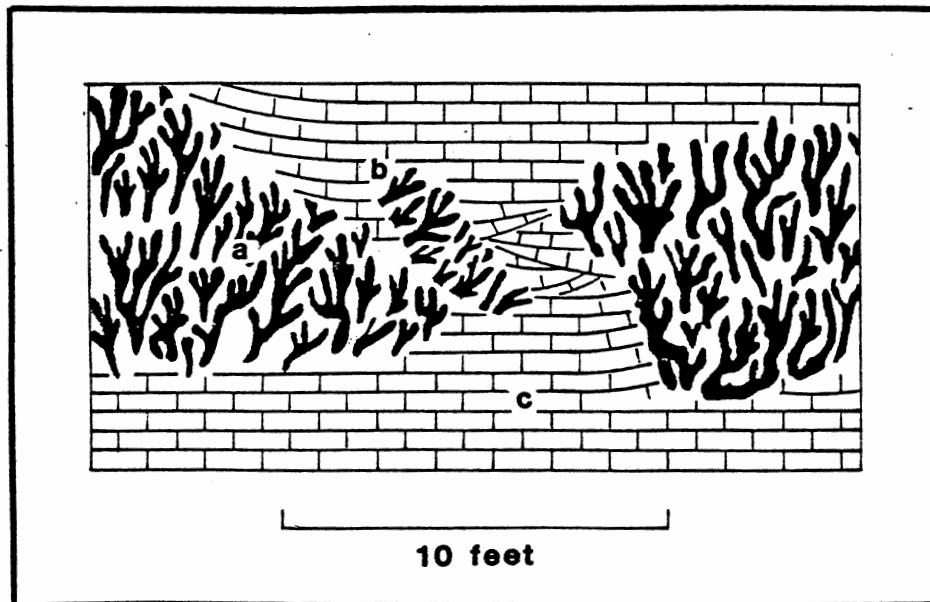


Figure 19. Penecontemporaneous Deformation of a Miniherm (a), Showing a Dislodged Fragment of the Algal Colony (b); (c) Silty Micrite, Cross-Laminated and Parallel Laminated. (Located 133 m (435 ft) Above Base of Section Measured in Blue Creek Canyon)

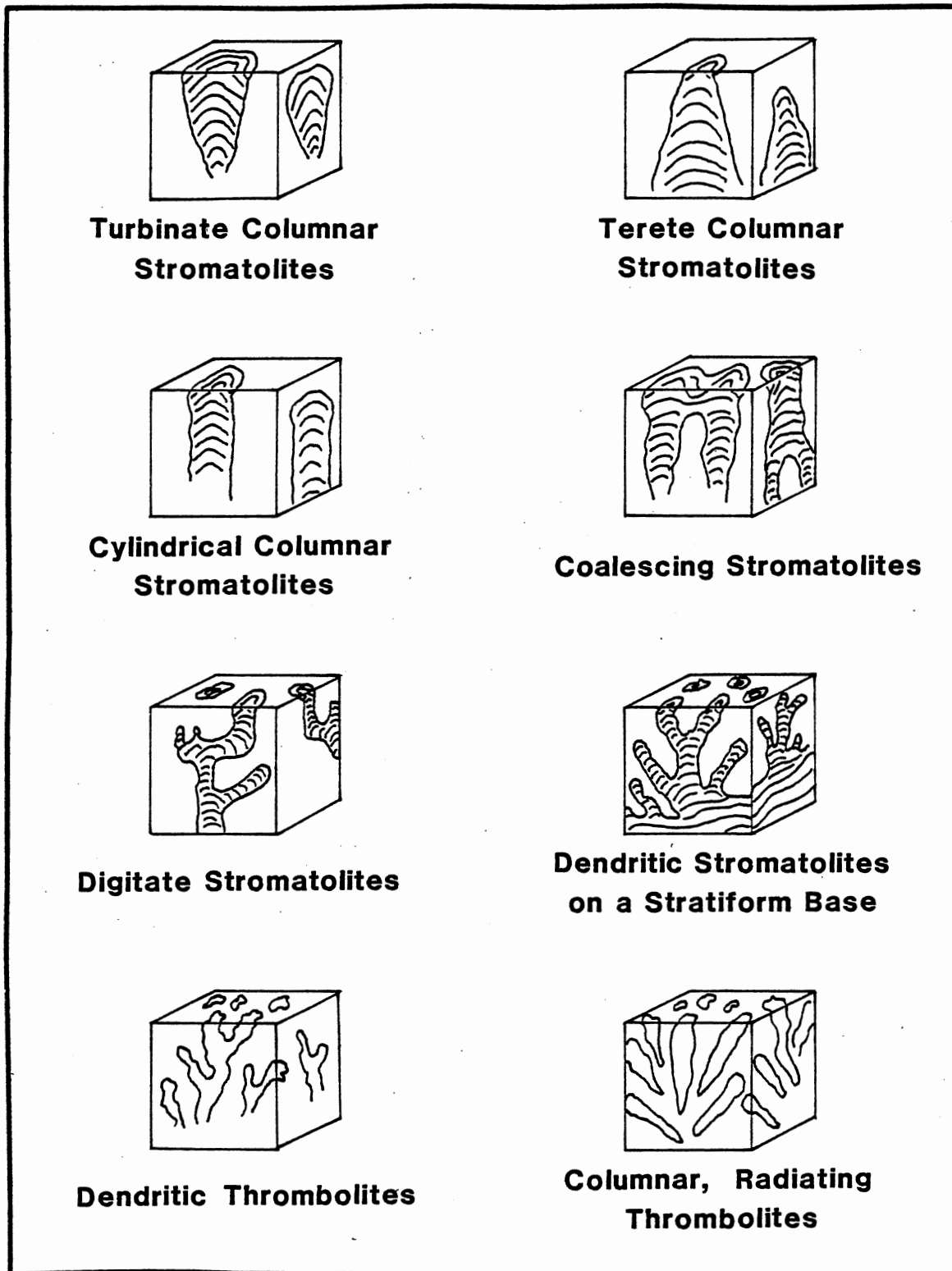


Figure 20. Stromatolite and Thrombolite Morphologies in Algal Reefs and Bioherms as Developed in the Cool Creek Formation in Blue Creek Canyon. (Terminology from Hoffman, 1969)



Figure 21. Encrusting Stromatolites

### The Micrite Lithotype

Microcrystalline limestone (micrite) is found throughout the Formation. It generally forms either massive or parallel laminated beds which are from 0.3 to 3 cm (0.1 to 1 in) thick. The massive micrite layers are of medium grey color. Laminated layers exhibit variations in color. The two most common color combinations are light grey and dark grey (perhaps due to slight variations in organic content) and light grey and pink (perhaps due to presence or absence of hematite particles). Some small scale trough cross-bedding has been observed, most commonly in channels between algal mounds (Figure 19).

Minor amounts of silt- and sand-sized quartz grains are found in several of the micrite units. Commonly, the quartz detritus is dispersed evenly throughout a unit, but the quartz particles sometimes serve to define cross-bedding.

Near the base of the Formation several micrite layers are bioturbated. The vertical burrows are less than 3 cm (1 in) in length (Figure 22). Horizontal burrows are rare, having only been identified in three locations. One of these is located 95 m (310 ft) above the base (Figure 22). The burrows were formed on a ripple-marked surface and were subsequently filled with micrite and oolites.

Subaqueous shrinkage cracks (Donovan and Foster, 1972) are located in micrite layers throughout the Formation (Figure 23). Sub-aerial mudcracks also occur in several horizons in the measured section (Figure 24). Rare small scale penecontemporaneous deformation is present in some horizons.

In thin section micrites show little variability. More than



(a)

(b)

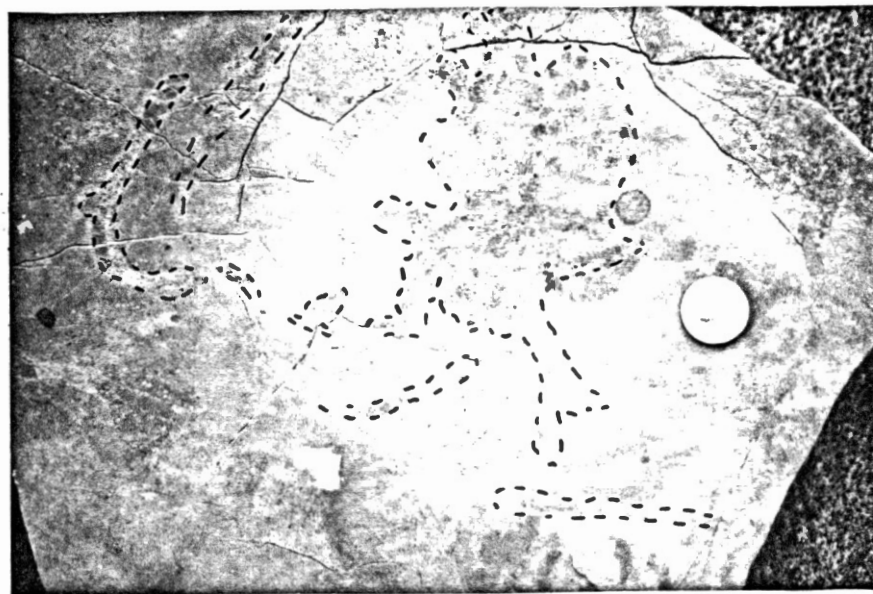


Figure 22. Bioturbated Micrite: (a) Vertical Burrows, Cross-Profile; (b) Ooid-Filled Horizontal Burrows, Plan View



(a)

(b)

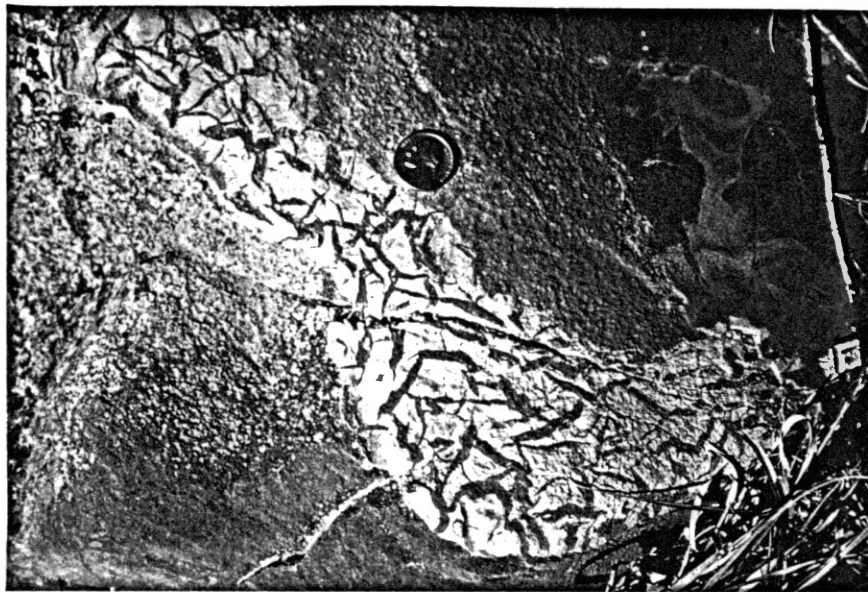


Figure 23. Subaqueous Shrinkage Cracks: (a) Cross-Profile; (b) Plan View. Lighter Micrite was Cracked, Later Infilled with Darker Micrite and Distorted When Compacted

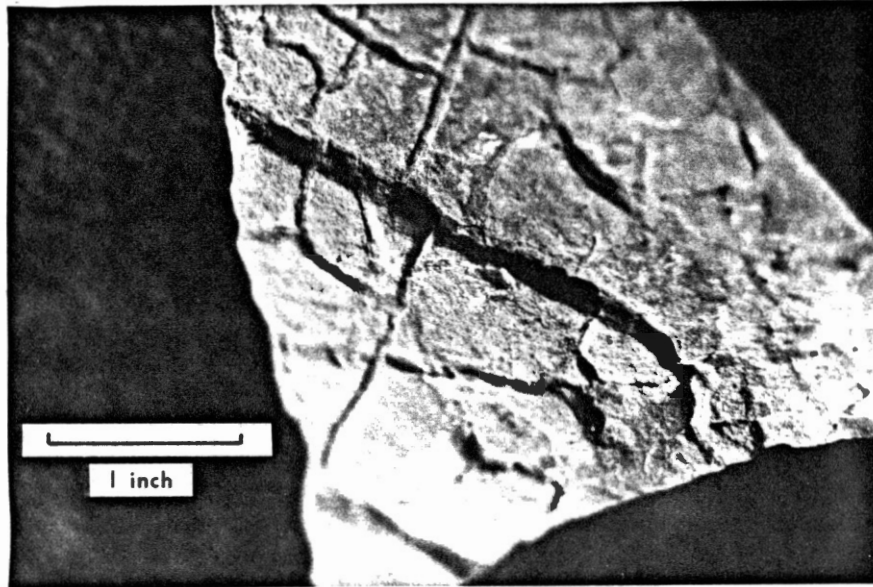


Figure 24. Subaerial Mudcracks, Plan View

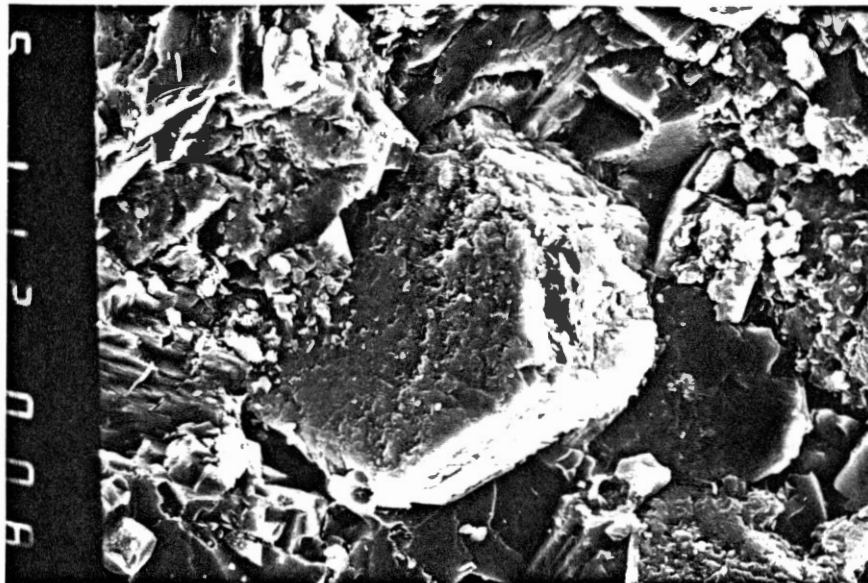


Figure 25. Authigenic Feldspar in Micrite Matrix  
(X1100, Scanning Electron Microscope)

90% of the rock is composed of lithified lime mud. The remaining constituents are detrital quartz silt, pellets, hematite, organic carbon, and traces of muscovite and feldspar. Authigenic feldspars, identified only in thin section, are found almost exclusively associated with micrites (Figure 25).

#### The Intraformational Conglomerate Lithotype

Intraformational conglomerates (IFC) form a substantial portion of the Formation. There are two main types of IFC: those comprising distinct beds (1 to 60 cm (0.5 to 24 in )) and those "filling in" between algal buildups. The IFC beds usually have sharp erosive bases and irregular upper surfaces (Figure 26). The topographic highs on the upper surfaces were often colonized by stromatolite-building algae.

The IFC's consist of elongate disc- and blade-shaped pebbles 8 cm (3 in) in maximum length, together with variable amounts of pellets, ooliths, quartz sand and silt, and shell fragments. The matrix may be lime mud with or without quartz sand or silt, or the pebbles may have formed an open framework subsequently cemented by sparite.

Most pebbles are micrite but fragments of stromatolites are also found (Figure 27). Thin section studies demonstrate that while in some IFC's only one type of clast appears to be present, in others the composition of the micrite fragments can range from pure micrite clasts to clasts that originated from a variety of other lithologies, including peloidal, oolitic, and quartz sand lithotypes. In some IFC's oblate chert pebbles, similar to those present in situ elsewhere in



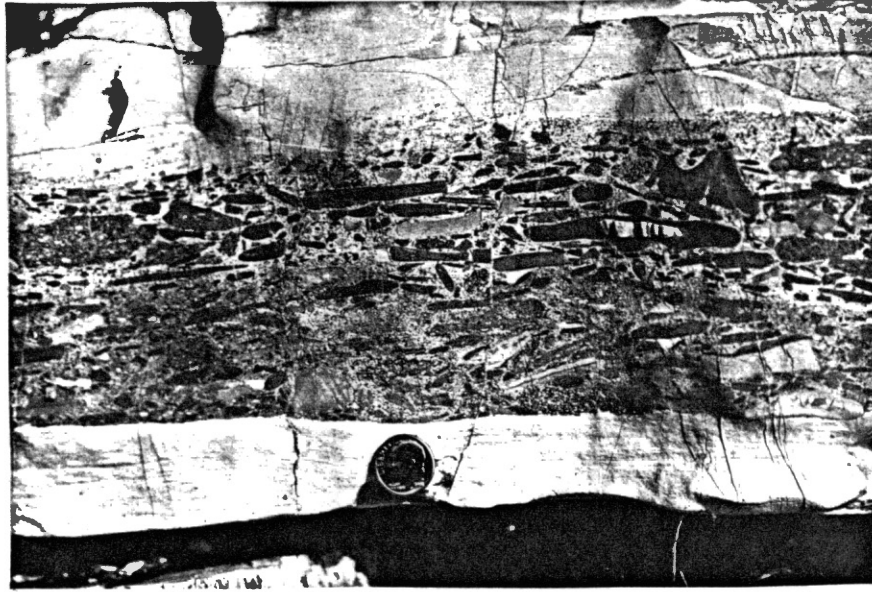


Figure 26. IFC Bed Showing Erosive Base and Gradational Upper Contact. Packing is Horizontal (Long Axis Parallel to Bedding) and Random



Figure 27. Algal Fragments Comprising IFC Clasts

the sequence, are present (Figure 28).

In most cases the discs and blades are packed with their long axes parallel to bedding (Figure 26). More rarely, imbrication (Figure 29), vertical packing (Figure 30) (Sanderson and Donovan, 1975), and random packing are seen (Figure 26).

#### The Intraformational Breccia Lithotype

Intraformational breccias are an uncommon feature in the Formation. Beds vary in thickness and form lenses that range from 15 cm to 1 m (6 in to 3 ft). The breccias often grade laterally into laminated micrite (Figure 31).

The breccia pebbles are angular to subangular micrite set in a micrite matrix. Fragment sizes are usually less than 8 cm (3 in), but blocks as large as 30 cm (1 ft) have been found (Figure 31). A well exposed unit containing three intraformational breccias found at Turner Falls in the Arbuckle Mountains illustrates the IFB's typically found in the Formation (Figure 32).

#### The Oolitic Limestone Lithotype

Oolitic limestone is found at a number of horizons in the Formation. The ooids do not appear to form distinct beds but rather, are dispersed throughout certain micrite and sparite horizons. These horizons can be as little as 15 cm (6 in) thick or as much as 10 m (30 ft) thick. The ooids can be associated with all lithotypes, most often with quartz sand, more rarely with algal boundstone. Individual ooids are less than 2mm (0.08 in) in diameter and usually average 0.5 mm (0.02 in). Oomolds may be present on weathered surfaces or the

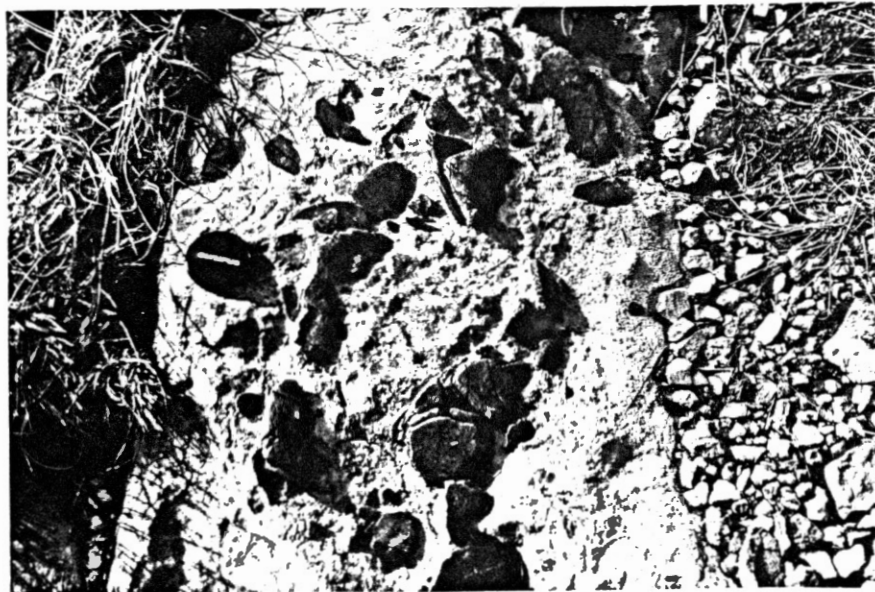


Figure 28. IFC Containing Imbricately Packed, Rounded Chert Pebbles



Figure 29. Imbricately Packed IFC Clasts

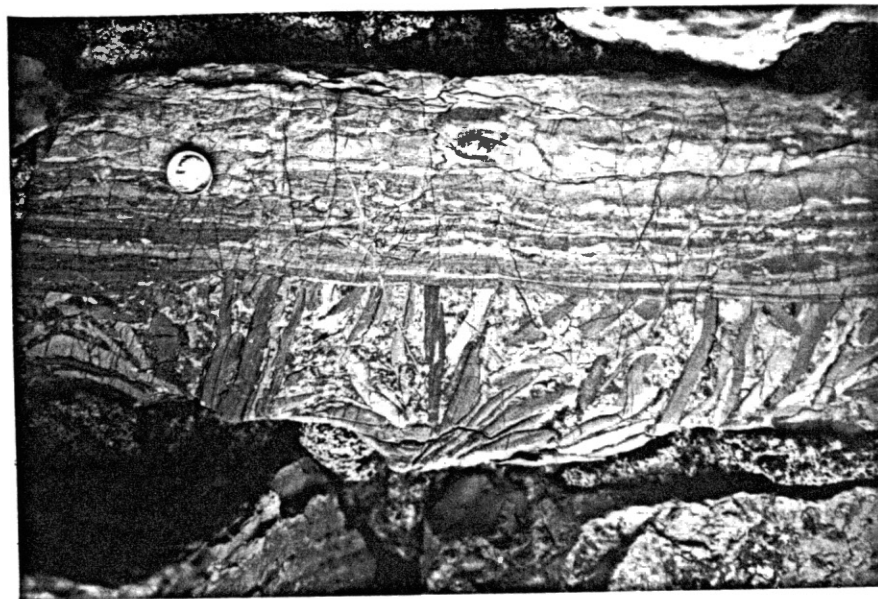


Figure 30. Vertically Packed IFC Clasts; Interareas are Filled with Micrite and Detritus. (Photograph is Upside Down--Block is Imbedded in Wall of Building at Turner Falls Overlook)



(a)

(b)



Figure 31. Collapse Breccias: (a) Stromatolites Initiated Growth on Top of Breccia after Stabilization; (b) Small Cavity Containing Collapse Breccia

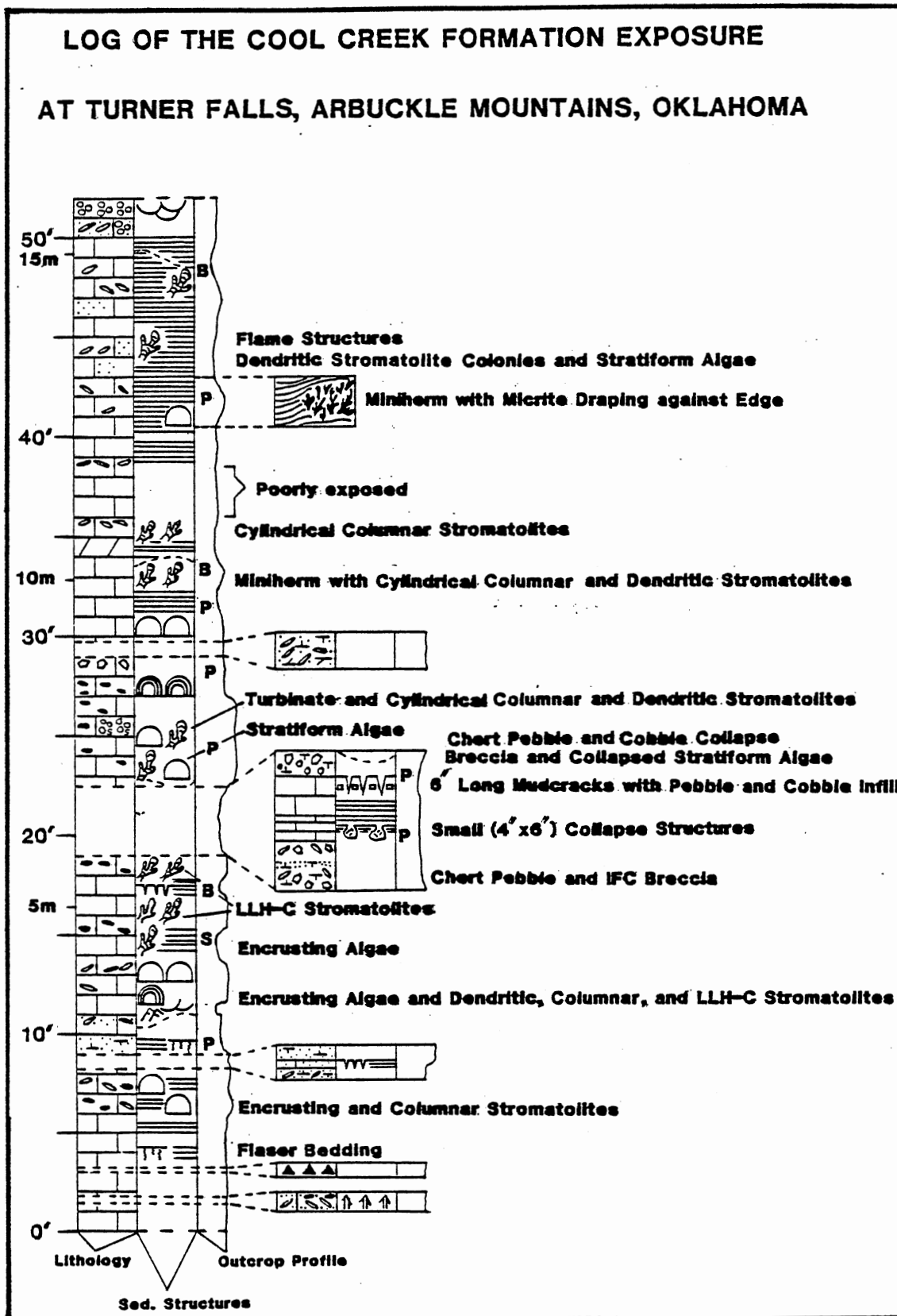


Figure 32. Stratigraphic Logs Measured at Turner Falls, Arbuckle Mountains, Southern Oklahoma

## LOG OF THE COOL CREEK FORMATION AT TURNER FALLS ROADCUT

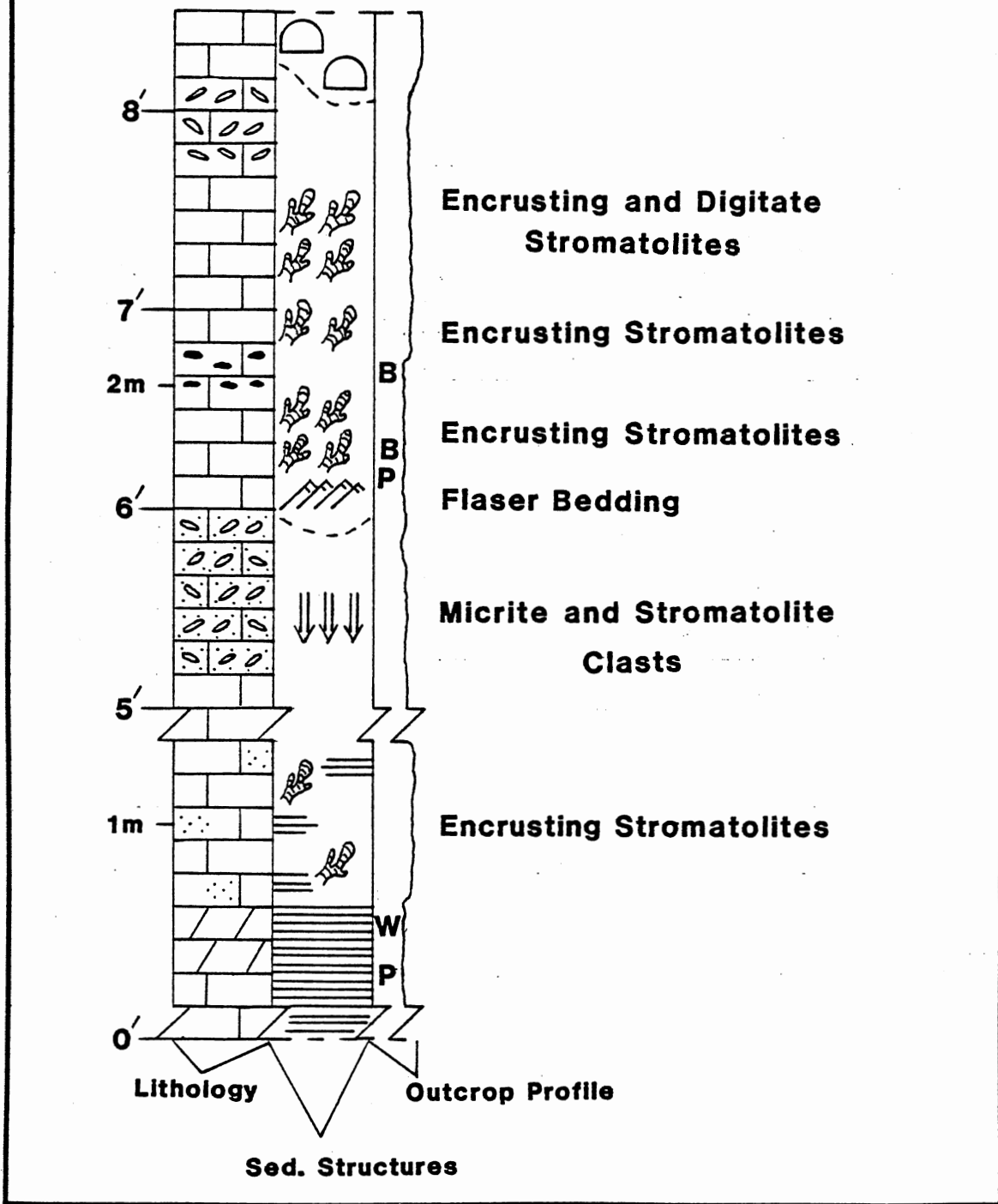


Figure 32. Continued

## EXPLANATION

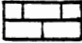
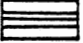

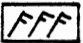
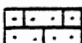

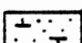
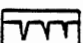
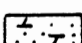
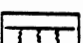
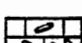

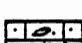
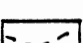

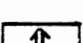
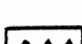
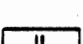
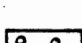
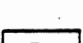
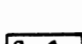

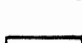
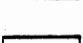

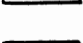
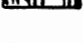
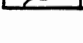
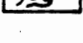
	<b>Limestone</b>		<b>Parallel laminations</b>
	<b>Dolomite</b>		<b>Small scale trough cross-bedding</b>
	<b>Sandy limestone</b>		<b>Medium scale trough cross-bedding</b>
	<b>Limey sandstone</b>		<b>Subaerial mudcracks</b>
	<b>Dolomitic sandstone</b>		<b>Subaqueous shrinkage cracks</b>
	<b>Intraformational conglomerate</b>		<b>Iron oxide pseudomorphs</b>
	<b>Sandy intraformational conglomerate</b>		<b>Indistinct bedding</b>
	<b>Chert nodules</b>		<b>Graded bedding</b>
	<b>Bedded chert</b>		<b>Reverse graded bedding</b>
	<b>Oolitic limestone</b>		<b>Pink</b>
	<b>Oolitic chert</b>		<b>Buff</b>
	<b>Chert pebble breccia</b>		<b>White</b>
			<b>Algal mound</b>
			<b>Algal mat</b>
			<b>Stromatolites</b>
			<b>Thrombolites</b>
			<b>Salt pseudomorphs</b>

Figure 32. Continued



matrix may be weathered away to expose oolitic relief.

Thin section analysis reveals that there are two basic ooid morphologies: Concentric ooids and radial ooids. Concentric ooids are composed of alternating bands of micrite that vary in density and, therefore, appear as light and dark brown rings (Figure 33). Occasionally, a ring may be composed of spar or show some radial texture. Radial ooids consist of alternating spokes of micrite and pseudospar (Figure 34). The spokes may be continuous from the outer edge to the nucleus or they may be interrupted and offset by concentric rings. Superficial ooids have also been seen (Figure 35). Some of the ooids have been diagenetically altered resulting in the degradation of the grains leaving only a ghost structure (Figure 35).

Although most ooids are nearly circular in cross-section, some are irregularly shaped (Figure 36). Most of these spastoliths are found in micritic matrices with a small number found in oosparites.

An ooid nucleus can be any one of the following fragments: Quartz sand or silt, broken fossils, broken ooids, and micritic, pel-micritic, or oomicritic intraclasts. Composite ooids consisting of two or more ooids are rare but have been seen (Figure 37). In some cases, micritization or recrystallization has destroyed the original nuclei (Figures 35 and 38).

#### The Peloidal Limestone Lithotype

Peloidal limestone does not form thick distinctive beds in the Formation but rather, is interlayered with other lithotypes. The small size of the peloids, less than 0.1 mm (0.004 in), and grey color make it extremely difficult to identify the lithology in the

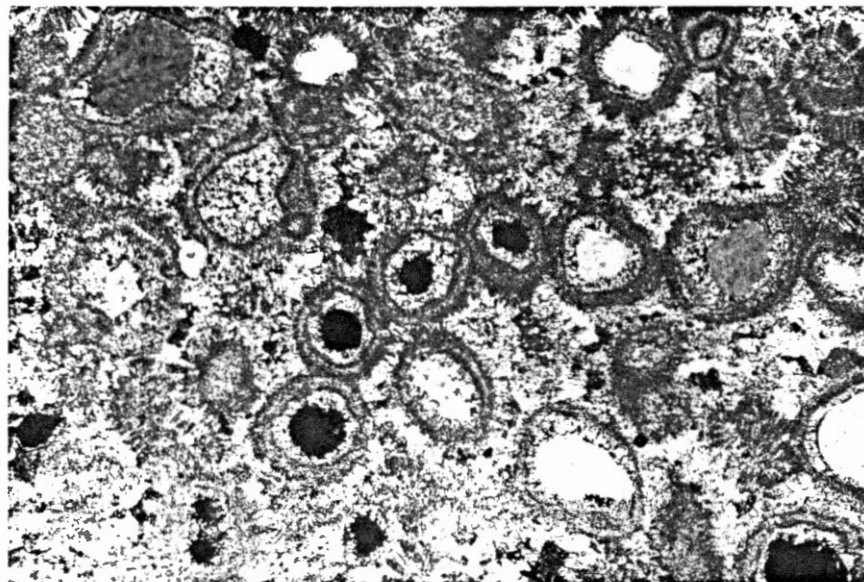


Figure 33. Concentric Ooids; Most Have Detrital Quartz Nuclei (X40, Crossed Nicols)

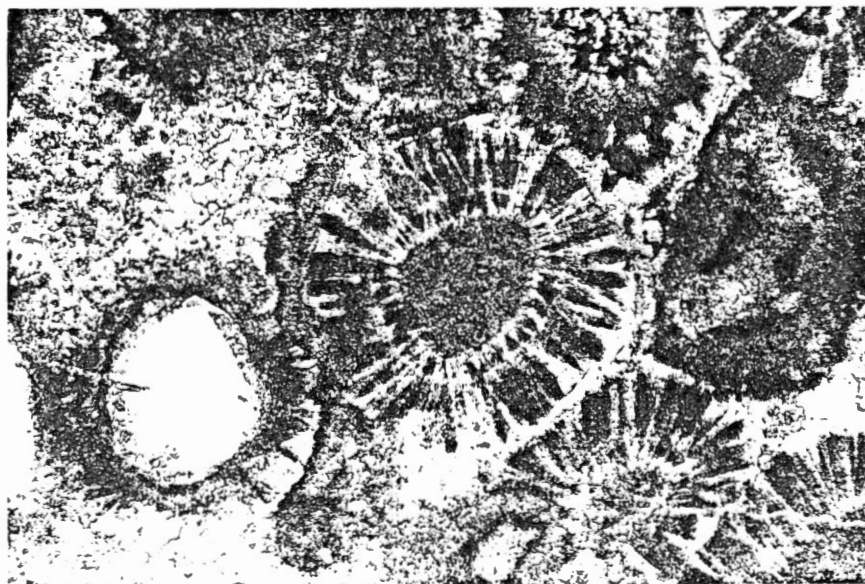


Figure 34. Radial Ooid with Micrite Nucleus (X100, Ordinary Light)

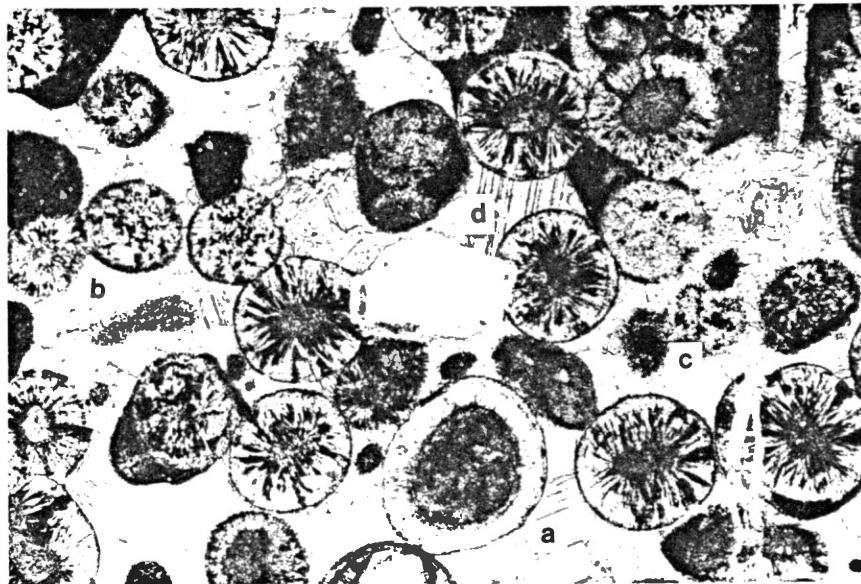


Figure 35. Oosparite. Superficial Ooid at (a) with Micrite Nucleus; Radial Ooids Show Several Stages of Disintegration from Partial (b) to Nearly Complete (c). Syntaxial Quartz Overgrowth on Intergranular Quartz Grain at (d). (X40, Ordinary Light)

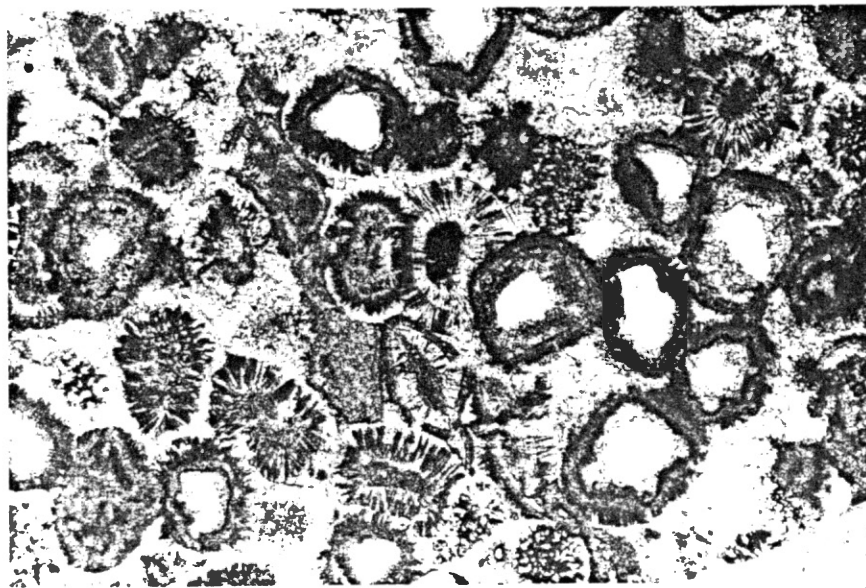


Figure 36. Spastoliths, Probably Caused by Compaction (X100, Ordinary Light)

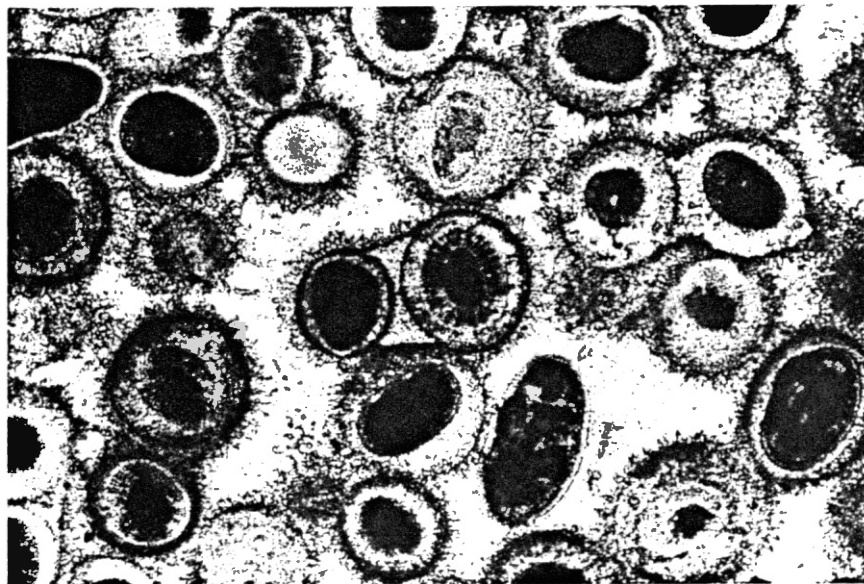


Figure 37. Partially Silicified Ooids Cemented by Siliceous Spar. Initial Cement was Iso-Pachous Calcium Carbonate. Note Composite Ooid in Center of Photo (X40, Ordinary Light)

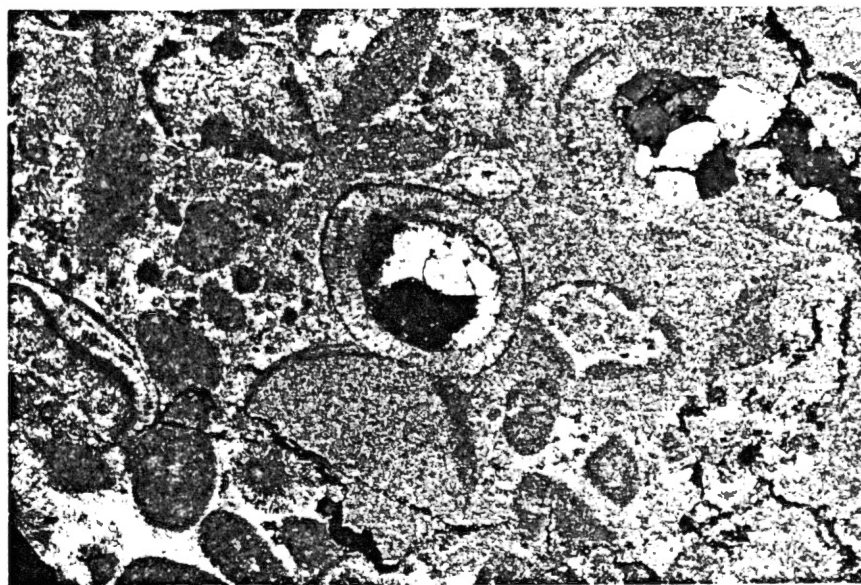


Figure 38. Ooids with Nuclei Replaced by Large Crystals of Non-Ferroan Dolomite. Pressure Solution Dissolved Ooids and Clasts (X40, Crossed Nicols)

field.

Thin section study shows the peloids are composed of dense micrite set in a micrite matrix or sparite cement (Figure 39). They are circular to elliptical in cross-section. Quite often they are associated with fossil fragments and are, therefore, interpreted as faecal pellets.

#### Quartz-rich Sandstones

As noted previously, the base of the Cool Creek Formation is defined by the first substantial appearance of detrital quartz sand. The basal sandy limestone is from 60 cm to 2 m (2 to 6 ft) thick; it is of great value in field mapping and is recognized as an ad hoc stratigraphic unit (the Thatcher Member). Small and medium scale trough cross-bedding, as well as parallel lamination, are prominent in this unit as they are in several other units of similar character higher in the Formation (Figure 40). Linguoid and symmetrical ripple marks have been seen on bedding planes in a few locations (Figure 41). Several of the quartz-rich units form lenses which pinch out laterally.

The quartz sand is generally medium grained throughout although fining upward and coarsening upward sequences in certain sections show a range in grain size from fine to coarse. In addition, as noted previously, some micrite layers contain silt-sized quartz grains. The grains are rounded to subrounded and white to light brown in color. Syntaxial overgrowths are developed to the point of being recognizable in hand samples. Associated clasts include ooliths, intra-clasts, rare fossil fragments (principally trilobites and gastropods),

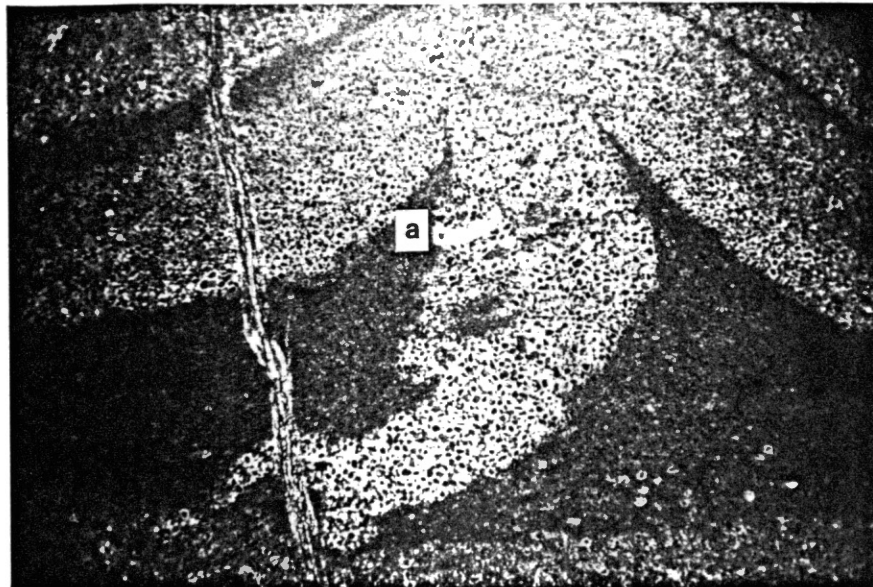


Figure 39. Subaqueous Shrinkage Crack Filled with Pel-sparite. Note Trilobite Fragment at (a) (X40, Crossed Nicols)



Figure 40. Small and Medium Scale Cross-Bedding in Quartz-Rich Sandy Limestone. Note Very Sandy IFC's Above and Below Cross-Bedded Unit



Figure 41. Sand in Troughs of Asymmetric Ripple Marks

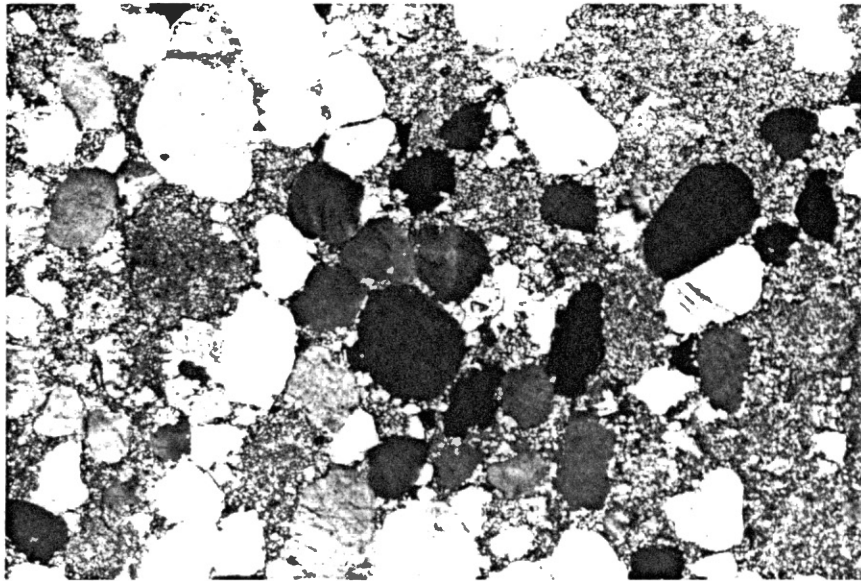


Figure 42. Photomicrograph of a Typical Quartz-Rich Limestone. Detrital Grains are Rounded; Some Show Syntaxial Overgrowths. Matrix is Micrite (X40, Crossed Nicols)

and accessory feldspar (principally microcline).

Studied in thin section, the quartz grains are seen to be sub-angular to rounded and usually, but not invariably, poorly sorted (Figure 42). The grains are predominantly monocrystalline although an occasional polycrystalline grain occurs (Figure 43). Vacuoles and Boehm lamellae occur infrequently.

#### The Chert Lithotype

Chert is found in many forms, of which nodules are the most common, being distributed throughout the Formation. These nodules range in size from less than 3 cm (1 in) to over 30 cm (12 in) in diameter and are roughly oblate in shape with their long axes parallel to bedding (Figure 44). In the lower two-thirds of the Formation the chert is predominantly flinty and white, grey, or pink in color; some nodules show color banding. The upper one-third of the Formation contains translucent chalcedonic chert that is mottled white, pink, or grey.

The nodules may be dispersed throughout a unit or they may occur as rows along certain bedding planes. Nodules may be so abundant along bedding planes that they may coalesce and form anastomosing networks. Occasionally, the chert fills vertical fissures.

Oolitic and peloidal limestones may be silicified to form very resistant chert layers. Such layers are white or pink in color and may be up to 0.3 m (1 ft) in thickness. Partial silicification of such beds produces a honeycomb weathering texture due to differential weathering (Figure 45).

Several varieties of partial silicification occur in algal



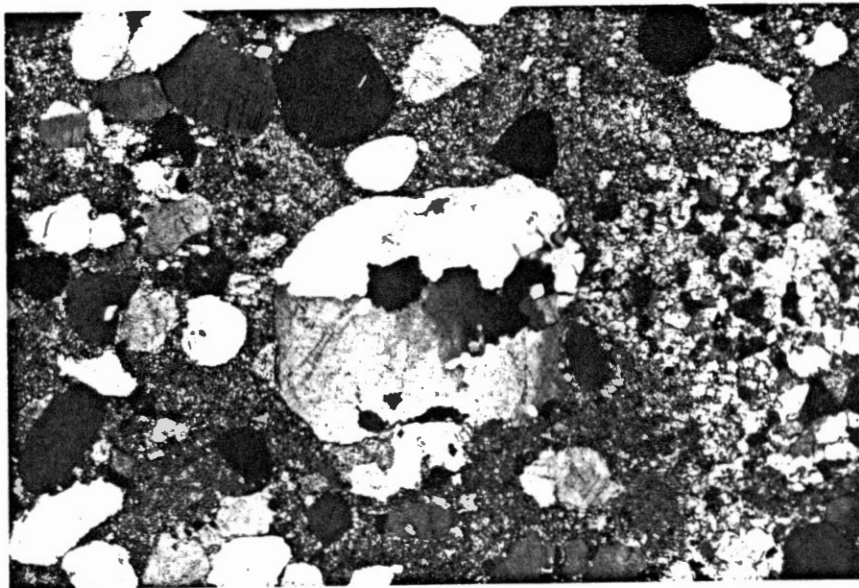


Figure 43. Rare Polycrystalline Quartz Grain in Quartz-Rich Limestone (X40, Crossed Nicols)



Figure 44. Chert Nodules Along a Bedding Plane Surface; Some Nodules are Discrete; Others Coalesce to Form an Anastomosing Network

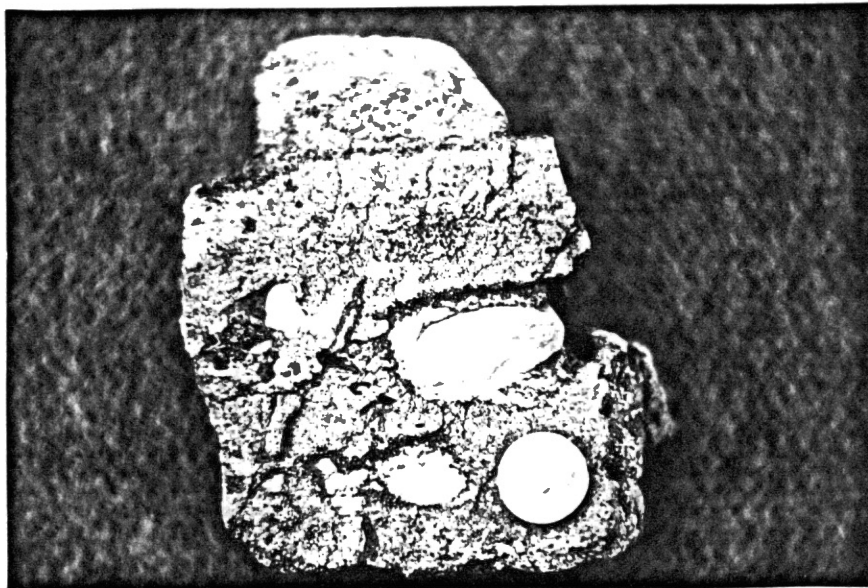


Figure 45. "Honeycomb" Texture Produced by Partially Silicified Oolitic Unit

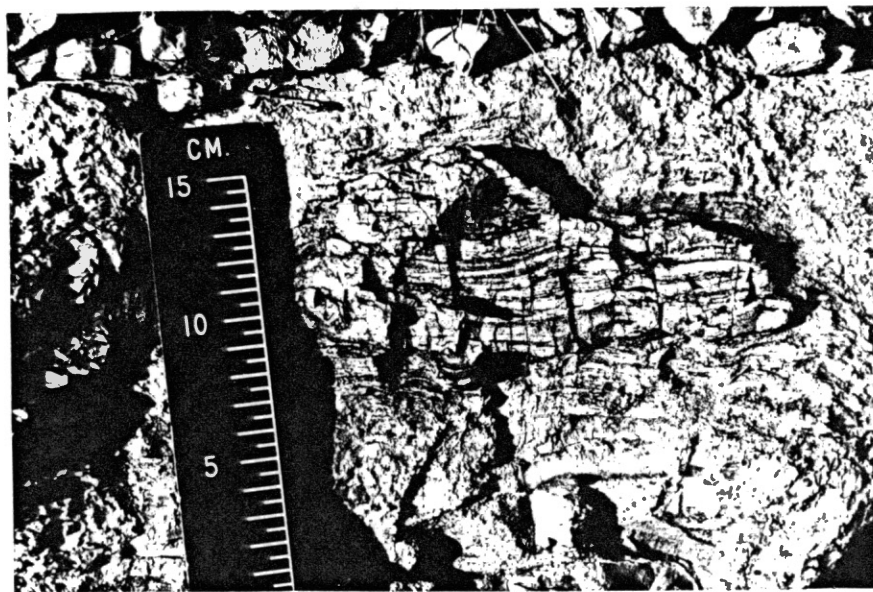


Figure 46. Silicified Core of an Algal Mound

structures. For example, some mounds contain cores of replacement chert or alternating rings of chert and micrite (Figure 46). In other cases, thrombolites are replaced preferentially to their surrounding matrix (Figure 15).

Only one true layered chert bed exists in the Formation. It is a distinctive 15 cm (6 in) thick bed located 350 m (1145 ft) above the base in which charcoal grey and orange layers alternate with grey micrite (Figure 47).

Several chert breccias from 10 to 100 cm (3 in to 3 ft) thick, have been identified in the Formation. In these units the chert pebbles are angular, pink or white, and range in size from 0.6 cm to 5 cm (0.25 to 2 in). The matrix of these beds is grey or pink micrite. Pebble content can be as high as 30% of the rock (Figure 48).

The most diverse and distinctive chert breccia occurs 305 m (1000 ft) above the base of the Formation. This unit is a sandy, chert pebble breccio-conglomerate. Some of the chert pebbles are rounded whereas others are angular. Medium grained quartz sand and ooids are also present.

The three main types of silica, megaquartz, microquartz, and chalcedony, have been identified in thin section studies. The silica occurs both as a replacement mineral and as a pore filling cement.

Megaquartz occurs primarily as syntaxial overgrowths on detrital quartz grains (Figure 49) and, less often, as pore-filling cement (Figure 50). Algal filament tubes and fenestrae are occasionally filled with secondary megaquartz (Figure 16). Very rarely, euhedral megaquartz crystals have been seen to be replacing carbonate cement (Figure 51) or fossil fragments (Figure 52).

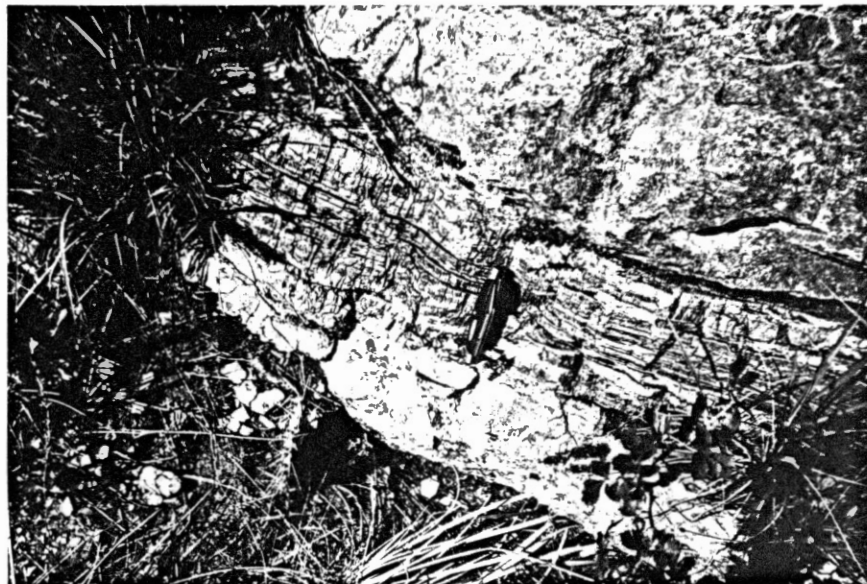


Figure 47. Bedded Chert. Dark Laminae are Orange and Grey Microcrystalline Chert; Light Layers are Micrite



Figure 48. Chert Pebble Breccia. Very Angular Chert Fragments Set in a Micrite Matrix

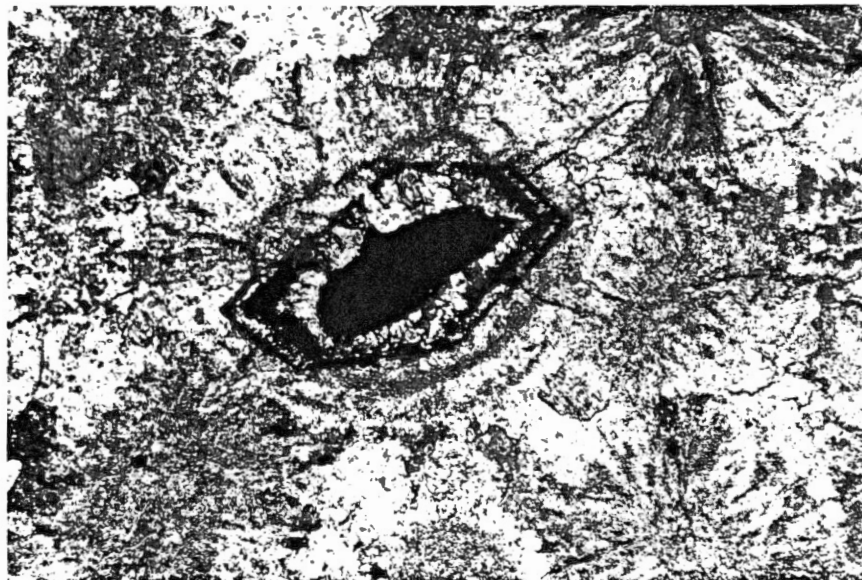


Figure 49. Multiple Generations of Syntaxial Quartz Overgrowths on a Detrital Quartz Grain that Forms the Nucleus of an Ooid (X100, Crossed Nicols)

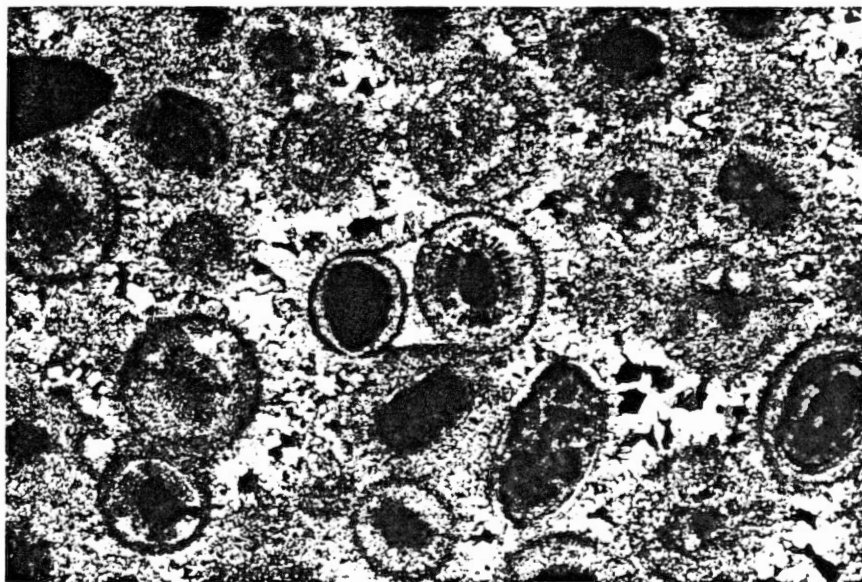


Figure 50. Megaquartz as Pore-Filling Cement. Same View as Figure 37 with Crossed Nicols (X40)

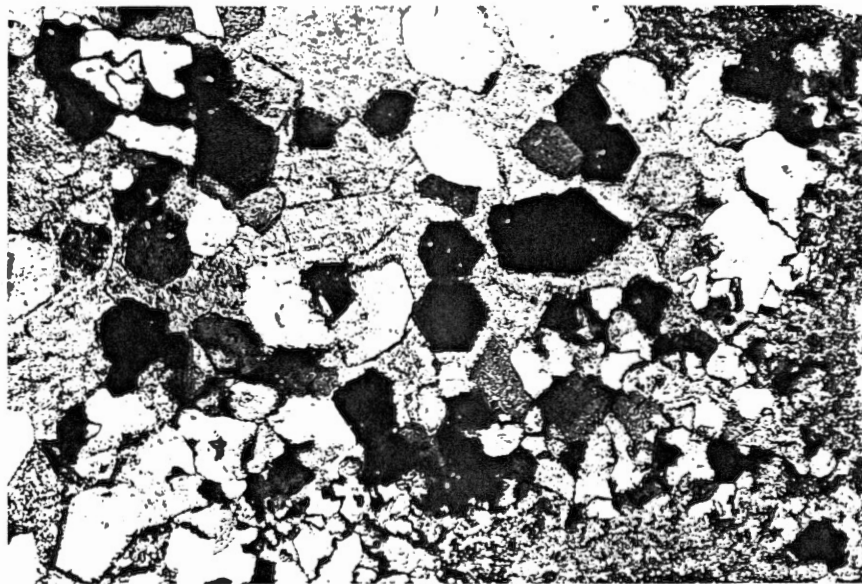


Figure 51. Rare Euhedral Quartz Crystals Replacing Calcite Spar (X100, Crossed Nicols)

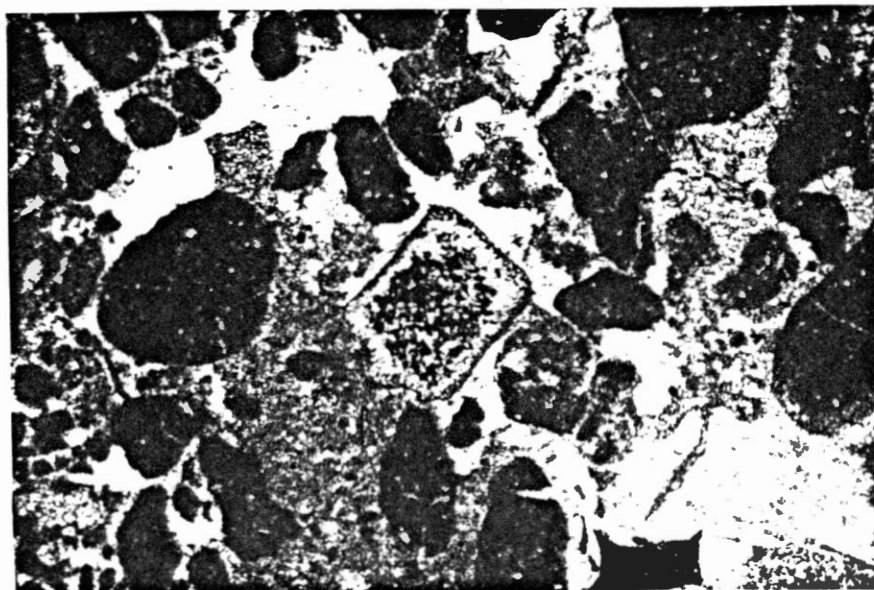


Figure 52. Microquartz Replacing the Interior of an Echinoid Fragment (X40, Crossed Nicols)

Microquartz is found throughout the Formation as primary bedded chert and as a replacement mineral. In thin section replacement chert and bedded chert are seen as crystals only a few microns across which show uniform pinpoint extinction. Ooids and fossils are the grains most commonly replaced by such microquartz. Replacement of the fossils begins at the core and continues outward. Both partially replaced fossils and completely replaced fossils have been indentified. Ooids may also be partially or completely replaced (Figures 37 and 53). The concentric rings have been selectively replaced by silica crystals of different sizes preserving the general outlines of the rings.

Fibrous chalcedony occurs most frequently in the upper one-third of the Formation. Three morphologies have been seen in thin section: fibrous chalcedony with continuous coloration along fiber packets (Figure 54); zebraic chalcedony with alternating light and dark colors along fiber packets (Figure 55); spherulitic chalcedony in which small spherulites (0.3 mm (0.01 in)) show pseuduniaxial extinction (Figure 56). Most of the chalcedony is length slow (quartzine) with only minor amounts of length fast chalcedony (chalcedonite). Chalcedonic chert is found as pore filling cement and as a replacement of calcium carbonate. Some pore filling cement is banded and may show alternating rows of length slow and length fast fibers.

In the upper part of the Formation evaporite pseudomorphs and dolomite are associated with secondary chert. They are recognized in both hand samples (Figure 57) and thin sections (Figure 58) and are commonly associated with length slow quartzine and zebraic chalcedony. Dolomite rhombohedrons have been seen in thin

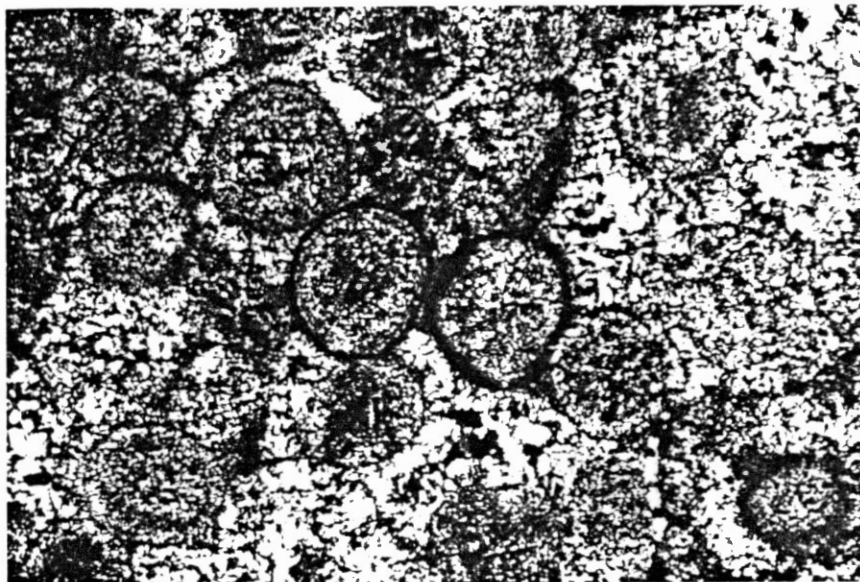


Figure 53. Completely Silica-Replaced Ooids Showing Little or No Compactional Deformation (X40, Crossed Nicols)

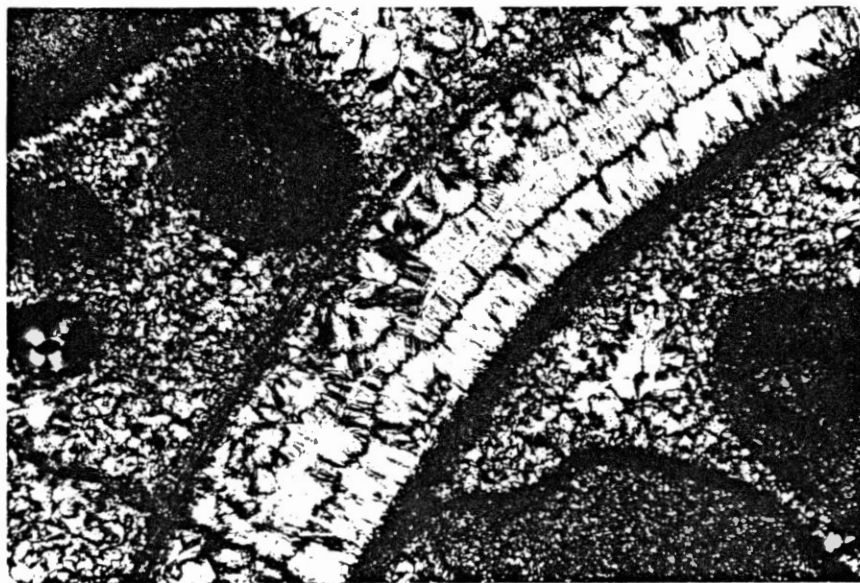


Figure 54. Chalcedonite Filling in a Fossil Mold (X100, Crossed Nicols)





Figure 55. Zebraic Chalcedony Filling In Pore Space  
(X100, Crossed Nicols)

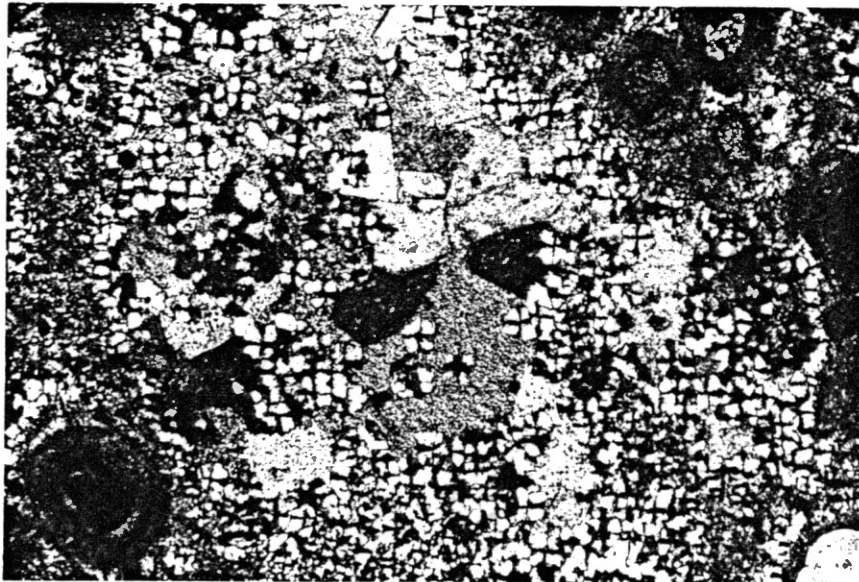


Figure 56. Spherulitic Chalcedony Replacing Calcite  
Spar Cement (X40, Crossed Nicols)

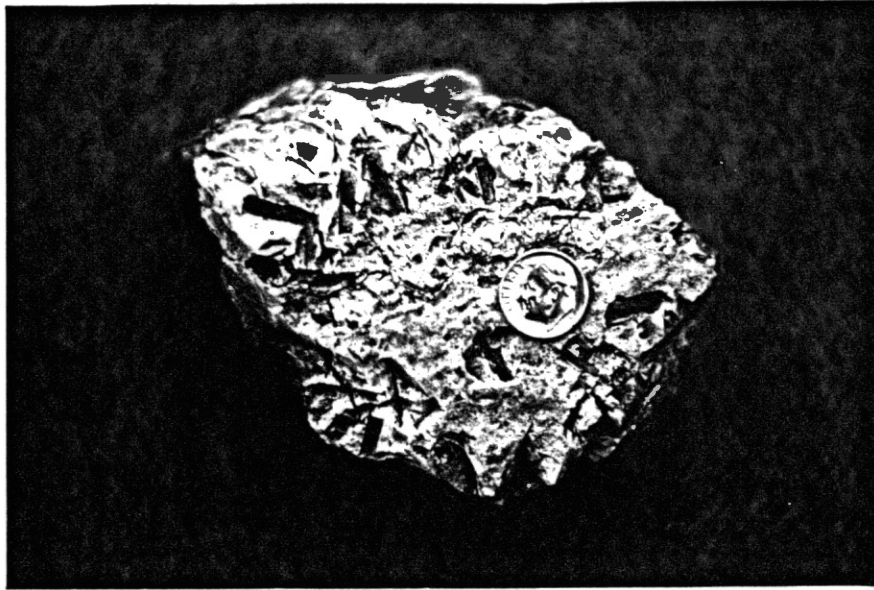


Figure 57. Evaporite Pseudomorph Molds in a Micro-Crystalline Chert Nodule

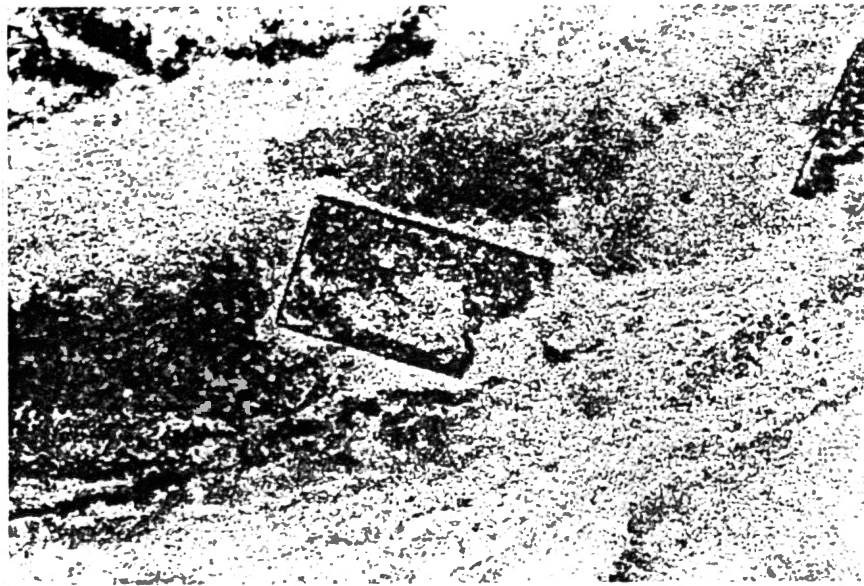


Figure 58. Evaporite Pseudomorphs in Microcrystalline Chert. Pseudomorphs are Calcite with Some Silica in Fractured Centers of Crystals (X40, Ordinary Light)

section associated with both microquartz and chalcedony (Figure 59).

### Dolostone

Although rock forming dolomite ("dolostone") is common in the Cool Creek Formation in other areas of the Slick Hills, it is rare in the Blue Creek Canyon measured section. A 2 m (6 ft) layer of dolomite occurs 52 m (170 ft) above the base of the Formation. The dolomite is brown-grey in color and is distinguished in the field by a more blocky weathered profile than the limestone. Dolostone in other areas of the Slick Hills exhibits a more weathered honeycomb appearance and is generally more abundant in the western part of the Hills. No dolostone has been observed east of Blue Creek Canyon.

An unusual section of dolostone was discovered in the western section of the Slick Hills (Beauchamp, 1982) and was measured as a supplementary section (Figure 60). In this section dolostone is either interbedded with secondary silica (mostly chalcedony) or contains nodules of silica. The morphology of the silica suggests that it may be pseudomorphing evaporative sulphates and hints at the existence of a sabkha environment. This will be discussed more fully in Chapter 4.

Thin section analysis shows that diagenetic dolomite occurs in small percentages (less than 10%) in many limestones throughout the Formation. Dolomite rhombohedrons are found replacing calcium carbonate in micrite matrix and clasts (Figure 61) and are also associated with microcrystalline chert (Figure 59). Minor zoning is seen on some rhombohedrons. Sizes range from 0.01 mm to 0.3 mm (0.0004 in to 0.01 in) in the partially dolomitized rocks to 1 mm (0.04 in) in



Figure 59. IFC Clast Replaced by Microcrystalline Chert. Dolomite Crystals Formed in the Nodule Before Silicification (X40, Crossed Nicols)



(a)

(b)

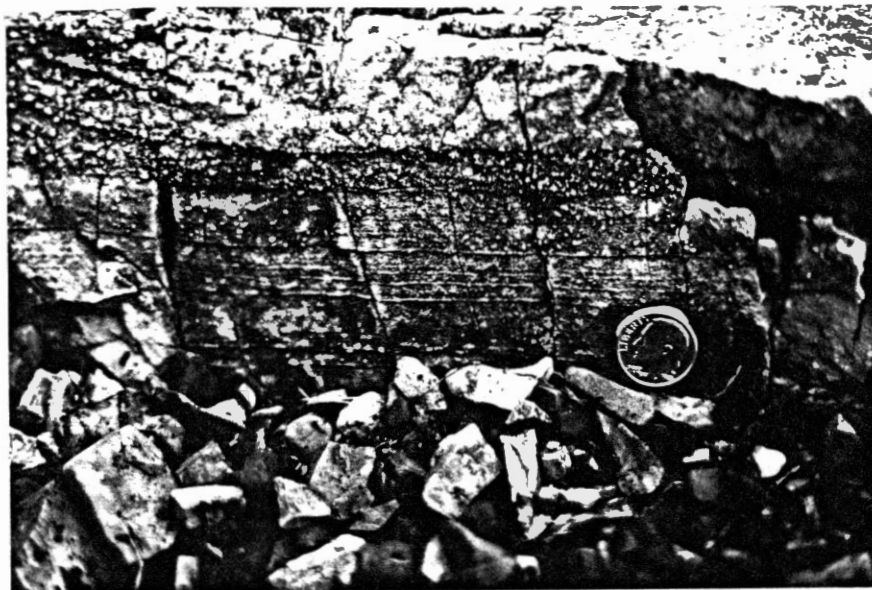


Figure 60. Sabkha Sequence:

- (a) "Cauliflower" Chert Nodules after anhydrite
- (b) Very Small "Cauliflower" Chert Nodules and Thinly Laminated Chert and Dolomite
- (c) Layered Dolomite and Chert after Anhydrite
- (d) Thickly Layered Dolomite and Chert after Anhydrite



(c)

(d)



Figure 60. Continued

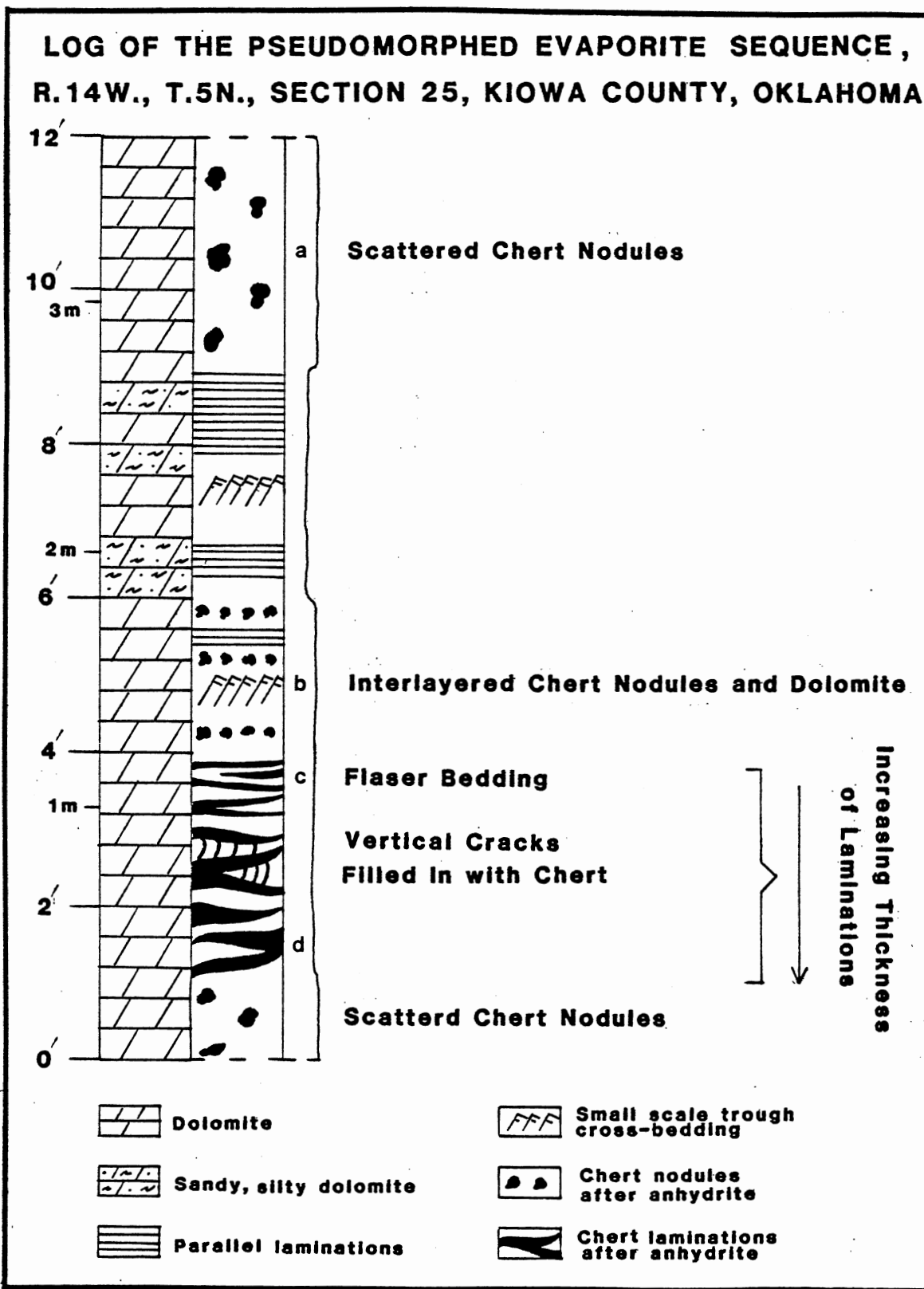


Figure 60. Continued



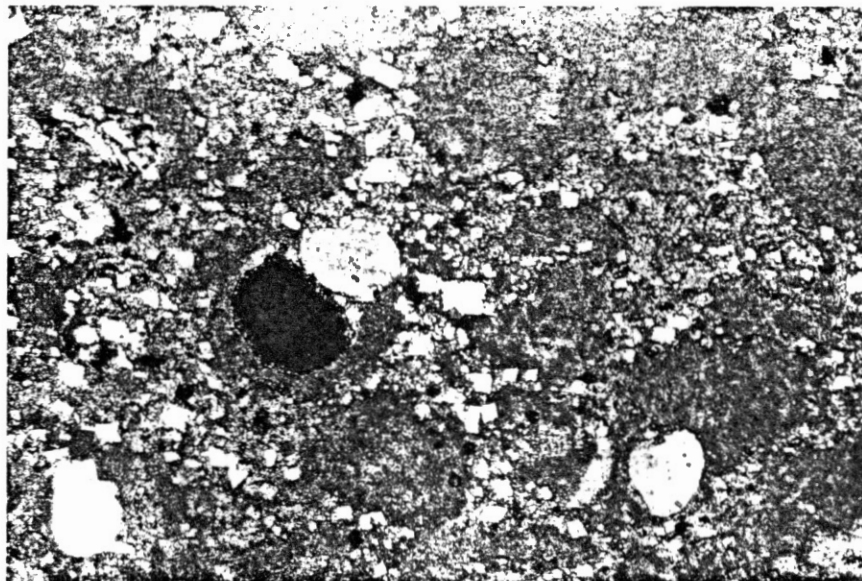


Figure 61. Secondary Dolomite Crystals Replacing Micrite in a Sandy IFC (X40, Crossed Nicols)



Figure 62. Interlocking Mosaic of Zoned Secondary Dolomite Crystals. Cement is Late Calcite Spar (X40, Ordinary Light)

in the interlocking crystals of the dolostone. Comprehensively dolomitized lithologies have secondary porosity which has usually been filled with a late sparry calcite (Figure 62).

### Body Fossils

Apart from lithified algae, the fossil content of the Cool Creek Formation is sparse. Most distinctive are the silicified gastropod shells of the genus Lecanospira which are found in the upper one-third of the Formation. They range in size from 6 mm to 38 mm (0.25 in to 1.5 in) in diameter (Figure 63).

Brachiopods are seen near the Cool Creek-Kindblade Formation boundary. They are less than 6 mm (0.25 in) across. Weathering makes their identification difficult but they are probably of the genus Diaphelasma.

Layers of sponge remains are found near the top of the Formation. Individual fossils are 6 mm to 13 mm (0.25 in to 0.5 in) in length. Usually, however, they are found in confused masses along bedding planes (Figure 64).

Although not visible in hand samples, trilobites and echinoids have been recognized as broken fragments in thin sections (Figure 65). They usually constitute less than 5% of the rock, but a few fossil hash units have been recognized and are generally associated with IFC's (Figure 66).

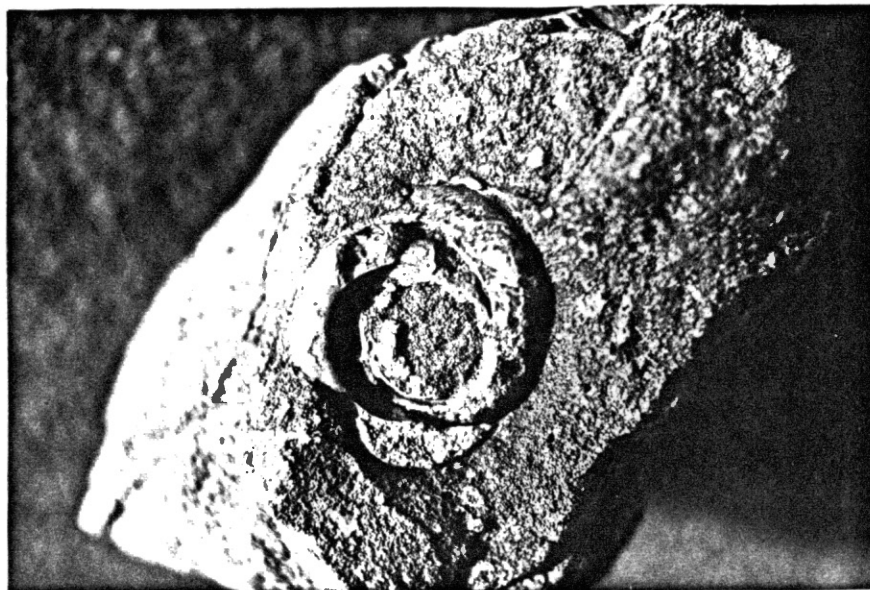


Figure 63. Gastropod, Lecanospira (?). Diameter =  
4 cm (2 in)

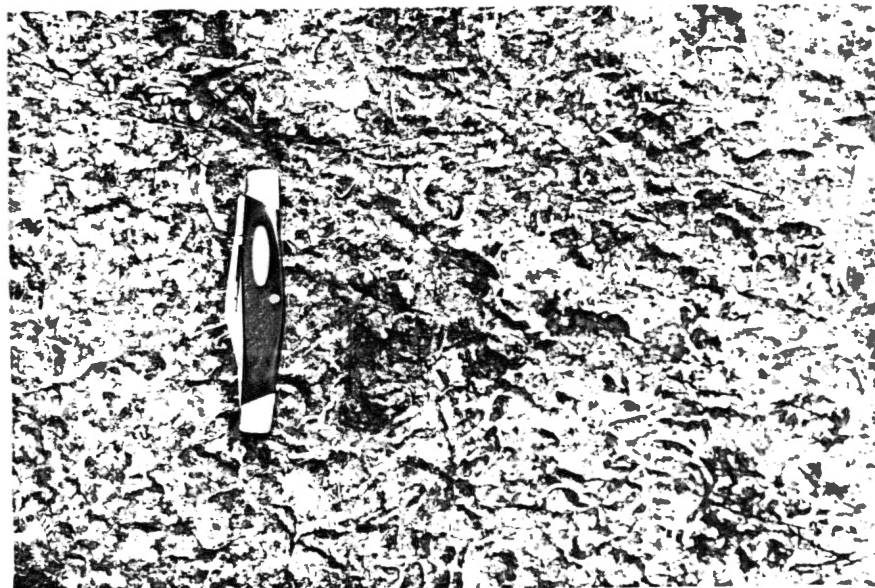


Figure 64. Masses of Sponge Remains on Bedding Surface

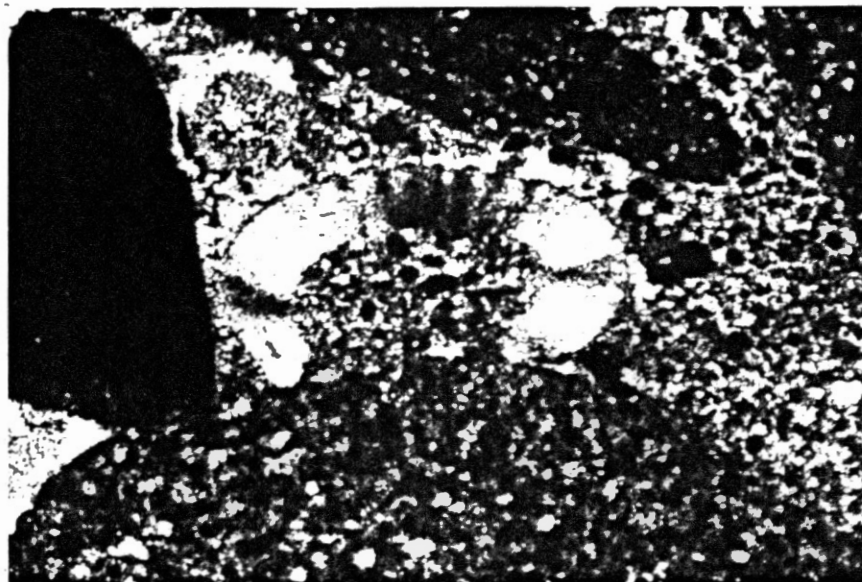


Figure 65. Trilobite Fragment (X40, Crossed Nicols)



Figure 66. Trilobite Hash Associated with an IFC  
(X10, Ordinary Light)

CHAPTER IV  
ENVIRONMENTAL ANALYSIS OF THE  
COOL CREEK FORMATION

Introduction

The Paleoenvironment during the Early Ordovician

Interpretation of past environments relies heavily on the Principle of Uniformitarianism. This Principle is reasonably valid as an interpretive tool for the recent geologic past, but as one goes farther back in time it is less useful because it is clear that the state of the earth during the Early Ordovician was considerably different than that of the present. For example, the present balance of carbon dioxide and oxygen was unlikely to be similar to that which exists today (following the rise of land plants).

500 million years ago the North American continent was far removed from its present location (Figure 67). Paleomagnetic data show that Southwest Oklahoma was located approximately 25° south of the Ordovician paleoequator (Habicht, 1979). Thick sequences of fossiliferous limestone and evaporites, deposited across much of the continent during this time, support the paleomagnetic data. Less substantial deposits of limestone and evaporites in areas that were more than 40° away from the paleoequator suggest that the worldwide climate was warmer and drier than the present average climate

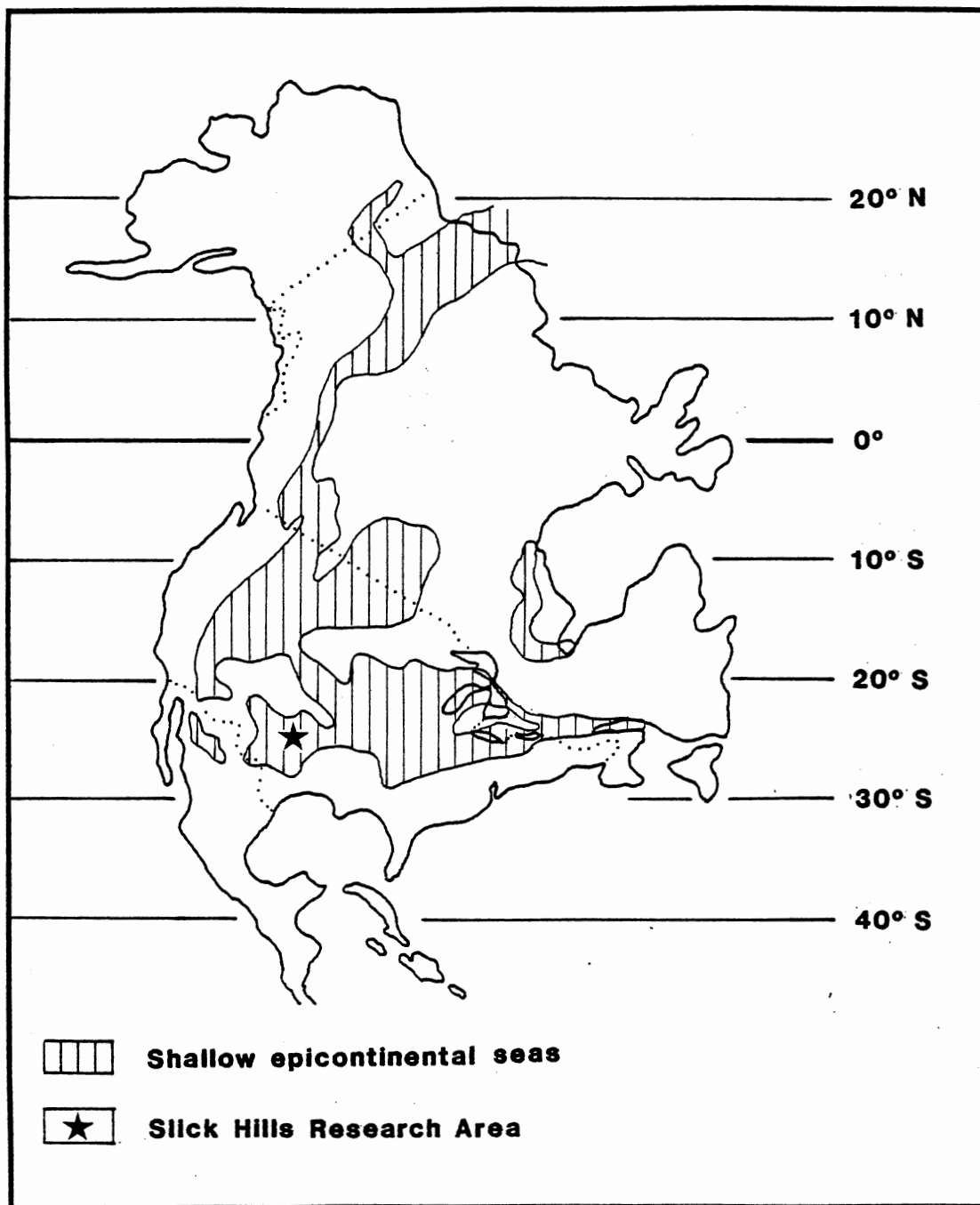


Figure 67. Paleoposition of North America during the Early Ordovician (Modified from Habicht, 1979)

(Levin, 1978).

Life in the Early Ordovician was restricted to the marine environment. The atmosphere contained only 1% to 10% free oxygen (based on the present level of oxygen at 100%), prohibiting the evolution of terrestrial animals and plants (Windley, 1977). Free oxygen in the atmosphere not only enables aerobic respiration in biota, but is responsible for the ozone layer which protects emergent life from ultraviolet radiation. Blue-green algae, of which traces have been found as far back as the Proterozoic (up to 3.5 billion years ago), are more resistant to ultraviolet radiation than most biota and were, therefore, responsible for the early introduction of oxygen into the atmosphere.

The salinity of the oceans is postulated to have been less in the Paleozoic than it is now (Levin, 1978). Salts weathered from terrestrial rocks have increased the salinity of the oceans through time. Although weathering and erosion of land surfaces would have been high because of the lack of land cover, the North American continent had very little relief during the early Ordovician. Therefore, introduction of salts into the oceans may have been minimal. However, the same lack of relief that prevented extensive transportation of salts was also responsible for the great extent of shallow epicontinental oceans. Shallow water and high temperatures would have created conditions favorable to the formation of evaporites due to the high concentration of salts that would have ensued.

#### The Algal Environment

As noted in Chapter 3, algal boundstones are the dominant litho-

type in the Cool Creek Formation, having been formed by the lithification of the various types of algal buildups. The algal units serve as an indicator of the general paleoenvironment of the area; the morphologies of the individuals comprising the units serve as indicators of the local environments within the area (Figure 68, Table II).

The stromatolites, thrombolites, and algal mats were built by the nonskeletal blue-green algae, Cyanophyta (Wray, 1977). Mucilaginous organic films trapped and bound detrital or chemical sediment. The availability of the sediment, the type of sediment, and the growth rate of the algal film controlled the morphology of the internal structure.

The laminae of the stromatolites and algal mats were formed by the alternation of organic-rich layers and sediment-rich layers. Thin section study shows that the sediment-rich layers in Cool Creek algae are composed predominantly of chemically precipitated calcium carbonate or recycled calcium carbonate (pellets or clasts) (Figure 17). Very fine grained quartz sand and silt are found in minor amounts (usually less than 1%). Siliciclastic material found in modern stromatolites along the Trucial Coast are known to be wind-blown (Park, 1976). It is here suggested that in most cases, the siliciclastic grains are probably of aeolian origin in the Ordovician algae (Wilson, 1975; Donovan, 1982). The small size of the grains, the small quantity, and the semi-arid environment with no land cover serve as indirect evidence of aeolian origin.

The organic laminae are darker than the sediment laminae thereby accentuating the layering. Filament tubules perpendicular to the



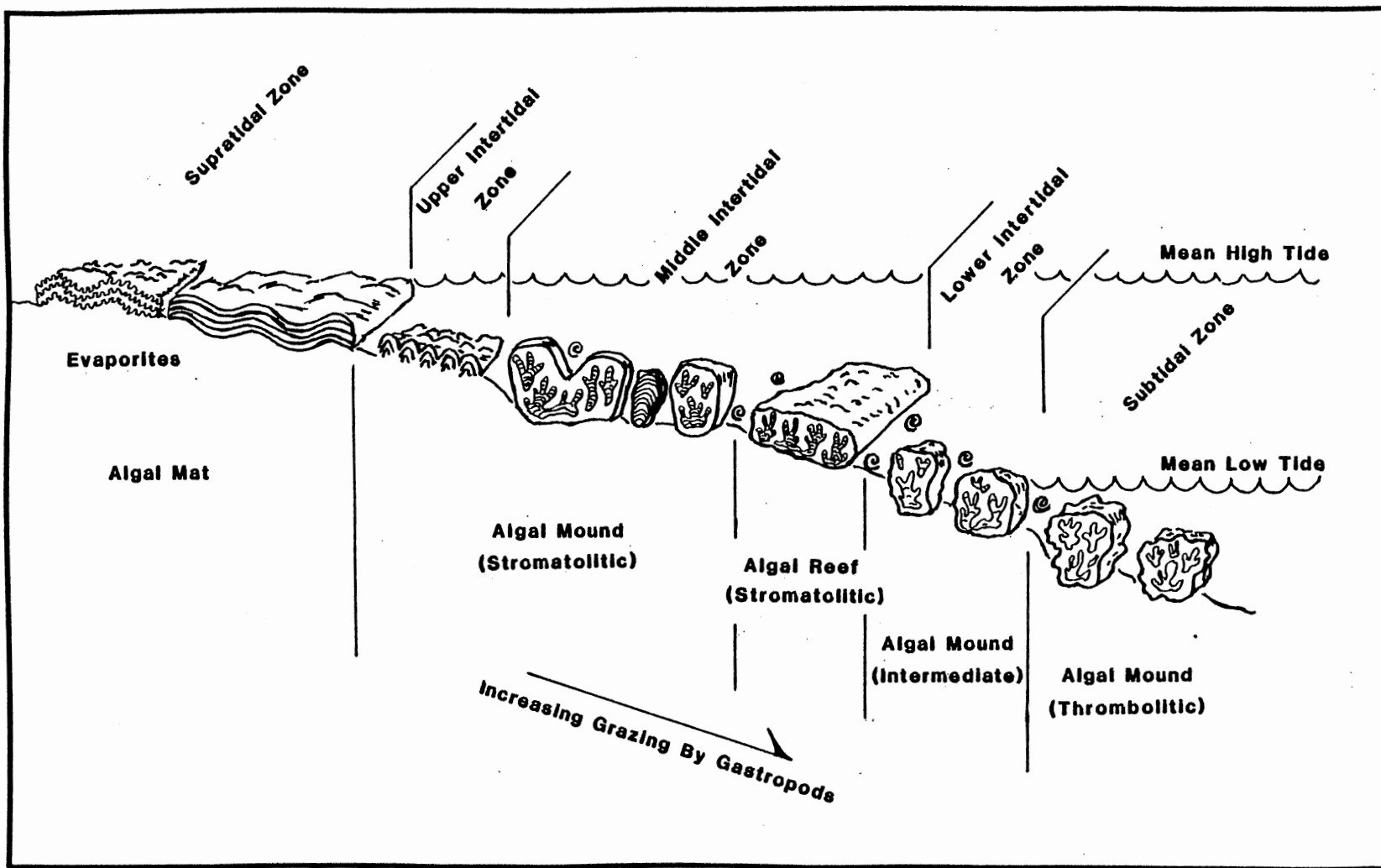


Figure 68. Interpretation of Environmental Relationships between Algal Types and Depth of Water as Developed in the Cool Creek Formation

TABLE II  
 LOCAL ENVIRONMENTS OF ALGAL BOUNDSTONES

Algal Type	Depth of Water	Water Turbulence	Clastic Input/ Chemical PPT	Biological Activity
Algal mat smooth profile	supratidal	gentle overwash; aperiodic	minor	very minor
crinkly profile	supratidal	gentle overwash;	minor; possible	none
Algal mound/reef/bioherm stromatolitic	intertidal	moderate	minor to moderate	moderate
intermediate	lowest intertidal- upper subtidal	moderate	minor	moderate
thrombolitic	subtidal	moderate	aperiodic	moderate

laminae indicate upward growth during daylight. Tubules parallel to laminae may represent horizontal night growth or gas fenestrae along laminae contacts (Gebelein, 1969) (Figure 69).

Alternating laminae have been hypothesized to represent cyclicity, perhaps diurnal, seasonal, or annual (Gebelein, 1969). Gebelein's study of modern algal growth in Bermuda has shown that one organic-rich-sediment-rich couplet is formed in each 24 hour period. This, however, occurs only in a subtidal zone with relatively constant diurnal conditions. Stromatolites that grow in intertidal zones and mat that grows in supratidal areas are subject to variable sediment supply, nongrowth due to lack of water, and weathering and erosion (Park, 1976). Therefore, periodicity in modern algal growth in subtidal areas cannot be projected back in time to be used as a guide to growth rates for ancient algae. The alternating layers can only be used to show that there were times of mainly organic growth when the sediment supply was limited and times when there was an influx of sediment which could be trapped by the filament.

Algal mat, which today is found only on supratidal mudflats, shows less distinct laminae than the stromatolites of mounds and reefs. By uniformitarian analogy the mats were less frequently washed with water, consequently only minor amounts of sediment were introduced. Lack of wetting inhibited both the growth of the algae and the precipitation of calcium carbonate, causing laminations to be vague and tubules rare. The intervals between overwashes may have been so long that subaerial mudcracks formed on the tops of the mats (Figure 70).

Thrombolites are characterized by a disrupted or clotted appear-

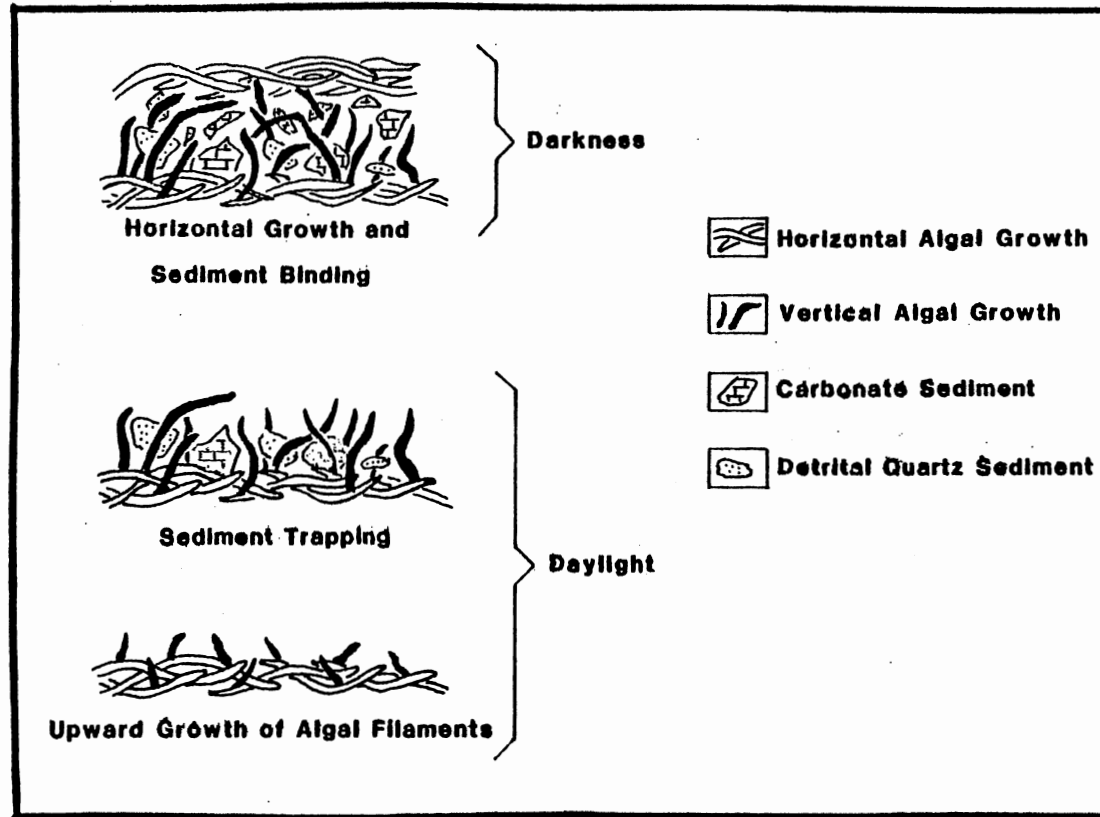


Figure 69. Diagrammatic Representation of the Cyclic Growth of Stromatolitic Laminae (Modified Slightly from Gebelein, 1969)



Figure 70. Subaerial Mudcracks Formed on an Algal Surface

ance and lack of internal laminations (Figure 16). These features resulted from irregular sediment supply, moderately turbulent water, and burrowing organisms (Pratt and James, 1982). Such conditions were most commonly found in the subtidal zone.

Increased distance from the shore limited the amount of water-borne clastic input. Very minor amounts of well-rounded quartz silt are found in the thrombolitic structures and may be attributed to aeolian sources. Sedimentation consisted primarily of calcium carbonate precipitation which occurred only when the water was relatively clear allowing photosynthesis. The soft algae may then have been disrupted by turbulent water with the change of tides or occasional storms. The mounds could probably have tolerated moderately agitated water, but violent storms would have torn the fragments from the thrombolites and redeposited them as IFC clasts.

Fossils (trace or body) of burrowing organisms are rarely found in the thrombolitic lithologies of the Formation, but some amount of disruption may have been caused by them. Pellets are intimately associated with most thrombolites indicating that some type of invertebrate, probably gastropods or trilobites, did inhabit the zone in some abundance.

A form of algal boundstone intermediate and gradational between thrombolites and stromatolites, exists (Figure 14). Such intermediate forms have vague suggestions of laminae and are not as disrupted as thrombolites. Figure 14 shows a gradational sequence from thrombolites at the bottom to stromatolites at the top. As the water gradually shallowed and became less constantly turbulent, thin, irregular laminae began to form. The water was much less murky with

sediment so that light could penetrate to the algal surfaces more regularly. During the initial stage of laminae development the algae are termed stromatolitic-thrombolites (Aitken, 1967). As the water depth continued to decrease, sediment was deposited more frequently and laminations became more prominent. This stage is known as thrombolitic-stromatolite. All stages are gradational into the next, from thrombolitic to stromatolitic with decreasing water depth.

Stromatolite and thrombolite morphologies are variable within algal reefs. By uniformitarian analogy, in the upper intertidal zone, algal mat gave way to algal mound. LLH-C stromatolites were formed as advancing and retreating tidal water established small channels eventually leading to the development of troughs between mounds. Doming was enhanced by irregularities on the initial surfaces and by gas bubbles caused by algal decomposition and respiration (Logan et al., 1964). Water turbulence in the channels was not so great as to disconnect the algae. Conditions for algal growth were more favorable on the crests; consequently, mounds developed with the greatest growth on the crests and least growth in the troughs (Figure 71). Upper intertidal flats located in bays and behind barrier bars provided the best environments for these mounds (Logan et al., 1964).

Slightly more turbulent water led to the LLH-S morphology. The mounds were spaced farther apart as channels widened and deepened. Troughs have thinner layers of algae than LLH-C stromatolites and the mounds tend to be larger.

SH-V and SH-C stromatolites are also formed in the intertidal zone. Logan et al. (1964) list six factors most important in the

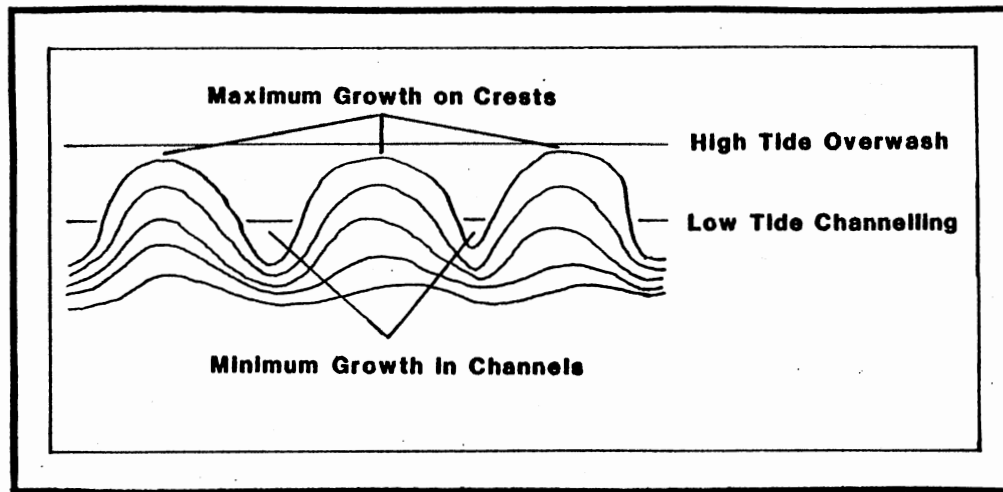


Figure 71. Diagrammatic Representation of Algal Dome Formation in the Cool Creek Formation



development of discrete domes. These are: 1) that algae formed only on tops and sides of high relief domes; 2) that rapid induration during dessication solidified the mound and caused algae to grow on the uppermost, moist areas; 3) that prolonged wetting in pools of water inhibited algal growth; 4) that scouring and abrasion in channels prohibited growth; 5) that dessication on the sides caused flaking off of algal pieces; 6) that scour due to unusual flooding caused mechanical formation of mounds.

The growth of such stromatolites began as cryptalgal encrustations usually on irregular surfaces. They may have continued to grow as discrete columnar mounds with a single vertical axis or they may have branched as rivulets formed on the irregular surfaces of the mounds. As channels shifted or were abandoned the various forms of branching developed (Figure 20). The mounds then became aggregations of small stromatolites or thrombolites separated by sediment. The interareas in thrombolite mounds of this type are normally filled with micrite and peloidal micrite. Interareas in stromatolite mounds contain more clastic material in the form of quartz sand and silt, fossil fragments, clasts, and pellets due to their proximity to the shoreline and shallower water.

The paleomorphology of a typical intertidal flat is provided by the 25 algal mounds exposed on the Oliver Syncline (Figure 12). The mounds were measured and their eccentricities calculated in order to determine if channelling could have had some effect on the shape of the mounds (Table I). The greater the eccentricity ( $e$  approaches 1) the more elliptical the mound and, therefore, the greater the possibility that channelling had some effect on shaping the mounds.

72% of the mounds show that  $e$  is greater than 0.5 indicating that channelling probably was a relatively important process in the formation of the mounds. The greater the water velocity and scouring effect on the mound, the greater the eccentricity. Lower water velocities and abrasion mean a lower eccentricity and more irregularly shaped mounds (Gebelein, 1969). The orientation of the long axis indicates the direction of flow in the channels, which, in a tidal flat, would have been bimodal.

Algal reefs were formed in the mid to lower intertidal zone in areas where there was less channelling. They are composed of columnar and branching stromatolites which form continuous "forests" of algae. Minor channelling caused branching and separation between individuals, but the water activity was not great enough to cause the formation of major channels and, consequently, mounds. Intertidal areas with little relief provided the best environments for reef formation.

Reefs cannot, of course, extend laterally indefinitely. The terminal end of a reef forms a bioherm (greater than 5 vertical feet) or a miniherm (less than 5 vertical feet). Major channels, entrances to embayments, and headlands were some of the features responsible for breaks in the reef. Lime mud with minor quartz sand and silt and IFC clasts were draped against the sides of the bioherms (Figure 18).

#### Intraformational Conglomerates

Intraformational conglomerates, a second important environmental indicator, are found as discrete beds, as infill between individual

algal members, and as channel fill. Because IFC's are a result of at least six processes, they are found associated with all other primary lithotypes in the Formation. These six processes are: 1) transgressions; 2) regressions; 3) storms, major and minor; 4) tides; 5) channels; 6) waves (Table III).

Transgressions, regressions, and major storms are the processes that were most likely to have resulted in the formation of discrete, areally extensive beds. In such beds, clast lithologies are heterogeneous including all types of micrite lithologies, algal fragments, chert pebbles, quartz sand, and minor amounts of fossil fragments (gastropods, echinoids, brachiopods, and trilobites), oolites, and pellets. Assuming (as seems likely) that the carbonate platform was of low relief, transgressions would have covered vast areas and consequently, would have eroded many variable lithologies. The relatively long period of time associated with transgressions would have led to constant reworking of clasts. Hence, pebbles deposited seaward of the shoreline would have become rounded and deposited with the elongate clasts generally flat-lying (long axis parallel to bedding) due to gentle washing and reworking. The IFC's were formed in the intertidal to upper subtidal zone and eventually buried under marine micrite as the transgression continued. Most transgressive/regressive clasts are large (up to 5 cm (2 in)); quartz sand is a common accessory particle. The abundance of quartz detritus reflects both the length of the transgressions and also the increasing proximity to the presumed source area (landward). Transgressive IFC beds are thicker than IFC beds formed by other processes.

Theoretically, regressive IFC's would be expected to be thinner

TABLE III  
DEPOSITIONAL ARRANGEMENTS OF IFC CLASTS

Process	Packing Arrangement	Zone	Turbulence	Clastic Input
transgression/ regression	flat-lying, vertical, imbricate, or random	intertidal to lower subtidal	low to moderate	high
storms	random	supratidal to subtidal	high	low to moderate
tides	flat-lying, random, imbricate	intertidal	moderate	low
channelling	imbricate, flat-lying	supratidal to subtidal	moderate	low to moderate
waves	vertical, flat-lying	intertidal	moderate	low

than transgressive IFC's and, as the seas receded, would have been subjected to other processes which altered their initial character. Though the clasts may resemble those in transgressive IFC beds, regressive IFC's would have been subsequently exposed to very shallow water and subaerial processes (desiccation). Subsequently, subaerial erosion would have destroyed the clasts and possibly have removed them entirely from the record.

Major storms (equivalent to hurricanes or typhoons) could have also formed discrete layers of IFC clasts. Though such layers may have been laterally extensive parallel to the shoreline, they were only as wide as the area covered by the zone of storm-generated destructive turbulence. Beds attributed to this mechanism are only a few centimeters thick since storms are of much shorter duration than transgressions or regressions. Because the storms cover only a limited area the clasts are more homogeneous than transgressive/regressive IFC's. Clasts are moderately rounded, but very poorly sorted and randomly packed due to the short, but violent nature of the process. Most storm-generated IFC's have a high percentage of mud matrix since the deposits were not cleanly worked over a relatively long period of time (Figure 27).

Minor storms (equivalent to daily thunderstorms) could have produced thin layers of IFC's which would have draped over pre-existing lithologies. This type of deposition is known to occur in the intertidal areas of most modern marine algal environments (Logan, 1961; Logan et al., 1964; Shinn, 1983). Clasts generated in this manner would have consisted primarily of local material and would have been randomly packed. Many minor storm IFC's may have been very quickly

removed from the record by subaerial exposure or the next day's thunderstorm. The clasts of IFC's attributed to this mechanism are very poorly sorted with sizes ranging up to 5 cm (2 in). Accessory particles such as detrital quartz and ooids are less common than in transgressive/regressive IFC's or even major storms. Micrite matrix forms a large part of the lithology as it does in major storm deposits.

The repetitive short term processes of tides, channelling, and waves probably account for the majority of the IFC's in the Formation (Figure 72). The beds assumed to have been formed in this fashion are not laterally extensive nor more than 0.3 m (1 ft) thick, but they form the most lasting record of IFC's. The movement of tides across the intertidal zone picked up and redeposited pieces of lithologies that had dried and loosened during low tide exposure. Tidal channels may have transported the clasts away from the immediate source area, but many clasts were deposited very close to their sources.

Tides and tidal channels later deposited the clasts in random, imbricate, or flat lying patterns depending on the supply, current velocity, and shape of the clasts. Most clasts fell into algal intermember or intermound areas although a small percentage became trapped in the algal layers. Clasts range in size from 1 mm to 2 cm (0.04 in to 0.8 in) in length; accessory particles are common only if a source area was proximal. Invertebrate fossils (mainly gastropods) are the most common nonclast detritus.

Major channels distributed IFC clasts away from their source area. Some terrigenous detritus, especially quartz sand was mixed in as an

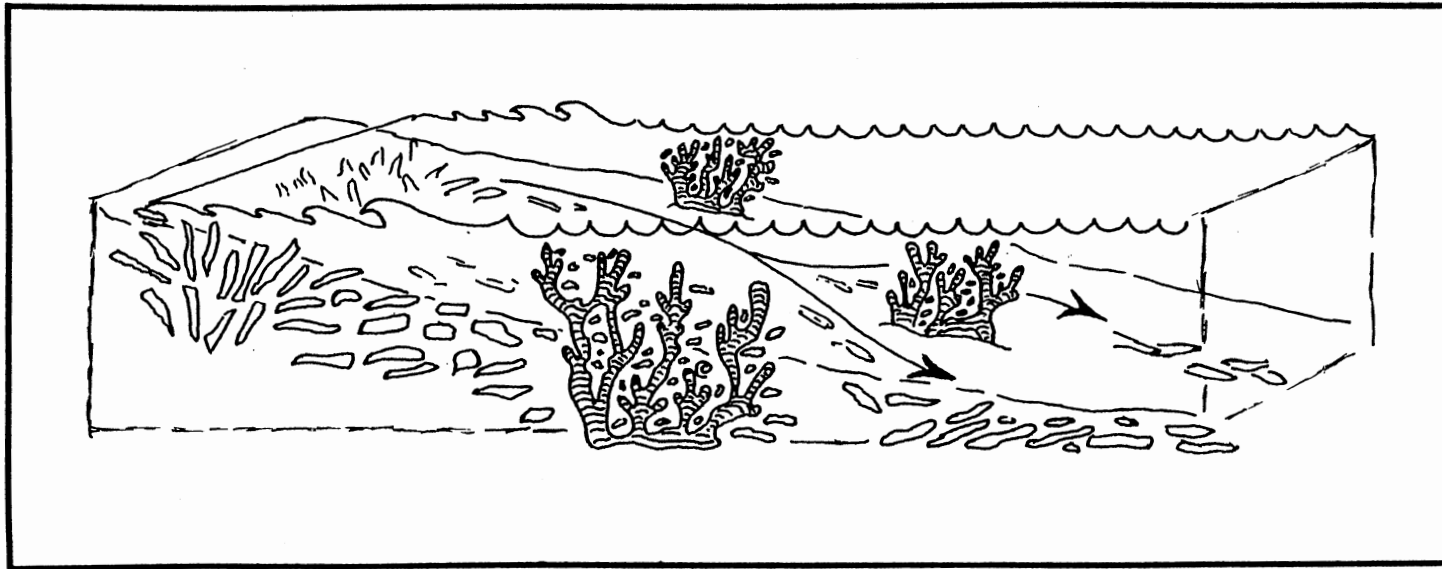


Figure 72. Interpretation of Environmental Relationship between IFC Morphology and Water Turbulence as Developed in the Cool Creek Formation

accessory that presumably decreased in amount with increasing distance from the shore. Clasts often show imbrication though they are commonly aligned with their long axes parallel to bedding.

Vertically stacked clasts were produced by moderate energy waves along shorelines (Sanderson and Donovan, 1974). Blade- or disc-shaped clasts were wedged into depressions producing fan-shaped, vertically-oriented, relatively stable deposits (Figure 30). Unlike vertically packed siliciclastic deposits, IFC clasts were deposited with a relatively dirty matrix. Small bits of detritus (fossil fragments, quartz sand and silt, ooids) were washed into the areas between clasts and quickly encased in micrite. The framework clasts of such deposits are relatively large (up to 6 cm (3 in)).

#### Other Environmental Indicators

##### Introduction

The algal boundstones and IFC's are the most definitive environmental indicators in the Cool Creek Formation. As established in the previous sections, the environment ranged from shallow subtidal to supratidal. Conditions were generally stable although occasional major events occurred. This is substantiated by the nature of the remaining lithotypes.

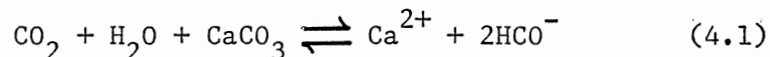
##### Micrite

Micrite can be formed in a number of environments and is, therefore, in itself not a diagnostic indicator of a tropical, shallow marine environment. However, its presence in large amounts in the Cool Creek Formation, plus its associated sedimentary structures and



detrital inclusions suggest that the lime mud was deposited in such an environment.

Calcium carbonate precipitation is controlled by the partial pressure of carbon dioxide in the following net reaction:



Several factors can lead to the removal of carbon dioxide from the aqueous system and the consequent precipitation of calcium carbonate (Blatt, 1982). These can be used as valid environmental indicators for the Cool Creek Formation.

1) Previous work has shown that Southwestern Oklahoma was located at approximately 25° south latitude during the early Ordovician (Habicht, 1982). Warm water temperatures at such latitudes would have been conducive to the release of carbon dioxide as gases are less soluble in warm waters.

2) Agitated water would have caused carbon dioxide to be released. Agitated waters were common from the shallow subtidal zone to the upper intertidal zone favoring carbonate precipitation in the region.

3) Warm water and subsequent evaporation in a semi-arid to arid climate led to an increase in salinity, also a condition leading to the release of carbon dioxide and precipitation of calcium carbonate.

4) Biotic activity involved the release of carbon dioxide due to photosynthesis. Calcium carbonate would have been precipitated during daylight hours when the algal activity was the greatest (Figure 69).

Laminated dark grey and light grey lime muds could reflect seasonal changes in shallow pools and lagoons (Pettijohn, 1975).

Though seasonal temperature changes were probably not great, the temperature may have dropped enough in the "winter" to cause a certain amount of algae to die and form the organic rich dark laminations. Calcium carbonate precipitation predominated during the summer creating the lighter grey, usually thicker layers. The very shallow conditions of some ponds and lagoons coupled with the inclusion of iron may have led to the dark pink and light pink laminations found in some micrite units. Evaporation of the water could have led to subaerial exposures and fixing of the iron in the ferric state.

Other indicators of the shallow water lagoonal environment are ripple marks, small scale cross-bedding, bioturbation, pellets, and subaqueous shrinkage cracks. The calm lagoonal waters constituted a restricted environment generally hostile to stromatolite growth. Depending on the amount of fresh water input from the continent (as surface flow and rainfall), the lagoonal waters could have contained high concentrations of salts, thereby prohibiting any biota, (including stromatolites) or the waters could have been freshened, thereby supporting a somewhat restricted faunal assemblage tolerant of brackish water (Leeder, 1982). The invertebrates in fresher water would have occupied the niche otherwise utilized by algae, and, in fact, would have fed on any algae that was present. Although body fossils are rarely found, pelleted micrites with some bioturbation are common throughout the Formation (Figures 22 and 39).

Subaqueous shrinkage cracks are associated with calm water such as would be found in a lagoonal system (Donovan and Foster, 1972). An extended period of evaporation or the migration of a channel that had been providing fresh water to the lagoon could have raised the

salt content of the brine, thereby causing the mud on the floor of the lagoon to crack (Figure 23). The cracks were subsequently filled in by sediment, compacted, and preserved. The infill was often quartz silt or fine sand probably of an aeolian origin.

### Oolitic Lithologies

Oolitic micrites were formed in agitated, comparatively more saline, shallow marine waters. Oolitic shoals were built in areas of strong tidal currents or deposited as beaches (Leeder, 1982). The thick oomicrites in the Formation (up to 10 m (30 ft)) generally contain unbroken ooids indicating tangential crystalline growth at the time of formation, and, hence, are better preserved (Figure 33). Some of the oomicrites contain no other detritus after the initial influx utilized as nuclei. Other units contain clastic debris indicating that intermittent periods of optimum oolitic growth alternated with periods of clastic input under conditions not suitable for the formation of oolites (Figure 33). Oolitic layers were also occasionally reworked and deposited as oolitic sandstones.

Some layers of revitalized ooids occur indicating a short term cessation of agitated conditions followed by the renewal of the high energy environment. Unbroken ooids were utilized as nuclei during the revitalization. This is evidenced by the original ooid showing initial regular concentric rings and later offset rings (Figure 35).

### Quartz Sand Lithologies

Quartz sands form an important lithotype in the Formation, indicating that a mechanism existed that was capable of moving sand-

and silt-sized grains from a terrigenous source into the shallow marine environment. Though the source for the quartz sand is not definitely known it is hypothesized that two cratonic regions of low relief may have existed, one to the northwest of Oklahoma, another to the southwest (Reading, 1980) (Figure 73). From these areas broad meandering rivers could have moved large quantities of terrigenous detritus, eventually depositing their loads in the vast tidal flats of the Early Ordovician seas. Some areal variability did occur as illustrated by the differences in lithology between the Cool Creek Formation and the Roubidoux Formation of Northeastern Oklahoma and Missouri (Figure 74). The Roubidoux source area may have been nearer to a quartz sand source as that Formation contains considerably more sand than the Cool Creek Formation (McCracken, 1955).

Deposition of the discrete quartz sand units occurred in broad sheets across tidal flats or in channels meandering across the flats accumulating to thicknesses up 2 m (6 ft). Both morphologies show small and medium scale trough cross-bedding, parallel laminations, fining upward sequences (normal grading), and coarsening upward sequences (reverse grading). Small and medium scale trough cross-sets were formed in the lower flow regime (Leeder, 1982), again indicating the relative lack of relief of the continental source area. The streams moved sluggishly across the tidal flats depositing their loads in sinuous channels that migrated across algal mat and between algal mounds. In relatively flat tidal zones that were uncut by stream channels sheet sands were deposited. These sheet sands were persistent layers that were usually parallel laminated. Both channels and beds exhibit fining upward sequences and coarsening upward se-

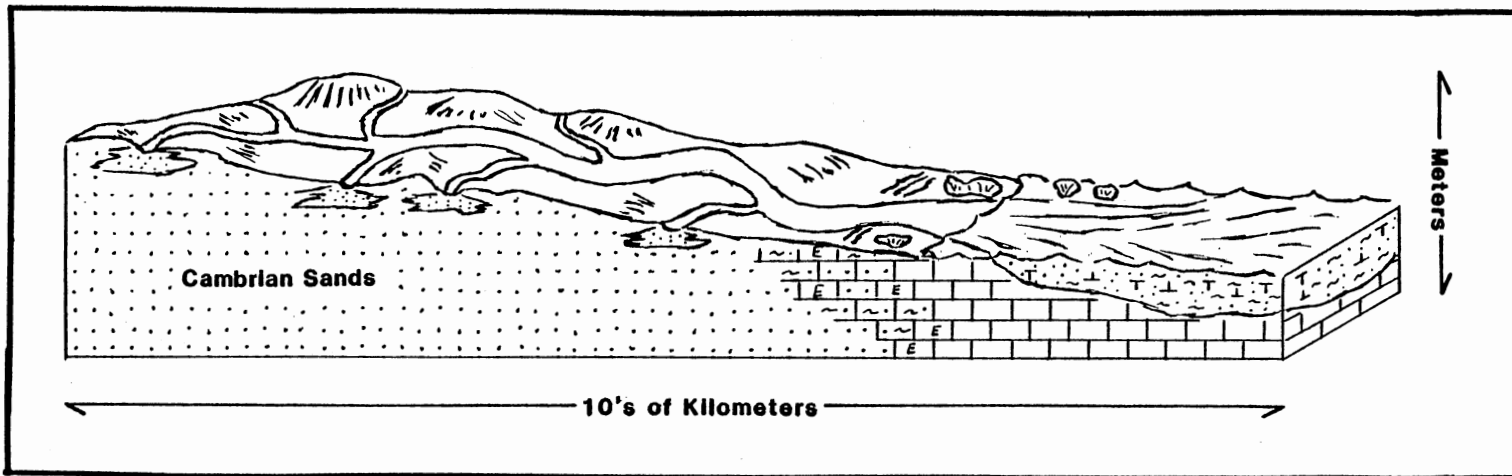


Figure 73. Block Diagram Illustrating the Transport of Quartz Sands from the Continent to the Shallow Marine Environment during the Deposition of Cool Creek Sediments

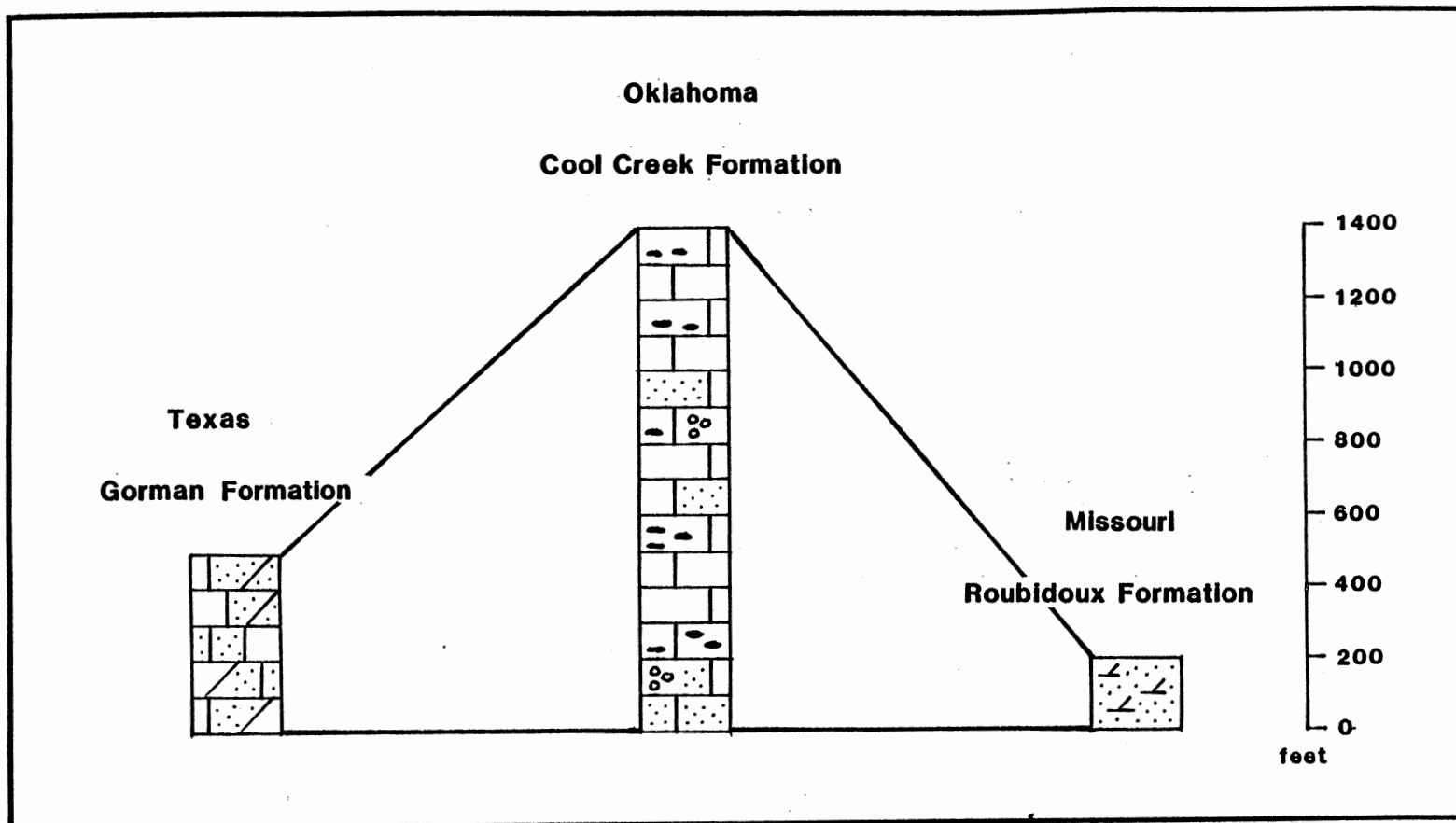


Figure 74. Stratigraphic Correlation of the Time Equivalent Cool Creek, Gorman, and Roubidoux Formations. Data for Gorman Formation Derived from Loucks and Anderson, 1980; Data for Roubidoux Formation Derived from McCracken, 1955

quences reflecting the variable rate of flow of the streams (Reading, 1980). Fining upward sequences were deposited as the flow power decreased across the flat or as the channel migrated laterally creating a point bar or filling in a channel. Coarsening upward sequences were deposited as the flow power increased across the flat due to a shallowing along the shoreline or progradation of the stream channel (Reading, 1980).

Once transported from the source area to the site of deposition, the quartz sands may have been subjected to reworking by local processes. Daily tides would have rounded and sorted the grains. Some grains falling into agitated waters became the nuclei of ooids; others were washed into cross-bedded sandy shoals. Distally from the shore the overall size of the sand grains decreased and the fine sands and silts were incorporated into lime muds (Tucker, 1981). Very fine quartz sands and silts were also trapped in the algal mat and stromatolitic laminae.

Most of the medium to coarse grained quartz sand grains were initially deposited by water, while the majority of the finer sands and silts were probably deposited by aeolian processes. Reworked quartz grains deposited on the tidal flats would have been periodically subjected to subaerial drying and wind erosion. Some of the grains may have been blown into algal laminae and trapped. Most of the quartz grains seen in thin section are well rounded, but this criterion can be applied to reworked water-lain grains as well, particularly in view of the mineralogical maturity of the sands. Consequently, no positive identification of the origin can be made.

The most prominent of the quartz sand units marks the base of

the Cool Creek Formation (the Thatcher Member). The bed varies from 60 cm to 2 m (2 to 6 ft) in thickness and is persistent throughout the Slick Hills and the Arbuckle Mountains. Oomicrite and minor IFC's are associated with the quartz sands. The uppermost 10 m (30 ft) of the underlying McKenzie Hill Formation consists of quartz silts and fine sands in carbonate matrix. These quartz sands grade upward into the medium to coarse grained quartz sands of the Cool Creek Formation thus exhibiting a coarsening upward sequence (Figure 75). The sands contain small and medium scale cross-bedding and parallel laminations. The homogeneous character of the Thatcher Member sands suggests that a transgression was not the cause of the influx of quartz sand. It is more likely that a gradual uplift of the surrounding continental area led to an increase in the amount of quartz sand introduced to the area. The coarsening upward sequence from the McKenzie Hill Formation to the Cool Creek Formation could have resulted as the tidal flat prograded seaward. The continental relief was not great enough to create deltas, per se; instead, vast tidal sheets and coalescing channels gradually built up the quartz sand sequences. With cessation of the uplift the tidal flat stabilized, water turbulence slowed, and algal colonies were established. Other quartz sand beds within the Formation may reflect continued continental uplift, but none is as extensive as the basal quartz sand.

#### Dolomite and Vanished Evaporites

Pseudomorphed evaporites provide an important environmental indicator in the Cool Creek Formation. Present sabkha environments exist only in hot, arid climates with evaporation that exceeds pre-



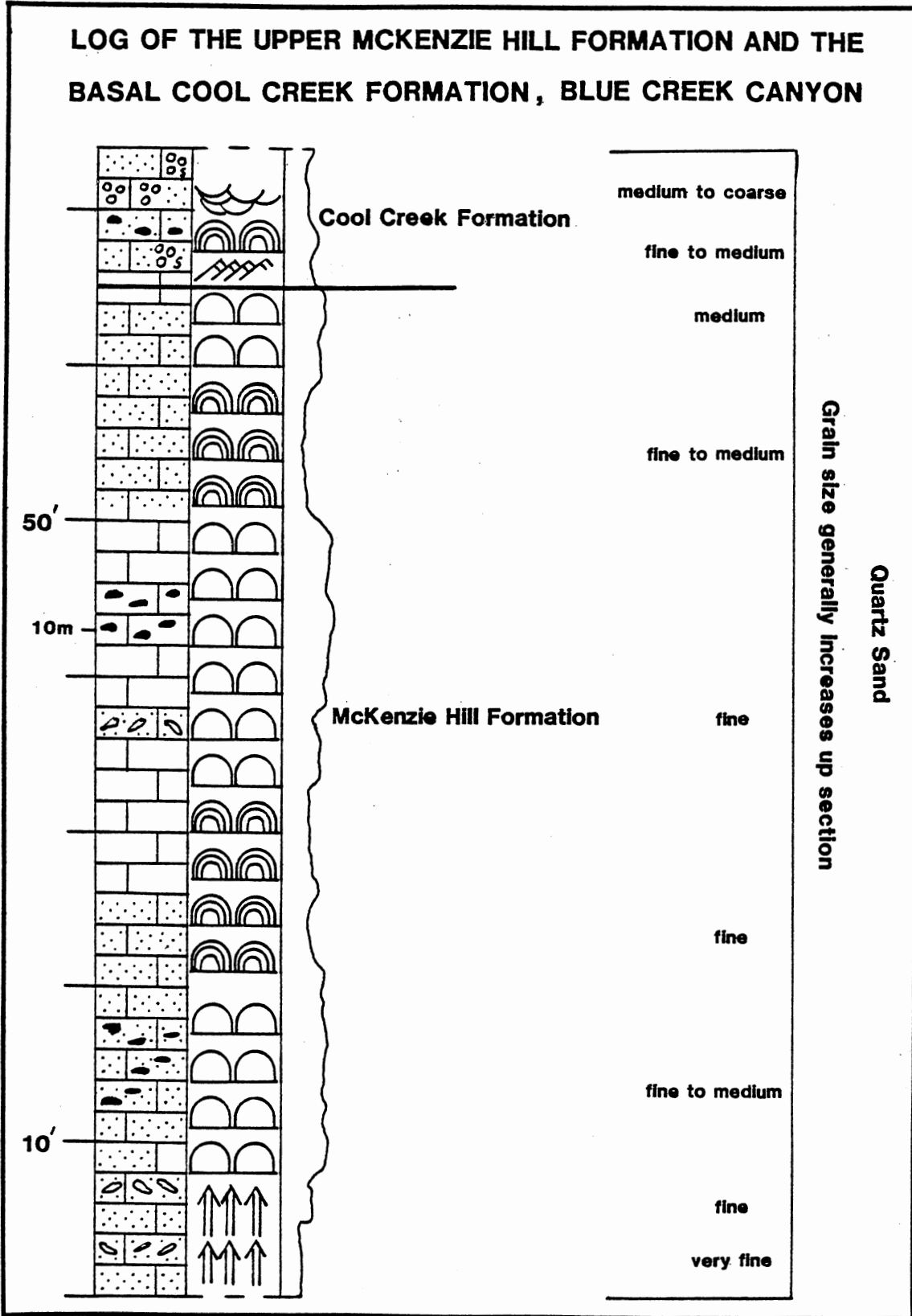


Figure 75. Log of the McKenzie Hill Formation-Cool Creek Formation Contact Showing Increase in Grain Size Up Section

precipitation and runoff. On the sabkha of Khor al Bazam in the Persian Gulf excessive temperatures (up to 60°C (140°F)) with very little precipitation lead to very high salinities (chlorinity up to 165‰) (Bathurst, 1975). Gypsum and aragonite are formed as the brine becomes supersaturated with respect to  $\text{SO}_4^{--}$  and  $\text{Cl}^-$  thereby removing the  $\text{Ca}^{2+}$  cation from the system and increasing the  $\text{Mg}^{2+}/\text{Ca}^{2+}$  ratio. Within the top few centimeters dolomite is formed as the high  $\text{Mg}^{2+}/\text{Ca}^{2+}$  ratio in the pore water exceeds the  $\text{Mg}^{2+}$  barrier (with respect to the formation of dolomite), allowing the replacement of  $\text{Ca}^{2+}$  ions with  $\text{Mg}^{2+}$  ions in the aragonite lattice.

Some sabkhas of the Persian Gulf type appear to have existed at the time of Cool Creek deposition (Figure 60). Quartz-rich sandy dolomites alternate with pseudomorphed anhydrite layers and "cauliflower" nodules in a manner similar to the Abu Dhabi sequence (Leeder, 1982) (Figure 60). Penecontemporaneous dolomitization destroyed any original algal mat texture that may have existed in the sabkha; however, in some areas salt pseudomorphs have been preserved by early silicification of algal mat. Aperiodic events such as storms may have covered the mat with thin layers of sediment (Leeder, 1982). With subsequent drying of the sediment and evaporation of pore waters, the sulphates grew on the tops of the algae.

The high solubility of the evaporites led to the formation of another lithology in the Formation---collapse breccias. After burial of the evaporite layers, circulating ground water dissolved the salts leading to the collapse of the overlying sediments. Minor karst topography was formed in several units of the Formation, but they are especially well exposed at the Turner Falls section in the

Arbuckle Mountains (Figure 32). Relatively large caves (up to 2 m by 1 m (6 ft by 3 ft)) and smaller cavities (10 cm by 15 cm (4 in by 6 in)) were filled with micrite pebbles, cobbles, and boulders, and quartz sand from the overlying units (Figure 31). In the Slick Hills, some collapse breccias also contain chert pebbles attesting to the early silicification of some of the overlying units.

### Bedded Chert

Inorganically precipitated chert is very uncommon in the Formation, but at least one distinct horizon is known to exist. Microcrystalline chert is interlayered with calcite in a bed that varies from 50 mm to 150 mm (2 in to 6 in) in thickness (Figure 47). The chert and calcite were probably deposited in a lagoonal setting resembling the modern Coorong Lagoon of Southern Australia (Peterson and von der Borch, 1965)

The interlayering of the chert and calcite may have resulted from seasonal changes in pH (Peterson and von der Borch, 1965). Algal photosynthesis could have raised the pH of the lagoon above 9 thereby dissolving detrital quartz sand, the probable source of the silica, while at the same time calcium carbonate would have been precipitated (Blatt, 1982) (Figure 76). During drier seasons that were unfavorable to algal growth, the pH would have been lowered, silica deposited amidst decaying algae, and calcium carbonate dissolved.

The calcium carbonate and chert layers have gradational contacts showing the gradual seasonal change when calcium carbonate and silica were precipitated almost simultaneously (pH = 7 to 9).

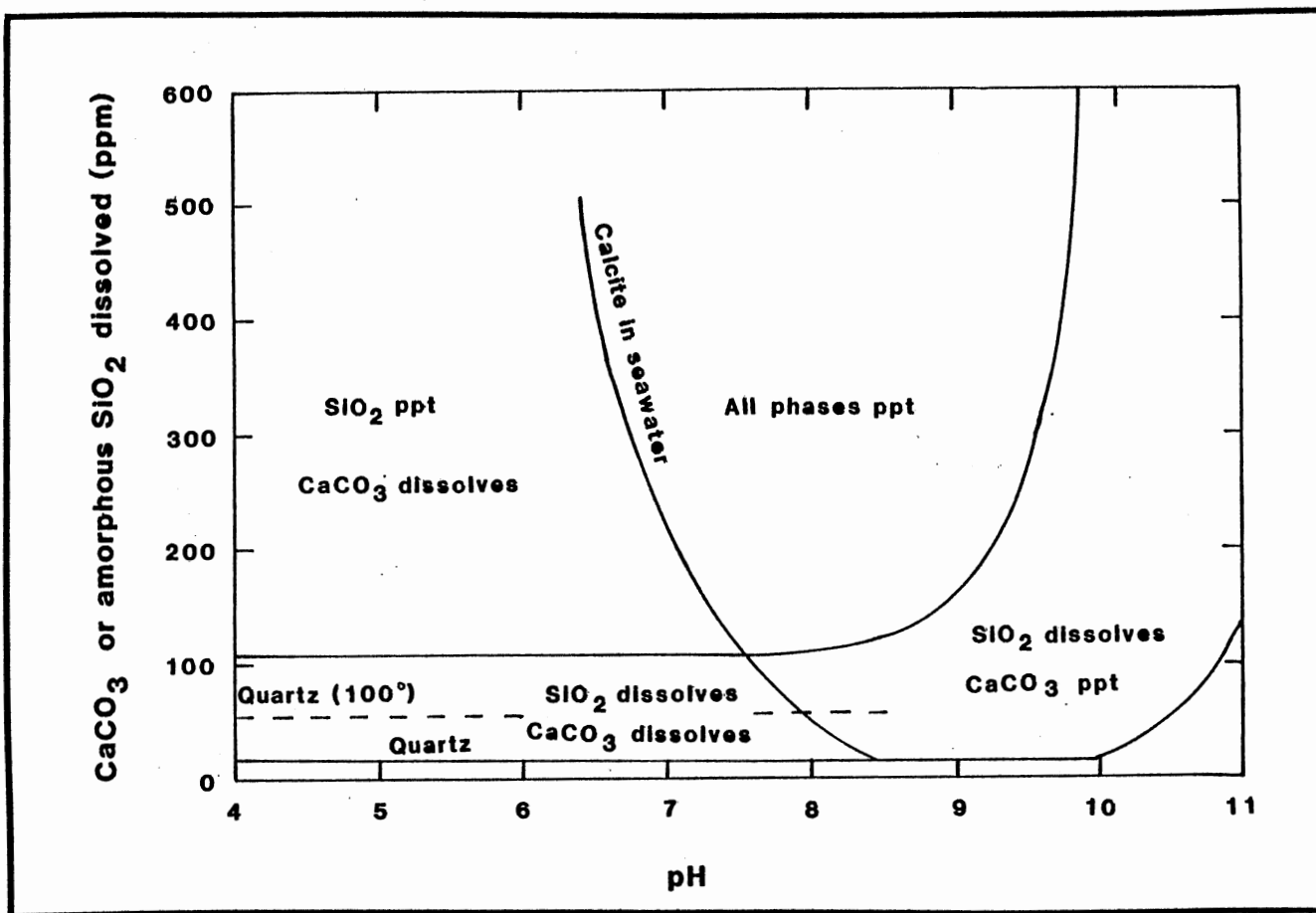


Figure 76. Phase Diagram Showing the Relationships between Calcium Carbonate or Silica Concentration Versus pH. From H. Blatt, 1982, Sedimentary Petrology

From thin section study, calcium carbonate appears to have been the primary precipitate, not dolomite or magnesite as is the case in the present Coorong Lagoon. No relict dolomite rhombohedrons are visible although if dolomite had been precipitated it would have been in the form of dolomicrite. Though the layers are slightly distorted, this is probably due to penecontemporaneous deformation rather than as a result of the  $\text{Ca}^{2+}$  cation (atomic radius =  $0.99\text{\AA}$ ) replacing the  $\text{Mg}^{2+}$  cation (atomic radius =  $0.66\text{\AA}$ ). A sufficient amount of magnesium may not have been available to the system in order to precipitate dolomite primarily or penecontemporaneously.

#### Overview of the Cool Creek Environment

##### Process Rates: Past versus Present

The combined lithologies of the Cool Creek Formation can be used as reliable indicators to reconstruct the general environment of the Slick Hills region during the Early Ordovician. However, the lithologies now present do not represent a complete and accurate representation of every event that occurred during that time. How much has been lost from the record cannot be determined, but based on processes that are currently operating, qualitative descriptions of what may have happened can be hypothesized. Once again, processes that are occurring in the present that are utilized to describe events of the past must be used with caution. Not only did processes occurring during the Ordovician probably differ in rate from those of the present, but rates of processes occurring simultaneously varied greatly. As a modern example, the rate of accretion of stromatolites in Bermuda is estimated to be about 360 mm/year

(14 in/year) (Gebelein, 1976), whereas the rate of accretion of stromatolites along the Trucial Coast is from 2 mm/year to 10 mm/year (0.08 in/year to 0.40 in/year) (Park, 1977). These differences in growth result from differences in sediment supply, periodicity of wetting, and frequency of destructive processes. These three factors vary considerably not only from location to location in the present, but have undoubtedly changed from Ordovician times to the present.

#### Preservation versus Destruction

Modern stromatolites and thrombolites occupy only small areas protected from the open ocean and predators. By comparison, conditions in large areas of the epeiric seas during the Ordovician were very favorable for algal growth. Vast shallow shelves covered much of the area that is now Oklahoma. Though clastic sediment input was limited, carbonate production was high causing algae to grow at a reasonably fast rate. However, based on estimates of the percentage of algal lithology in the Formation, the growth rate appears to have been only about 0.07 mm/year (.003 in/year) (Basin Analysis, 1982). Perhaps the accretion was this slow; more likely, compaction, erosion, and nondeposition altered the record of events.

Early burial of the algae would have led to compaction of the laminae. Although the stromatolites would have been preserved qualitatively, the total quantitative growth record would not be accurately represented. Complete compaction before cementation would have eliminated all pore spaces; partial cementation, probably more often the case, would have reduced the size of the stromatolites by some intermediate value between 0% and 100%.

Rapid lithification of algae and surrounding sediments is evident from the high percentage of IFC's in the Formation. Early lithification not only tended to preserve many of the sediments, but also helped to record erosive events. Nearly 25% of the Formation is composed of IFC clasts showing that destructive events were common. The amount of sediment transported out of the area may have been considerable, but of course, cannot be determined.

Subaerial exposure leading to mudcracks and the growth of evaporites in sabkhas contributed to the IFC clast supply. As mounds and mats were exposed during low tide the surfaces became dessicated, fragments flaked off, and formed clasts (Figure 70). The growth of evaporites just under the surface of algal mat tended to separate layers of mat exposing them to dessication and removal by wind or water. This has been recorded on the Trucial Coast and is considered to be a major process by which mat, especially crinkle mat, is destroyed and removed (Park, 1977).

Nondepositional events undoubtedly occurred during the Early Ordovician, but the frequency and extent of such events is not known. However, the cumulative effect of short periods of nondeposition and erosion may have led to large gaps in the geologic history of the area.

#### Subsidence

The remarkable thickness of the predominantly algal lithologies of the Arbuckle Group may, at first, appear to be difficult to explain especially when compared to the relatively thin equivalent units in Texas and Missouri (Figure 74). This can be explained by the isostatic adjustment of the crust to accomodate loading (Matthews, 1974).

The Anadarko Basin, on the edge of which lie the Slick Hills, underwent such isostatic subsidence throughout much of the Paleozoic Era (Basin Analysis, 1982) (Appendix B). During Arbuckle time alone nearly 1680 m (5500 ft) of sediments were accumulated in the aulacogen. As the sediments were deposited in the shallow water their weight caused the basin to subside in order to maintain isostatic balance. Compaction and dewatering served to increase the mass of the overburden and accelerate the subsidence.

The basin was formed by the failure of an arm of a triple junction rift zone (Basin Analysis, 1982) (Figure 77). Marine waters invaded the shallow basin, a near ideal setting for the initiation of isostatic subsidence. The Gorman and Roubidoux Formations were deposited outside of the aulacogen on the stable craton causing total thicknesses in these areas to be much less than in the basin. Erosive forces on the craton probably played a much more important role than in the basin, thereby reducing the overburden in any one region.

The subsidence rate would not have been constant; periods of acceleration, deceleration, and steady state must have existed. This variable subsidence rate was probably the cause of the many transgressive and regressive units seen in the Formation. When subsidence rates were greater than sedimentation rates marine waters deepened and transgressive sequences were deposited. If subsidence rates decelerated, sediment would build up leading to a shoaling upwards sequence. Subsequently, the weight of the sediments would have caused another isostatic shift initiating a transgressive sequence.

Occasionally, these transgressive and regressive shifts may have



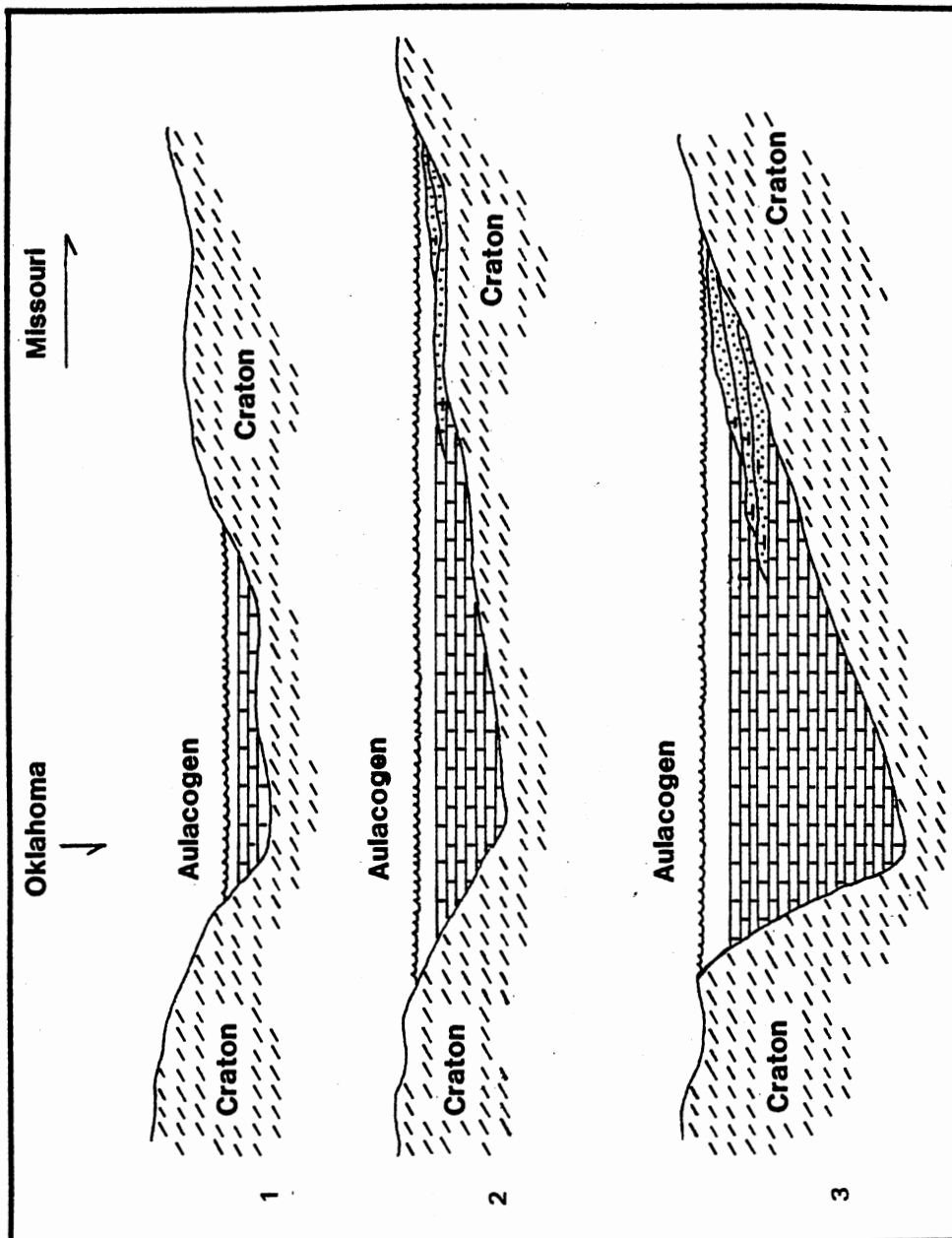


Figure 77. Diagrammatic Representation of the Theorized Subsidence of the Anadarko Basin: (1) Initial Rifting; (2) Subsidence Begins; (3) Maximum Subsidence

been relatively rapid and some stages of normal facies changes may have been skipped. One such sudden shift may account for the vertical facies change illustrated in Figure 9. Thrombolite mounds formed in the subtidal zone are cleanly overlain by LLH-C stromatolites, generally formed in the upper intertidal zone. A sudden shallowing (rapid evaporation with no subsidence? Slight tectonic uplift?) allowed LLH-C stromatolites to form directly on top of thrombolites. This occurrence appears to be a regional event as the unit can be traced laterally for several kilometers.

Sudden downshifts would have allowed rapid inundation of shallow-water facies. Some micrite layers overlying stromatolite mounds may have been the result of rapid deepening of water.

Normal sequences are also found in the Formation as illustrated in Figure 14. A shallowing upward sequence was formed as thrombolitic texture gave way to a partially laminated intermediate texture, then to a stromatolitic texture. Gradational changes from algal mat to digitate stromatolites illustrate gradual deepening of waters.

Steady state events were probably least common as the earth is, by nature, a dynamic entity. Some great thicknesses of algal mound do exist without apparent interruption, but these probably represent only a few tens of years and a period in which the preservation potential of the mounds was very high.

### Cycles

Cycles, as defined by Wilson (1975), do not appear to be present in the Formation. Although there are only a limited number of lith-

ologies, they are not repeated in the rhythmic patterns such as those seen in the Carboniferous cyclothems (true cycle: ABCBA; hemicycle: ABCABC).

There are several processes responsible for the production of cycles. Although some of them were operating during the Early Ordovician, other parameters cancelled the effects necessary to create cyclic deposits. The mechanism most widely recognized as a primary factor in the production of cycles is the transgressive/regressive couplet. As discussed previously, these two processes are accepted as having occurred frequently, but not rhythmically. The two primary causes of transgressive/regressive cycles are sea level changes due to ice cap fluctuation and sea level change due to major tectonic plate movements. It has been shown (Habicht, 1979) that glacial episodes were not major events during the Early Ordovician Period. This early part of the period was also relatively quiet with respect to plate movement (Windley, 1979). It was not until the Middle Ordovician that major plate shifting occurred in North America during the Taconic Orogenic Phase.

Periodic subsidence and stabilization of basins also cause transgressive/regressive cycles. Although this mechanism was probably responsible for the transgressions and regressions in the Cool Creek Formation, they appear to have been aperiodic. This, coupled with the great areal extent of the shallow marine seas, probably prohibited true cycles from forming. These intracratonic oceans were so shallow that there was very little change in the type of sediment that was deposited. No moderately deep or very deep water facies are found in any significant amount in any of the Arbuckle Group Formations,

nor, for that matter, in any of the Formations in the Slick Hills (Figure 78). Only a few very thin shales (a few centimeters thick) are found sporadically in the basin Formations.

The same flat ocean floors were mirrored in the low relief of the continent. Terrigenous input was usually minimal unless the depositional area was close to the land source. Uplifts and tectonism on the North American continent were not a factor during this time, and hence, could not supply vast quantities of material to the system (Windley, 1979).

One other parameter has been responsible for cyclic deposition of ancient lithologies. This is a periodic fluctuation in climate. In other periods the climate changed episodically over several hundred or thousand years affecting either terrigenous source areas or the marine depositional areas such that sedimentation patterns were cyclic. During the Early Ordovician the hot, dry climate appears to have remained nearly constant (Habicht, 1979). Even changes between seasons were negligible. Very short term seasonal changes occurred such as those seen in the banded chert, but the conditions were not permanent and caused only minor perturbations in the record.

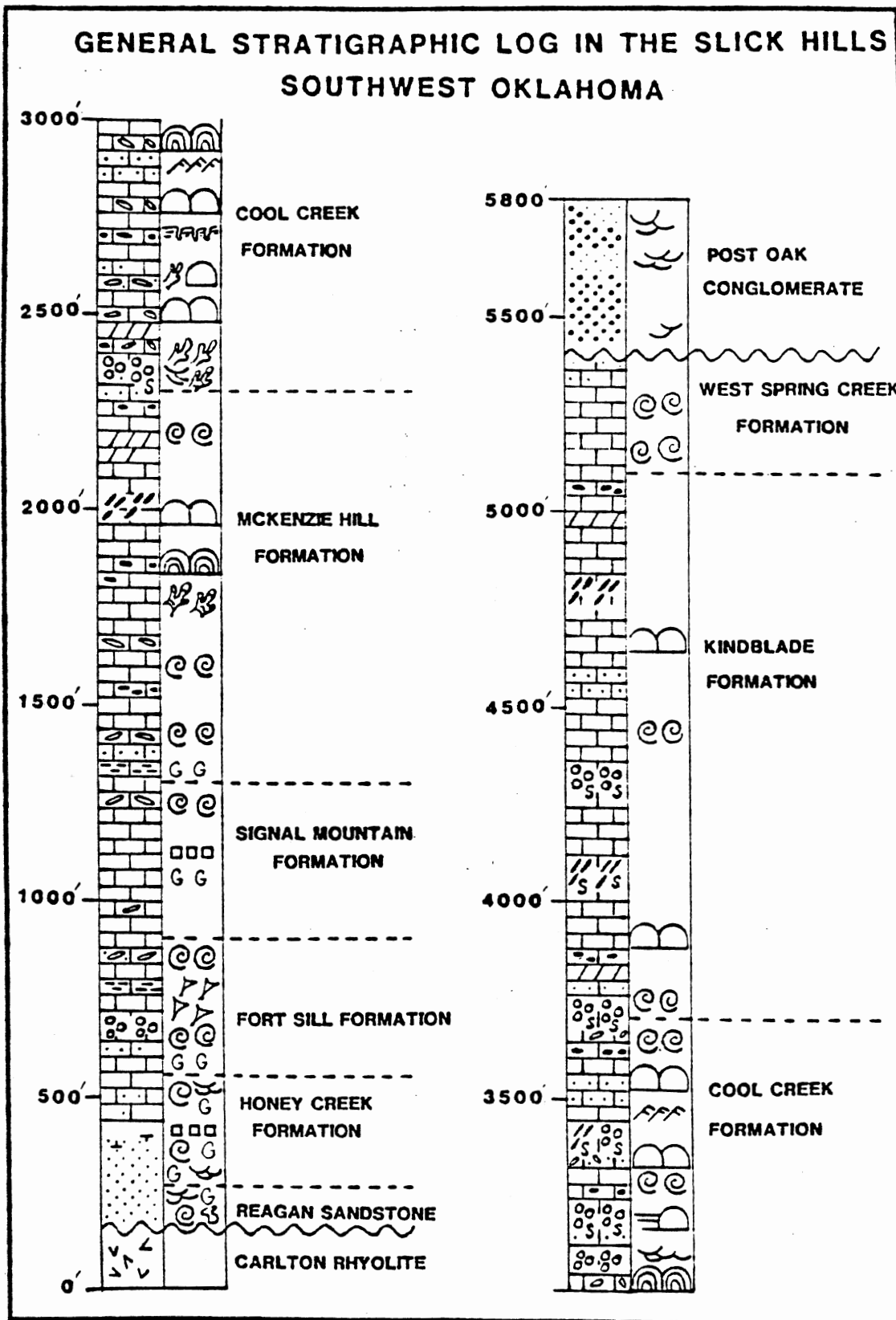


Figure 78. General Stratigraphic Log of the Formations Outcropping in the Slick Hills

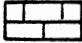
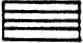
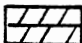
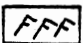
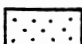

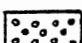
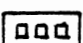

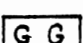
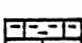

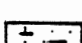

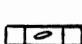
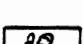
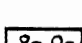
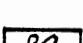
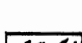
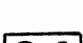

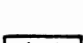
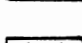
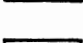
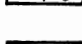
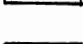
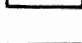
<b>EXPLANATION</b>			
	<b>Limestone</b>		<b>Parallel lamination</b>
	<b>Dolomite</b>		<b>Small scale cross-bedding</b>
	<b>Sandstone</b>		<b>Medium scale cross-bedding</b>
	<b>Conglomerate</b>		<b>Iron oxide pseudomorphs</b>
	<b>Sandy limestone</b>		<b>Glauconite</b>
	<b>Shaley limestone</b>		<b>Algal mounds</b>
	<b>Limy sandstone</b>		<b>Algal mat</b>
	<b>Intraformational conglomerate</b>		<b>Stromatolites</b>
	<b>Oolitic limestone</b>		<b>Thrombolites</b>
	<b>Peloidal limestone</b>		<b>Fossilized invertebrates</b>
	<b>Oolitic chert</b>		<b>Sponge remains</b>
	<b>Peloidal chert</b>		<b>Horizontal burrows</b>
	<b>Chert nodules</b>		<b>Bioturbation</b>
	<b>Rhyolite</b>		

Figure 78. Continued

## CHAPTER V

### DIAGENESIS OF THE COOL CREEK FORMATION

#### Introduction

Relatively few diagenetic processes have altered the original character of the Cool Creek sediments. The complexity of the diagenetic history is a result of the manner in which these processes took place. No single alteration can be taken as a separate event. Each process can be discussed separately but the diagenetic history can only be unraveled by the realization that all are inextricably intertwined.

#### Physical Diagenesis

The diagenetic history of the Formation has been both physical and chemical. Compaction comprises the primary physical change after deposition. Early compaction tended to reduce the pore space and extract water; burial compaction further decreased pore space, increased expulsion of pore water, and deformed and rotated some grains (Figures 36 and 42). Compaction and burial of algae reduced the thickness of colonies by closing of some fenestrae and tubules before they could be secondarily filled. Later tectonic stresses added to deformation of some lithologies.

## Chemical Diagenesis

The chemical diagenesis of the Formation has been more complicated than the physical diagenesis although only a limited number of processes have occurred. The complications arise as a result of the interaction between these processes. The four main chemical diagenetic processes were: 1) dissolution; 2) secondary precipitation; 3) replacement; 4) recrystallization.

### Dissolution and Reprecipitation

The two major secondary products in the Formation are calcite and silica. Calcite occurs principally as a cement (pore-filling and syntaxial), silica as a cement (pore-filling and syntaxial) and a replacement product. The source of the calcite presents no problem as the bulk of the primary lithologies are calcite. The main source of the silica appears to have been quartz grains. Very few siliceous sponge fragments have been found in the field or in thin section, but quartz sand was abundant throughout (Figure 79). If either the source of the silica was limited or the water chemistry tended to be favorable to the solid phase of silica, the secondary precipitation of silica was confined to syntaxial quartz overgrowths. In order to act as a replacement product or as a major pore-filling cement, a large quantity of source silica had to have been available (Figure 80). Where quartz sand was sparse, for example, in the lower intertidal or subtidal zones, dissolution and subsequent reprecipitation occurred as syntaxial overgrowths. Where quartz sand was more available, as, for example, on some supratidal flats or in tidal channels, silica cement occurred as syntaxial overgrowths and pore-filling



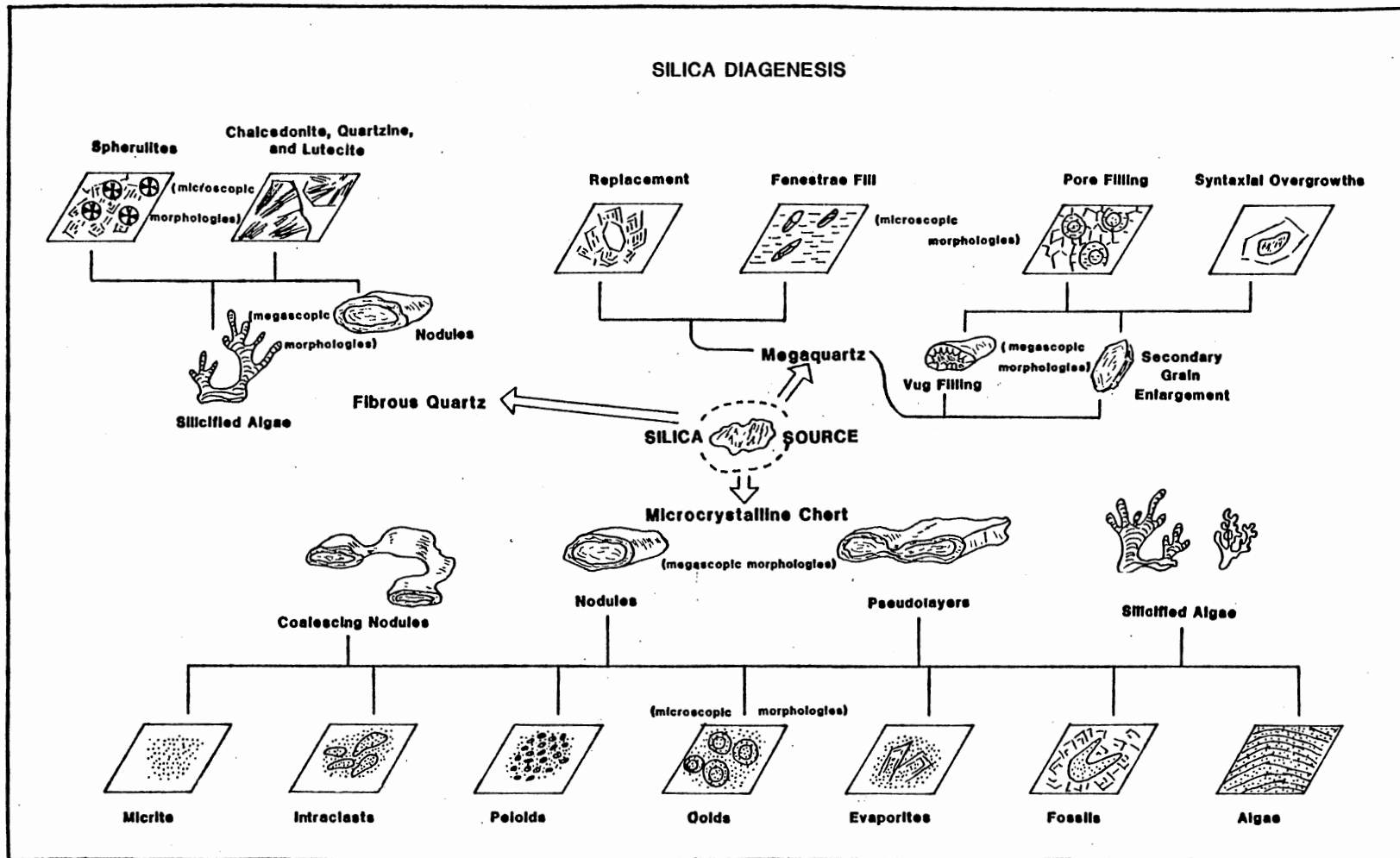


Figure 79. Summary of Silica Diagenesis in the Cool Creek Formation

Silica Concentration	Morphology	Mineralogic Type
very high	amorphous  minute, equant	<div style="display: flex; justify-content: space-between;"> <span style="writing-mode: vertical-rl; transform: rotate(180deg);">polymerized</span> <div style="text-align: center;"> <p>opal</p> <p>microcrystalline quartz</p> </div> <span style="writing-mode: vertical-rl; transform: rotate(180deg);">ionized</span> </div>
high	fibrous	<div style="display: flex; justify-content: space-between;"> <div style="text-align: center;"> <p>chalcedonite</p> </div> <div style="text-align: center;"> <p>quartzine</p> </div> </div>
low	coarse, equant	megaquartz
		<div style="display: flex; justify-content: space-between;"> <div style="text-align: center;"> <p>Environment: neutral to acid nonsulphate</p> </div> <div style="text-align: center;"> <p>Environment: alkaline and/or sulphate</p> </div> </div>

Figure 80. Diagram Illustrating the Silica Type Produced as a Function of Environment and Silica Concentration (Modified from Folk and Pittman, 1971)

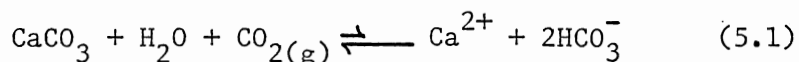
megaquartz and chalcedony.

Dissolution of the minerals was the result of pressure solution or from changes in the Formation fluids (Pettijohn et al., 1973). Pressure solution would have occurred during burial and tectonism. In most cases only calcium carbonate grains and matrix were dissolved along solution seams, the solute transported, and redeposited probably in an area relatively close to the source (Figure 38). Pressures were generally not great enough to dissolve silica, consequently, quartz grains concentrated along solution seams.

Changes in the fluid chemistry of the Formation were much more important in the dissolution of minerals and their reprecipitation. The solubility of the minerals, their concentrations, the temperature and pressure of the system, and the relative proportions of  $H^+$  and  $OH^-$  ions (pH) were the main parameters governing solution and reprecipitation. In a very simplified sense, when the Formation water was acid ( $pH < 7$  ( $[H^+] > 10^{-7}$ )),  $CaCO_3$  was dissolved; when the water was alkaline, ( $pH > 7$  ( $[OH^-] > 10^{-7}$ )),  $SiO_2$  was dissolved (Figure 76). However, calcite is more soluble than silica and will dissolve more readily in slightly acidic water than silica will in slightly basic water unless the concentrations are very small. Larger quantities of calcite can be held in solution than silica until a very high pH level is attained ( $pH > 10$ ).

Temperature and pressure of the ground water affect the solubility of both calcite and silica. Even at a relatively low pH silica can be dissolved if the temperature is high enough (Blatt, 1982). However, as the temperature of the solution increased in the presence of calcite, carbon dioxide was removed from the system and

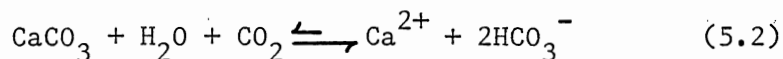
$\text{CaCO}_3$  would not dissolve:



Calcite was precipitated until a state of equilibrium between the temperature of the water and the  $\text{CO}_2$  in solution was attained.

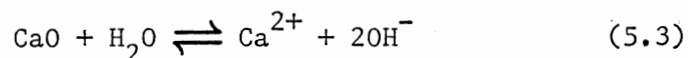
Therefore, at low pH, but high temperature  $\text{CaCO}_3$  was precipitated and silica dissolved.

If the system was closed and pressure due to burial or tectonism became a factor, then  $\text{CO}_2$  was retained in the system (Brady and Humiston, 1978). Equation 5.1 then becomes:



until equilibrium between pressure and  $\text{CO}_2$  was attained.

The ground water chemistry of the system changed periodically creating a rather complicated series of processes. Since only a weak acid is necessary to dissolve  $\text{CaCO}_3$ , little change would have had to take place in the water. Moderate fluctuations in pH and  $\text{CO}_2$  content would alternately dissolve and reprecipitate  $\text{CaCO}_3$ . However, in order to dissolve silica by the ground water method a very high pH or a high temperature must have been attained. As previously stated, increased temperature with burial may have caused some of the later dissolution. In order to increase pH, a chemical change in the water was necessary. If  $\text{Ca}^{2+}$  had been introduced to the system without a corresponding increase in carbon, the ground water would have become extremely alkaline with time by the following reaction:



This alkaline solution would have caused the corrosion of quartz grains with subsequent reprecipitation as the water chemistry returned to a more acid state or as the silica was transported to an

area of lower pH. That the ground water conditions varied quite often can be demonstrated in Figure 49. At least four alternating periods of calcite and silica cementation can be seen. A fifth period (actually the first event) may also be present. Note that the center quartz grain appears to be too large to have been the original ooid nucleus. Multiple generations of alternating calcite and silica cement are common throughout the Formation. As many as nine consecutive events have been recorded in some units as the ground water chemistry fluctuated.

The porosity and permeability of the lithologies controlled, in part, the timing of cementation and the rate at which it took place (Pettijohn et al., 1973). A lithology that consisted of rounded to subrounded grains and was relatively free of matrix (for example, an oolitic grainstone) would have had a very high initial porosity (Figure 81). In the phreatic zone, ground water would have percolated freely and, if chemical conditions permitted, precipitated an early cement. Rapid precipitation led to small crystals fringing the grains. As the crystals grew, porosity and permeability were reduced. As fluid circulation slowed, growth slowed, and the subsequent individual crystals were larger. Complete cementation had a drusy texture in many cases. In some instances, cementation was interrupted after the initial fringe of isopachous crystals had been precipitated. Reintroduction of ground water filled the remaining pore spaces usually with later calcite or, more rarely, silica (Figure 50).

If the grains were more angular forming an interlocking mosaic or the micrite matrix more abundant, the porosity and permeability

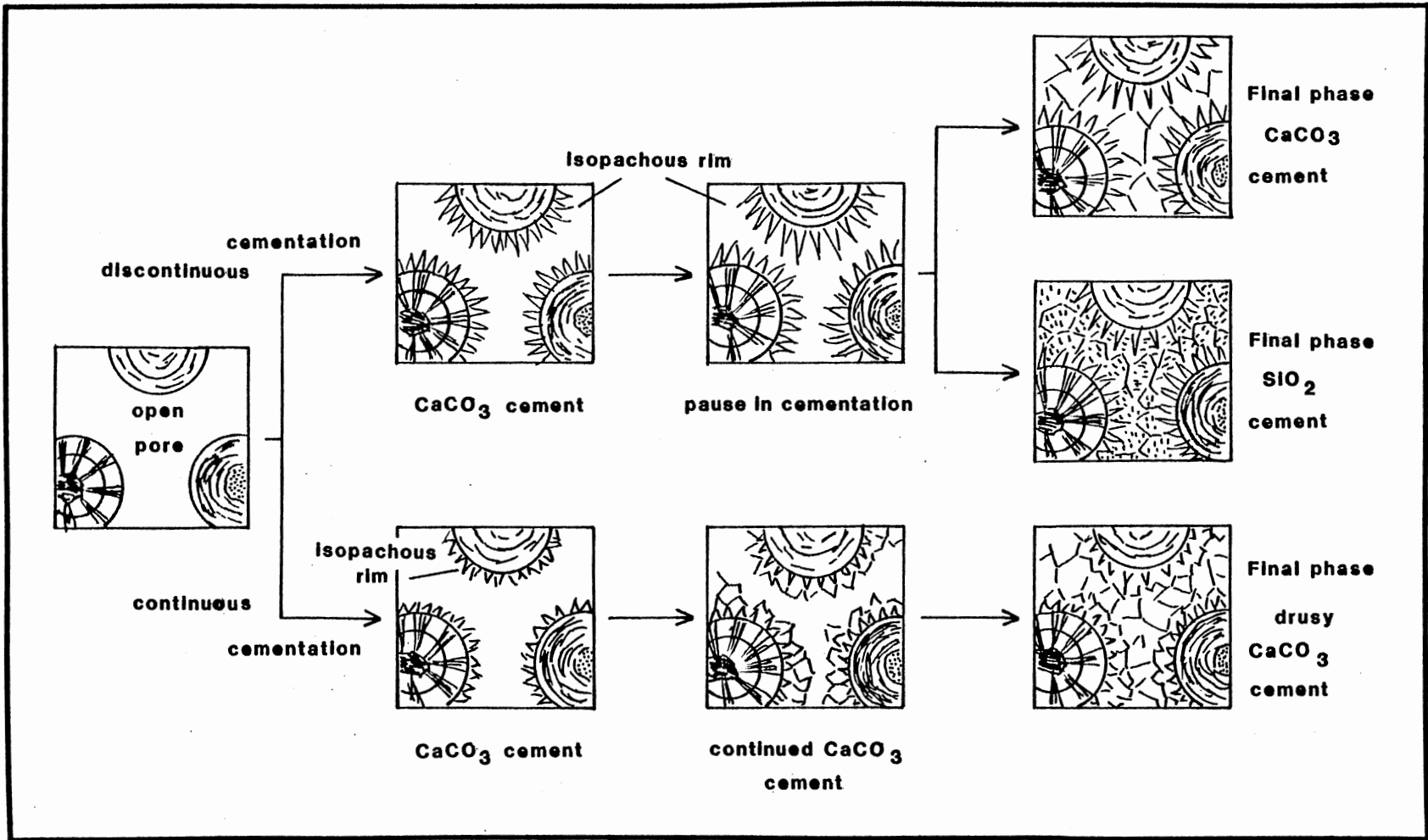


Figure 81. Illustration of an Example of Continuous and Discontinuous Cementation in an Oolitic Grainstone Found in the Cool Creek Formation

were reduced. Cementation occurred much more slowly filling in the pores with large crystals of spar.

Most of the pore-filling silica exists in the form of mega-quartz; equant microcrystalline quartz is most often associated with replacement. Fibrous microcrystalline quartz occurs both as a pore-filling cement and as a replacement product. This will be discussed more fully in the following section.

### Replacement

Mineral replacement was a very important diagenetic process in the Formation. The exact method by which two minerals replace each other is not well understood, but some hypotheses have been formulated (Pettijohn et al., 1973). In the case of silica to calcite or calcite to silica, the replacement appears to occur across a fluid film only a few microns in thickness allowing a very close replication of the morphology of the replaced grains (Figure 82). If the process alters some parameter during the change from one mineral to another, for example the calcite to dolomite volume change, the replication of the structures may not occur.

All lithologies in the Formation were susceptible to silica replacement, either partially or completely. Replacement usually began along a front of least resistance, for example, a fracture or some area of increased porosity and permeability, then spread outward exchanging silica for calcite as the fluid penetrated the rock. Microporosity and micropermeability controlled the movement of the fluid. Differences in these two parameters may account for some of the partially silicified units. For example, some stromatolites

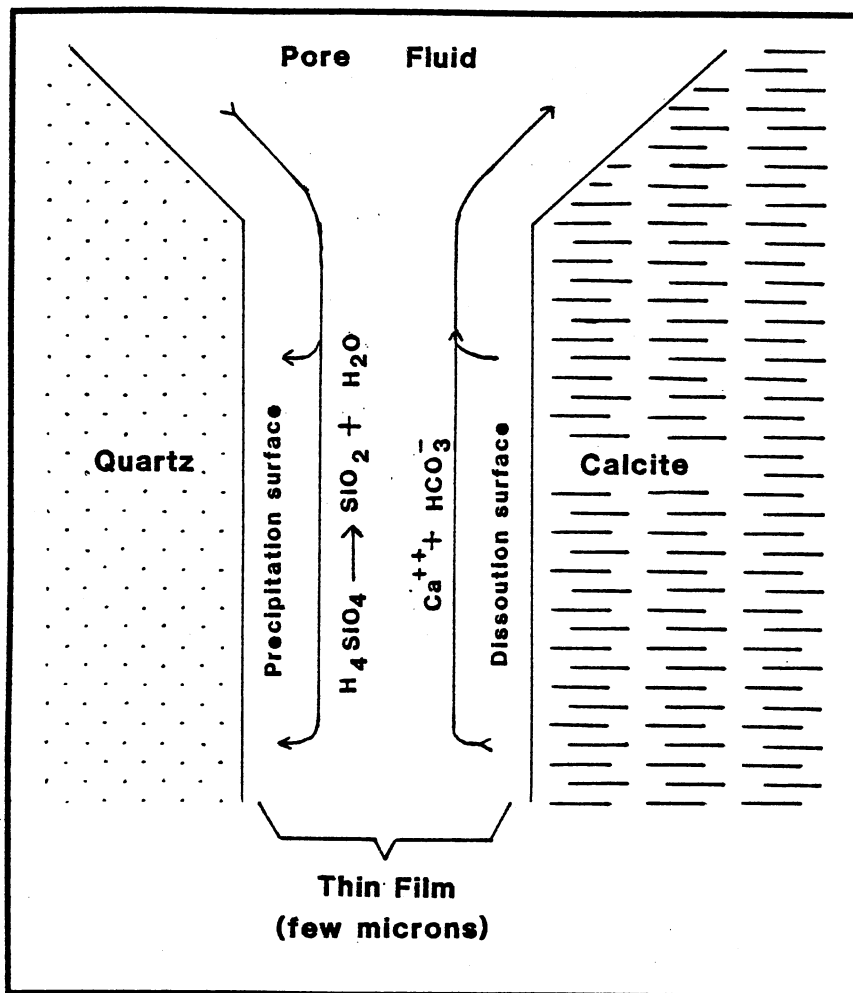
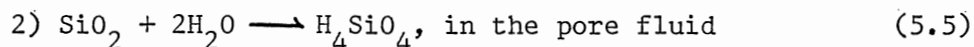
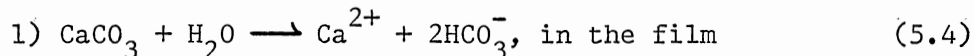


Figure 82. Diagrammatic Representation of the 1:1 Replacement of Calcite by Silica (Modified from Pettijohn, Potter, and Siever, 1972)



show alternating silica and calcite laminae.

Replacement may have occurred in the following manner (modified from Pettijohn et al., 1973):



3)  $[\text{H}_4\text{SiO}_4]$  is greater in the pore fluid; moves toward film

4)  $[\text{Ca}^{2+}] + [\text{HCO}_3^-]$  is greater in the film; moves toward pore fluid

5) If the ion activity product of the  $\text{H}_4\text{SiO}_4$  exceeds the solubility product,  $\text{SiO}_2$  precipitates:



The delicate balance of dissolution and reprecipitation of  $\text{CaCO}_3$  and  $\text{SiO}_2$  must occur near the junction of the calcite-silica fields (Figure 76). Much of the silica replacement occurred very early in the history of the individual units. Evidence of this is seen in oolitic lithologies that have been partially silicified. The areas replaced by silica show no compaction in the silicified areas, but considerable compaction and distortion in the zones that remained calcitic (Figures 36 and 53). Further proof of early silicification is seen in Figure 28. Chert nodules were formed in some unit. Soon after, weathering and erosion removed the nodules; they were rounded in transport and redeposited in an imbricate fashion as part of an IFC.

Most of the lithologic units that were replaced by silica are composed of equant microcrystalline quartz indicating a high concentration of silica in the ground water (Folk and Pittman, 1971) (Figure 80). Dissolution and replacement occurred nearly simultaneously. Chert nodules were formed when the silica in solution

was mobilized along fractures (both vertical and horizontal) and reprecipitated when the ground water chemistry became unfavorable to carrying the dissolved silica. The mobilization may have involved only limited amounts of silica allowing reprecipitation of individual nodules along lines of weakness. If large quantities of silica were mobilized, the nodules would have begun to coalesce forming pseudolayers along fractures (Figure 83). Most of the nodules were formed early as evidenced by the distortion of micrite laminae when the silica nodule was precipitated (Figure 84).

In rare instances sparry calcite cement was replaced by spherulitic chalcedony or euhedral quartz crystals (Figures 51 and 56). A relatively high concentration of silica in the ground water was necessary in order for equant microcrystalline chert to form (Folk and Pittman, 1971). With limited silica concentration replacement would have been limited to minor amounts of fibrous quartz or megaquartz.

#### Silica and Replaced Evaporites

Six types of secondary silica that are often associated with evaporites have been identified in thin section. These are: 1) fibrous chalcedonite (length fast); 2) fibrous quartzine (length slow); 3) fibrous zebraic chalcedony; 4) pseudofibrous lutecite; 5) equant megaquartz; 6) flamboyant megaquartz. Equant microcrystalline chert, though not confined to association with evaporites, is also found with them.

A thorough investigation by Folk and Pittman (1971) shows a close link between length slow quartzine and "vanished evaporites"



Figure 83. Discrete Chert Nodules and Chert Pseudolayer (Turner Falls)



Figure 84. Chert Nodule Distorting Micrite Laminae Through Growth

(Figure 80). The pseudomorphed sulphates discussed in Chapter 4 all contain quartzine as well as one or more of the other silica types. Quartzine most often occurs as a replacement of the sulphates; chalcedonite occurs as a pore lining followed by pore-filling megaquartz. The following sequence of events may explain the changes in micro-morphologies of the silica (modified from Chowns and Elkins, 1974):

- 1) Highly alkaline water was introduced to the sabkha. The sulphates were simultaneously dissolved and replaced by silica in much the same manner as calcite was replaced by silica. Ordinarily, the anhydrite would have been hydrated to gypsum, but in the presence of silicic acid ( $H_4SiO_4$ ) direct silicification took place. If the concentration of silica were very high, equant microcrystalline chert replaced the evaporites. With decreasing silica concentration but high pH and sulphate content quartzine was formed (Figure 85). Tiny laths of relict anhydrite were often trapped as inclusions in the secondary quartz.
- 2) Ground water dissolution of the salts began to exceed replacement, thereby creating voids. As the sulphates were transported away from the system the voids were lined by length fast chalcedonite. If the silica concentration remained high enough, the pore was filled with chalcedonite fibers (Figure 54).
- 3) If the concentration of silica diminished, the remaining pore space was filled with megaquartz (Figure 55).

Pore water chemistry rarely remained constant or changed in an orderly progression. Consequently, alternations in the type of silica formed took place. Pseudofibrous lutecite is a transitional form occurring after quartzine. It is characterized by a faint chevron

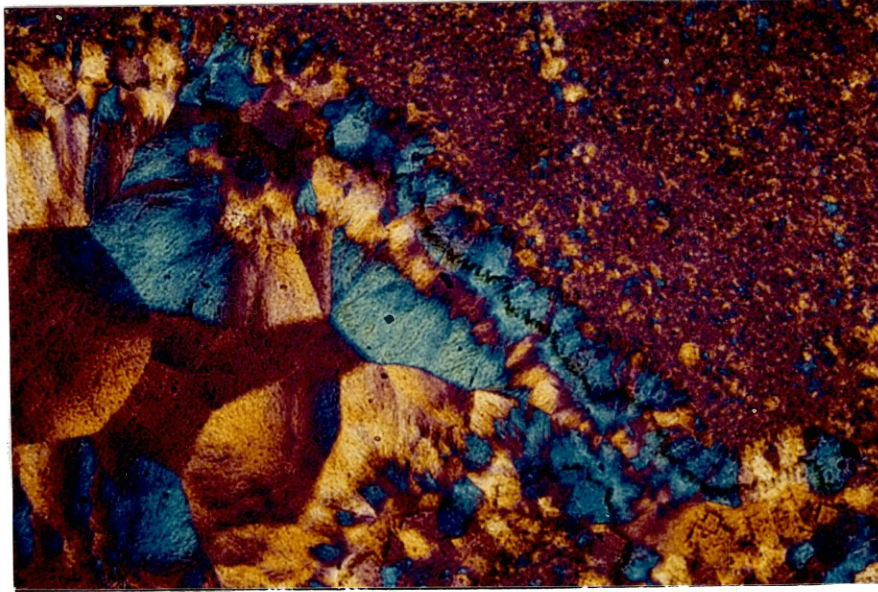


Figure 85. Fibrous Chalcedony: Quartzine Fibers are Yellow Northeast to Southwest; Chalcedonite Fibers are Blue Northeast to Southwest (X40, Crossed Nicols, Quartz Wedge)



Figure 86. Silica Nodule after Anhydrite. Lutecite at (a); Flamboyant Quartz at (b). (X100, Crossed Nicols)

pattern (under crossed polars) and generally occurs near the outer edge of a nodule (Figure 86). The fibers cross at approximately  $60^{\circ}$  giving the nodule a distorted appearance (Folk and Pittman, 1971).

Zebraic chalcedony shows alternating black and white fibers (under crossed polars) progressing outward from the fiber bundle (McBride and Folk, 1977) (Figure 55). It is associated with quartzine or lutecite and may represent slight fluctuations in pH or sulphate content as the alternating black and white is seen to represent changes from length slow to length fast chalcedony.

Flamboyant megaquartz represents a stage intermediate between quartzine and equant megaquartz (Chowns and Elkins, 1974). As the silica concentration decreased, fibrous quartz began forming large, elongate crystals. These crystals finally merged into equant megaquartz crystals as the pore space was filled (Figure 86).

Both the matrix and evaporites may have been silicified or only the matrix but not the evaporites. The preservation of the evaporites as silica ghosts may have occurred in two steps. First, the salts were dissolved and replaced by calcite. With the introduction of silica-rich water, replacement of both matrix and the previously pseudomorphed evaporite occurred. In some cases, only the matrix was silicified (Figure 58). During the initial replacement of the evaporite a very dense network of microcrystalline calcite was formed along the outside edge of the evaporite crystal forming an impermeable barrier. Most of the ghosts retained the first replacement mineral, calcite, except where microfractures allowed the penetration of silica-rich water. The pseudomorphed evaporites were then partially replaced from the inside out with silica before the silicifi-

cation process ended.

#### Conversion of Aragonite to Calcite

A major diagenetic problem with all ancient carbonates is the question of which polymorph was initially precipitated, aragonite or calcite? Orthorhombic aragonite is the more unstable carbonate phase at low temperature and, if it was the original polymorph, would have converted to calcite relatively quickly (Pettijohn, 1975). The argument of aragonite versus calcite centers around the presence or absence of the  $Mg^{2+}$  ion in the seawater (Bathurst, 1975). When the  $Mg^{2+}$  ion is present in sufficient quantity in marine water, inorganic precipitation of calcite is prohibited. In modern seawater, the  $Mg^{2+}/Ca^{2+}$  ratio is high, consequently, aragonite is the initial precipitate. In ancient seawater the  $Mg^{2+}/Ca^{2+}$  may have been considerably lower thereby permitting the direct precipitation of calcite.

The lithologies most often used to determine whether primary deposition was aragonite or calcite are oolites. Recent ooids are usually aragonitic whereas ancient ooids are comprised of calcite. Wilkinson and Landing (1978) used oolitic units from the Jurassic Twin Creek Formation of Wyoming to show that calcite comprised the primary mineralogy. Ooids with original aragonitic nuclei had had the nuclei dissolved and replaced by sparry calcite. The cortices retained their original structure. Ooids with original calcite nuclei and cortices remained unchanged in structure. They argue that if all of the ooids were originally aragonite, the conversion to calcite should have affected all of the structures.

The present study of ooids is not entirely conclusive as to

whether the original polymorph was calcite or aragonite, but Wilkinson's and Landing's hypothesis appears to be supported in most circumstances. In Figure 36 compactional breakage of the ooids follows the radii of the cortices in most cases. If aragonite replacement had occurred after compaction (which most authors feel would be the case) the calcite crystal formation should have crossed fracture lines and not conformed to primary radii.

In most of the oolitic lithologies the primary fabric of the ooids, whether radial or concentric, is well preserved. Again, if aragonite converted to calcite, the resultant crystal growth should have obliterated these structures. Figure 38 illustrates this very well. Nuclei of some of the ooids may have been originally aragonitic, probably gastropod fragments. Trilobite fragments (originally calcite) and polymorphed fossil fragments (originally aragonite) in the matrix support this conclusion. The aragonitic fragments were dissolved and removed from the system. They were later replaced not by calcite as is usual, but, in this case, by dolomite. The cortices of the ooids were not dissolved and retained their original radial structures.

The deposition of the Formation took many thousands of years and in such time, many changes in the fluid chemistry undoubtedly took place. However, from the ooid samples studied in this endeavor, the marine waters appear to have been lacking in the  $Mg^{2+}$  ion that would have prohibited primary calcite precipitation. The samples studied were collected from all levels in the Formation and nearly all seem to indicate the deposition of primary calcite rather than aragonite to calcite conversion.

A study by Gebelein and Hoffman (1973) has shown that  $Mg^{2+}$  can



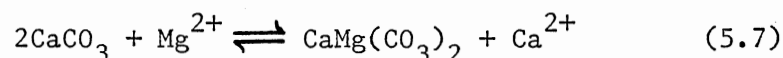
be taken up by algal growth and retained even after lithification. If the initial  $Mg^{2+}/Ca^{2+}$  ratio in the seawater was low relative to present conditions, the further abstraction of  $Mg^{2+}$  by algae could have lowered the  $Mg^{2+}$  content in the seawater below the threshold of primary aragonite deposition. Later decay of the organics would have released the  $Mg^{2+}$  thus providing a source for the formation of secondary dolomite (discussed below).

The penecontemporaneous dolomite of the sabkha appears to present an anomaly, that is, a high concentration of  $Mg^{2+}$  ions. The combination of extreme evaporation leading to high salt concentration and the withdrawal of  $Ca^{2+}$  in the formation of sulphates would have raised the  $Mg^{2+}/Ca^{2+}$  ratio high enough to accommodate dolomite precipitation.

#### Later Secondary Dolomite

Secondary dolomite does not form a large percentage of the formation in Blue Creek Canyon. Minor amounts are found throughout replacing primary lithologies but only one significant bed of dolomite exists.

In general, small dolomite rhombohedrons (less than 1 mm (0.04 in)) comprise less than 5% of a sample. The rhombohedrons replace all lithotypes and are concentrated in the zones that were most permeable (Figure 61). Magnesium-rich ground waters percolated through these units relatively early in their diagenetic histories. The source of the  $Mg^{2+}$  may have been the decay of organics as discussed above. As the salinity and  $Mg^{2+}/Ca^{2+}$  ratio increased, dolomite crystals were precipitated by the following reaction (Blatt, 1982):



Some dolomite was precipitated very early as seen in Figure 59. The dolomite is confined to the IFC clast showing that dolomitization occurred prior to complete lithification of some micrites. The process was interrupted as the micrite was ripped up and redeposited as an IFC. Silica was then introduced to the IFC unit replacing calcite preferentially to dolomite (Dietrich et al., 1963). Dolomite is more difficult to dissolve in mildly acidic water than calcite, therefore, the silica replacement took the course of least resistance.

The dolostone layer is composed of larger dolomite crystals (1 mm (0.04 in) and larger) in an interlocking mosaic (Figure 62). The unit must have been subjected to a continuous influx of  $Mg^{2+}$  ion-laden water to so comprehensively dolomitize the calcite (Blatt, 1982).

Evidence of secondary replacement is shown by the zoned crystals. Blatt (1982) has suggested two methods by which zoning can occur. By the first method, the dark central zone is contaminated with inclusions of some ion, usually  $Fe^{2+}$ , replacing minor amounts of  $Mg^{2+}$ . The clear rim on the rhombohedron would indicate a change in water chemistry, that is, a lack of  $Fe^{2+}$  in the circulating water. In order for the iron to be visible under the microscope, it would have to have been oxidized later in its diagenetic history.

The second method suggested by Blatt involves the inclusion of  $Ca^{2+}$  ions trapped in the centers of the crystals as dolomite began to replace calcite. The calcite was dissolved away from the growing dolomite crystal to accommodate the greater need for  $CO_3^{2-}$ . With continued growth, the edge of the dolomite crystal penetrated the pore space where no calcite was left. Consequently, a clear

inclusion-free rim formed around the cloudy center. The secondary porosity (13% total increase in porosity during complete dolomitization) created by dolomitization was usually filled by late sparry calcite.

#### Authigenic Feldspars

Authigenic feldspars comprise a very small fraction of the mineralogy of the Formation (less than 0.1%), but are significant in that they formed in a sedimentary environment. They were first reported in the Arbuckle Group by Baskin (1956) in samples from the Arbuckle Mountains.

The samples containing authigenic feldspars are predominantly micrite in the form of matrix, clasts, or seam fill. The secondary feldspars occur as overgrowths on detrital feldspars or as complete authigenic crystals showing no detrital core (Figure 87). The overgrowths are not always of the same composition as the fragment as seen in Figure 88 where an authigenic potassium feldspar appears to have overgrown a plagioclase fragment. Completely authigenic crystals may have grown by replacement of micrite as most crystals show inclusions of calcium carbonate.

Kastner and Siever (1979) have proposed two models for the formation of authigenic feldspars: 1) the isochemical model; 2) the exchange reservoir model. The isochemical model is a closed system involving the dissolution and reprecipitation of minerals already present. The exchange reservoir model requires the addition of water from another source containing the elements necessary to precipitate the feldspars. A combination of the two methods may have been re-

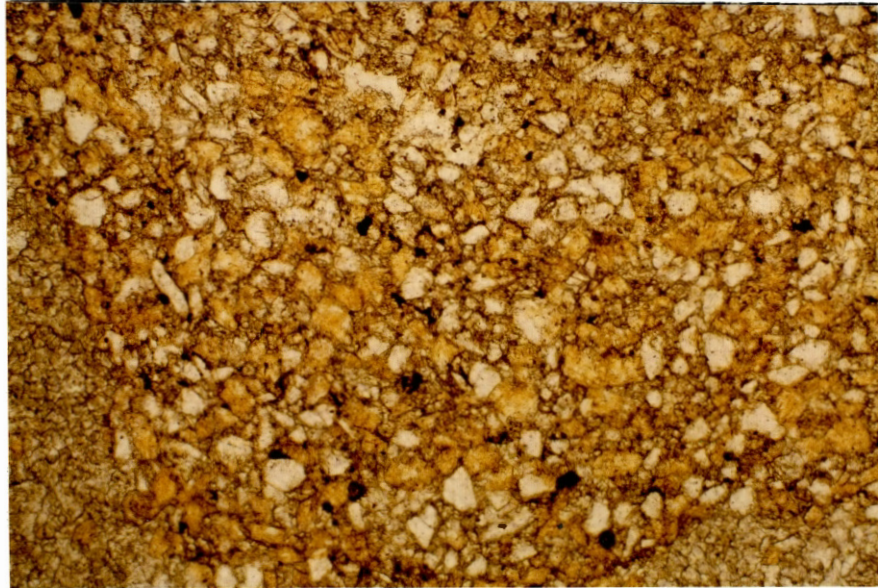


Figure 87. Authigenic Feldspars, Stained Yellow with Cobaltinitrite (X40, Ordinary Light)

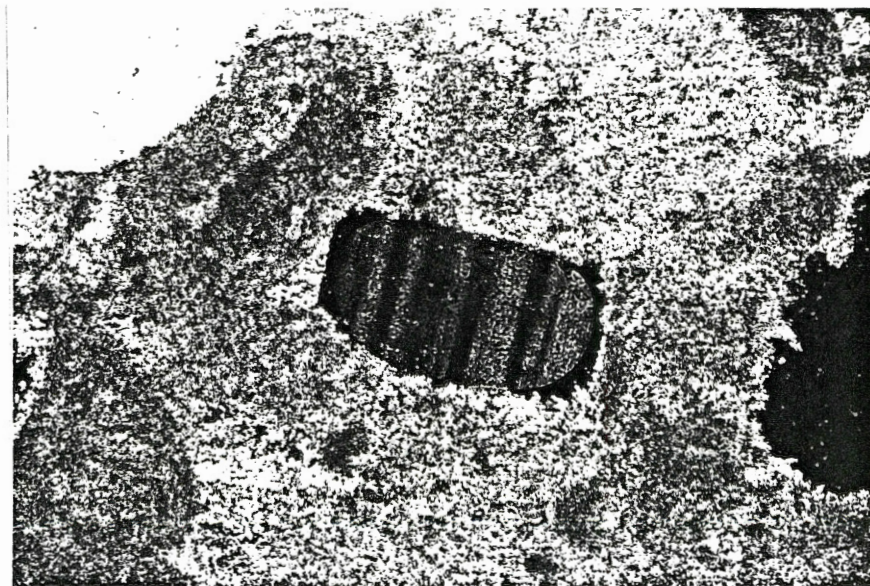


Figure 88. Detrital Plagioclase with an Overgrowth of Feldspar, Probably Orthoclase (X100, Crossed Nicols)

RECEIVED  
MAY 10 1964  
U.S. AIR FORCE  
HEADQUARTERS  
DALLAS, TEXAS

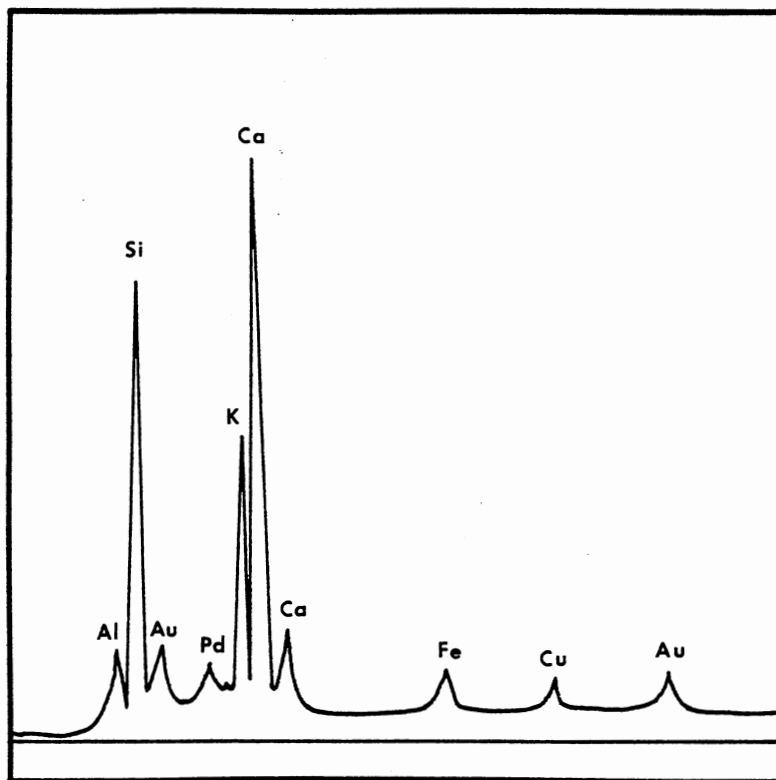


Figure 89. Qualitative Analysis of Authigenic Feldspar Crystal Seen in Figure 25. Potassium Peak Indicates Feldspars are Probably Orthoclase. EDAX Analysis Readout

sponsible for the feldspars in the Formation.

The two most common authigenic feldspars found in sedimentary rocks are potassium feldspars (orthoclase and microcline) and albite. SEM analysis shows that the feldspars found in this study are potassium-rich (Figures 25 and 89). Detrital quartz grains within the sediment were probably the source of the silica, but aluminum and potassium had to have been transported in from another area. Since the environment was conducive to evaporite formation potassium may have been supplied from ephemeral sylvite deposits on the sabkhas. Aluminum seems to be the most difficult element to supply. In order to adhere only to the isochemical model, the aluminum would have had to have been supplied by the entrapped pore water or the sediment in place. This hypothesis is valid for dissolution of detrital feldspars in place, but for sediment in which detrital feldspars were not a part, the aluminum must have been supplied from ground water mixing with another source. This source may have been patches of volcanic rocks on the continent. Minor amounts of rock fragments are found in some sections indicating that these may have been the source of the aluminum.

#### Aggrading Neomorphism

Tucker (1981) listed four criteria by which aggrading neomorphism, that is, grain enlargement, could be recognized in limestone thin sections. These are: 1) Irregular crystal boundaries, often containing embayments; 2) irregular, patchy distribution of crystal sizes; 3) gradational boundaries between original crystals and neomorphic crystals; 4) skeletal grains floating in coarse spar.

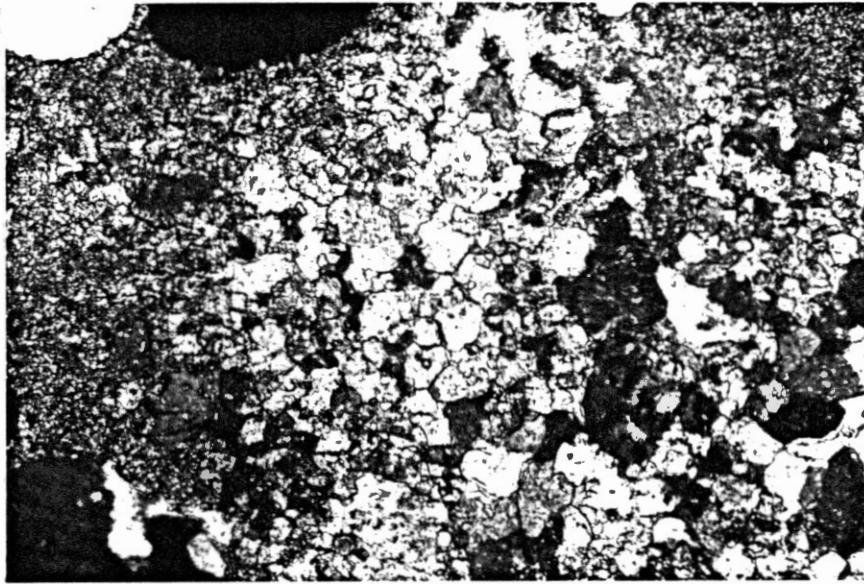


Figure 90. Aggrading Neomorphism (X100, Crossed Nicols)



The first three of these criteria are met in some of the Cool Creek samples (Figure 90). Calcite crystal sizes have increased from micrite (less than 4 microns) to microspar (4 to 10 microns) and pseudospar (10 to 50 microns). Some of the largest crystals measure up to 70 microns across. The crystal growth process appears to occur across a thin film surface in a manner similar to that of the silica-calcite replacement process (Bathurst, 1975). Calcite (micrite) was dissolved during wet transformation on one side of a thin film and slowly reprecipitated on the other side. The rate of the crystal growth determined the ultimate size of the new crystal; the slower the growth, the larger the new crystal. The irregular shapes were governed by the pre-existing crystals.

#### Paragenesis

As stated in the opening paragraph of this chapter, the diagenetic processes that took place in the Cool Creek Formation were relatively few. The complexity arises when an interpretation of the sequence of events is attempted. If each event occurred separately over long periods of time, then stopped completely before the next event, the paragenetic sequence would be a simple matter. However, diagenetic events do not conform to this rule. Nearly all of the processes had the ability to occur simultaneously or alternated at such rapid rates that the sequence is difficult to determine in many cases. Figure 91 is a summary of the paragenetic sequence seen in the Formation showing the overlap of nearly all of the processes.

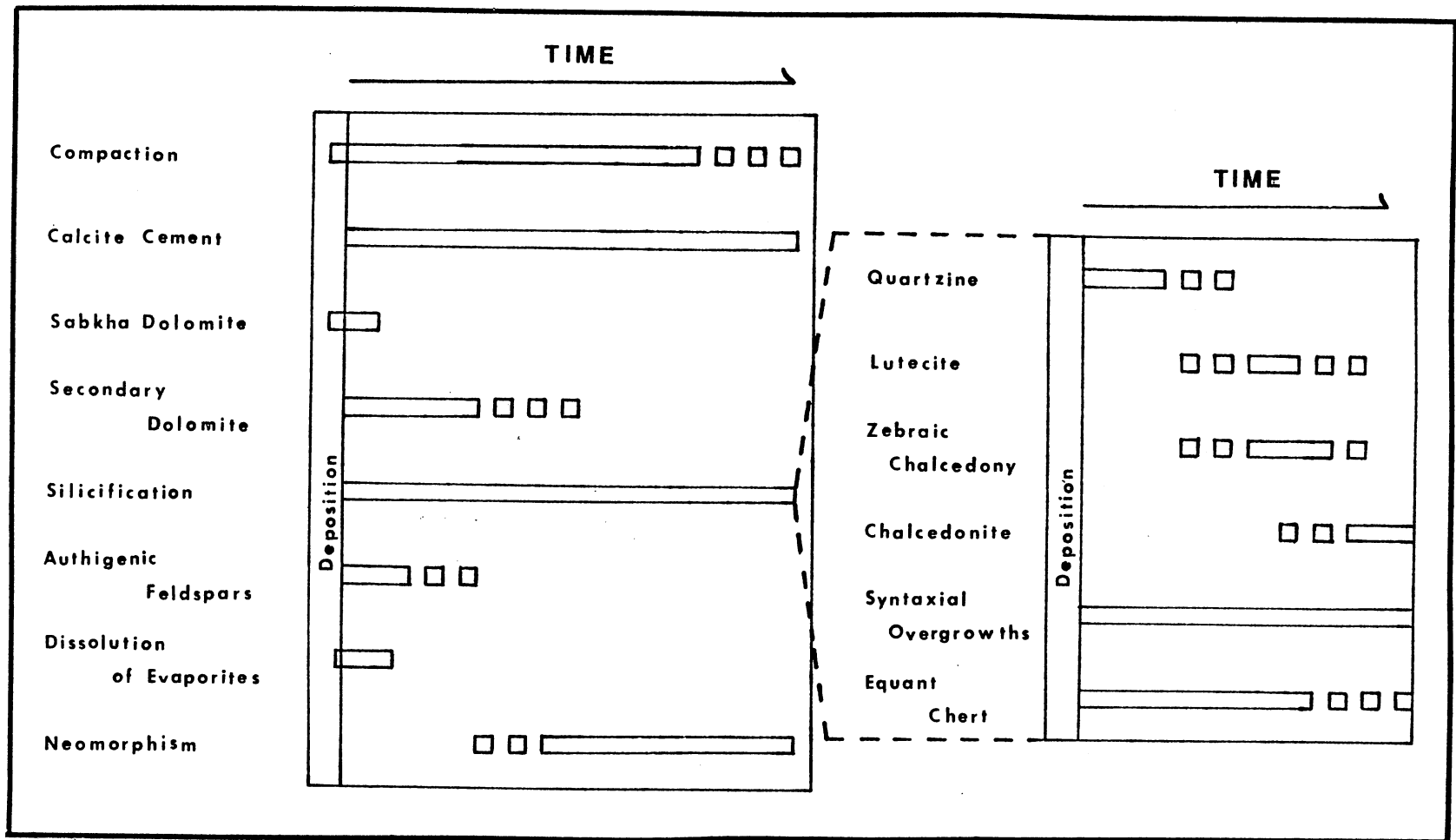


Figure 91. Summary of the Paragenetic Sequence of Events For the Cool Creek Formation

## CHAPTER VI

### SUMMARY AND CONCLUSIONS

The purpose of this Master's study is to describe the lithologies of the Ordovician Cool Creek Formation, to determine the environmental conditions during the deposition of the sediments, and to evaluate the diagenetic changes that occurred after deposition and the possible order of their occurrence. The area of study is located in Blue Creek Canyon in the Slick Hills of Southwestern Oklahoma.

The following lithotypes were recognized and described in the field and in the laboratory:

- 1) Algal boundstones: A modified classification scheme was devised to describe the various forms of boundstones. These forms include:
  - a) Crinkly and smooth algal mat with indistinct growth laminae;
  - b) LLH-C, LLH-S, SH-C, and SH-V algal mounds composed of laminated stromatolites, non-laminated thrombolites, and intermediate structures;
  - c) Algal reefs forming tabular outcrops;
  - d) Bioherms and miniherms that terminate abruptly in a lateral sense;
  - e) Encrusting stromatolites coating other lithotypes.
- 2) Micrite: Grey, buff, or pink micrites contain variable quan-

tities of quartz silt and sand. The micrite layers may show a variety of sedimentary structures including parallel laminations, small scale trough cross-bedding, bioturbation, subaqueous shrinkage cracks, and subaerial mudcracks. Authigenic feldspars are restricted to the micrite lithotypes.

3) Intraformational conglomerates: IFC's comprise nearly 25% of the Formation and are found as distinct beds or as infill between boundstone constituents.

4) Intraformational breccias: IFB's are relatively uncommon and are best exposed at Turner Falls.

5) Oolitic limestone: Ooids are found throughout the Formation. They are either radial or concentric in morphology and have nuclei that are composed of a variety of detritus.

6) Peloidal limestone: Peloids are most often identified only in thin section and are thought to be faecal in origin due to their association with fossil fragments.

7) Quartz-rich sandstone: The first substantial appearance of quartz sand marks the base of the Formation (Thatcher Member) and is frequently seen thereafter.

8) Chert: Flinty and chalcedonic chert nodules are found throughout the Formation. One layered chert and several chert breccias were recognized. Megaquartz, equant microquartz, and chalcedony were identified in thin section.

9) Dolostone: Only one dolostone bed was found in the Blue Creek Canyon section. Small quantities of dolomite rhombohedrons are found in thin section, usually replacing micrite.

Body fossils are sparse in the Formation. The gastropod Lecano-

spira and the brachiopod Diaphelasma have been identified. Sponges, trilobites, and echinoids are seen only as fragments.

In Ordovician times Oklahoma was situated in tropical latitudes. The paleoenvironment was warmer and drier than the present climate with life restricted to marine waters. The variable laminae structures of algal boundstone are used as the primary indicator of the shallow marine environment. IFC's indicate disturbances in the shallow water causing clasts to be ripped up from pre-existing lithologies. Daily events such as waves and channelling, and larger events such as storms, transgressions, and regressions, resulted in the deposition of IFC's. The interpretation of the environment is substantiated by other lithologies such as micrite, oolites, quartz sand, and pseudomorphed evaporites.

Though the general environment can be reasonably interpreted by applying the Principal of Uniformitarianism processes and process rates were, to some extent, different in the Early Ordovician. Considerable evidence of reworking of sediments and of nondeposition exists. Subsidence of the basin allowed great thicknesses of sediment to accumulate; classic cyclic motifs similar to Carboniferous cyclothems are not present.

The diagenetic history of the Formation is complicated only by the frequency and alternation of the few processes that affected it. Physical diagenesis consisted primarily of compaction and later deformation during folding and faulting.

Chemical diagenesis consisted primarily of cementation by calcite and cementation and replacement by silica. The source of the secondary calcite was the abundant primary organically and chemi-

cally precipitated calcite; the silica originated mainly from the abundant quartz sand grains throughout the Formation. If silica concentration was very high, equant microcrystalline quartz was precipitated. Lesser concentrations, differences in pH, and the presence or absence of sulphates controlled the precipitation of fibrous chalcedony. The most common secondary silica precipitate occurred at low concentrations and formed overgrowths on detrital quartz grains.

The problem of primary aragonite versus primary calcite was not conclusively determined but, using Wilkinson's and Landing's (1978) results of ooid studies seems to indicate that calcite was primary.  $Mg^{2+}$  concentration in Ordovician seawater may have been low enough to allow primary calcite formation.

Aggrading neomorphism is seen in some of the carbonate samples. Minor amounts of secondary dolomite and authigenic feldspars are found in the Formation usually associated with lithotypes containing micrite.

## BIBLIOGRAPHY

- Aitken, J. D., 1967, Classification and Environmental Significance of Cryptalgal Limestone and Dolomite, with Illustrations from the Cambrian and Ordovician of Southwestern Alberta: *Journ. of Sedimentary Petrology*, Vol. 37, pp. 1163-1178.
- Barthelman, W. B., 1968, Upper Arbuckle (Ordovician) Outcrops in the Unap Mountain-Saddle Mountain Area, Northeastern Wichita Mountains, Oklahoma: Unpub. M.S. Thesis, University of Oklahoma, Norman, Oklahoma.
- Basin Analysis Class, 1982, Subsidence Rates in Oklahoma During the Paleozoic: *Selenite Blade*, Vol. 1, pp. 75-78.
- Baskin, Y., 1956, A Study of Authigenic Feldspars: *Journ. of Geology* 64, pp. 132-155.
- Bathurst, Robin G. C., 1975, Carbonate Sediments and Their Diagenesis: Elsevier Scientific Publ. Co., Amsterdam.
- Beauchamp, Weldon, Personal Communication, Stillwater, Oklahoma, October 14, 1982.
- Beauchamp, Weldon, 1983, The Structure of the Southern Slick Hills in Southwestern Oklahoma: Unpub. M.S. Thesis, Oklahoma State University.
- Blatt, Harvey, 1982, Sedimentary Petrology: W. H. Freeman and Co., San Francisco.
- Blatt, Harvey, Middleton, G., and Murray, R., 1980, Origin of Sedimentary Rocks: Prentice Hall, Inc., Englewood Cliffs, New Jersey.
- Bradfield, H. H., 1964, The Ellenburger Group of North Central Texas: *Tulsa Geol. Soc. Digest*, Vol. 32, pp. 112-118.
- Brady, J. E. and Humiston, G. E., 1978, General Chemistry: John Wiley and Sons, New York.
- Brookby, H. E., 1969, Upper Arbuckle (Ordovician) Outcrops in Richards Spur-Kindblade Ranch Area, Northeastern Wichita Mountains, Oklahoma: Unpub. M.S. Thesis, University of Oklahoma, Norman, Oklahoma.

- Chafetz, Henry S., 1973, Morphological Evolution of Cambrian Algal Mounds in Response to a Change in Depositional Environment: Journ. of Sedimentary Petrology, Vol. 43, pp. 435-446.
- Chowns, J. M. and Elkins, J. E., 1974, The Origin of Quartz Geodes and Cauliflower Cherts Through Silicification of Anhydrite Nodules: Journ. of Sedimentary Petrology, Vol. 44, pp. 885-903.
- Clark, Joe Marsh, 1964, The Arbuckle of Northwest Arkansas: Tulsa Geol. Soc. Digest, Vol. 32, pp. 76-90.
- Cloud, P. E., 1952, in Nelson, H. F., Brown, C. W., and Brineman, J. H., 1962, Skeletal Limestone Classification: Classification of Carbonate Rocks-A Symposium, AAPG Memoir 1, pp. 224-252.
- Davis, Richard A., 1983, Depositional Systems: Prentice Hall, Inc., Englewood, New Jersey.
- Decker, C. E., 1939, Two Lower Paleozoic Groups, Arbuckle and Wichita Mountains, Oklahoma: GSA Bul., Vol. 50, No. 8, pp. 1311-1322.
- Decker, C. E. and Merritt, C. A., 1928, Physical Characteristics of the Arbuckle Limestone: OK Geol. Surv. Circ. No. 15.
- Deelman, John C., 1978, Experimental Ooids and Grapestones: Carbonate Aggregates and Their Origin: Journ. of Sedimentary Petrology, Vol. 48, pp. 503-512.
- Dietrich, R. V., Hobbs, C. R. B., and Lowry W. D., 1963, Dolomitization Interrupted by Silicification: Journ. of Sedimentary Petrology, Vol. 33, pp. 646-663.
- Donovan, R. Nowell, 1982, Geology of Blue Creek Canyon: in Gilbert, M. C. and Donovan, R. N., eds., Geology of the Eastern Wichita Mountains, Southwestern Oklahoma: OK Geol. Surv. Guidebook 21, pp. 65-77.
- Donovan, R. N. and Foster, R. J., 1972, Subaqueous Shrinkage Cracks from the Caithness Flagstone Series (Middle Devonian) of North-east Scotland: Journ. of Sedimentary Petrology, Vol. 42, pp. 309-317.
- Folk, R. L. and Pittman, J. S., 1971, Length Slow Chalcedony: A New Testament for Vanished Evaporites: Journ. of Sedimentary Petrology, Vol. 41, pp. 1045-1058.
- Garrett, P., 1970, Phanerozoic Stromatolites: Noncompetitive Ecologic Restriction by Grazing and Burrowing Animals: Science, Vol. 49, pp. 171-173.



- Gebelein, Conrad D., 1969, Distribution, Morphology, and Accretion Rate of Recent Subtidal Algal Stromatolites, Bermuda: Journ. of Sedimentary Petrology, Vol. 39, pp. 49-69.
- Gebelein, Conrad D., and Hoffman, Paul, 1973, Algal Origin of Dolomite Laminations in Stromatolite Limestone: Journ. of Sedimentary Petrology, Vol. 43, pp. 603-613.
- Habicht, J. K. A., 1979, Paleoclimate, Paleomagnetism, and Continental Drift: AAPG Studies in Geology No. 9, AAPG, Tulsa, Oklahoma.
- Ham, W. E., 1956, in Chase, G. W., Frederickson, E. A., and Ham, W. E., 1956, Petroleum Geology of Southern Oklahoma: AAPG, Tulsa, Oklahoma.
- Harlton, B. H., 1963, Frontal Wichita Fault System of Southwestern Oklahoma: AAPG Bul., Vol. 47, pp. 1552-1580.
- Harlton, B. H., 1964, Surface and Subsurface Subdivisions of Cambro-Ordovician Carbonates of Oklahoma: Tulsa Geol. Soc. Digest, Vol. 32, pp. 38-42.
- Hoffman, H. J., 1969, Attributes of Stromatolites: Geol. Surv. of Canada Paper 69-39, pp. 1-58.
- Hoffman, Paul, 1974, Shallow and Deep Water Stromatolites in Lower Proterozoic Platform-to-Basin Facies Change, Great Slave Lake, Canada: AAPG Bul., Vol. 58, pp. 856-867.
- Johnson, K. S., Branson, C. C., Curtis, N. M., Ham, W. E., Harrison, W. E., Marcher, M. V., and Roberts, J. F., 1979, Geology and Earth Resources of Oklahoma: OK Geol. Soc., Norman, Oklahoma.
- Kastner, Miriam, 1971, Authigenic Feldspars in Carbonate Rocks: American Mineralogist, Vol. 56, pp. 1403-1442.
- Kastner, Miriam, and Siever, Raymond, 1979, Low Temperature Feldspars in Sedimentary Rocks: Am. Journ. of Science, Vol. 279, pp. 435-479.
- Leeder, M. R., 1982, Sedimentology: Process and Product: George Allen and Unwin, London.
- Levin, Harold L., 1978, The Earth Through Time: W. B. Saunders Co., Philadelphia.
- Logan, B. W., Rezak, R., and Ginsburg, R. N., 1964, Classification and Environmental Significance of Algal Stromatolites: Journ. of Geol., Vol. 72, pp. 68-83.

- Loucks, R. G. and Anderson, J. H., 1980, Depositional Facies and Porosity Development in Lower Ordovician Ellenburger Dolomite, Puckett Field, Pecos County, Texas: in Halley, R. B. and Loucks, R. G., eds., Carbonate Reservoir Rocks: SEPM Workshop No. 1, Denver, Colorado, pp. 1-31.
- McBride, Earle F., and Folk, Robert L., 1977, The Caballos Novaculite Revisited: Part II: Chert and Shale Members and Synthesis: Journ. of Sedimentary Petrology, Vol. 47, pp. 1261-1286.
- McConnell, David, 1983, The Structure of the Northern Slick Hills in Southwestern Oklahoma: Unpub. M.S. Thesis, Oklahoma State University.
- McCracken, Earl, 1955, Correlation of Insoluble Residue Zones of Upper Arbuckle of Missouri and Southern Kansas: AAPG Bul., Vol. 39, pp. 47-59.
- Matthews, Robley K., 1974, Dynamic Stratigraphy: Prentice Hall, Inc., Englewood Cliffs, New Jersey.
- Monaghan, P. H., and Lytle, M. L., 1956, The Origin of Calcareous Oolites: Journ. of Sedimentary Petrology, Vol. 26, pp. 111-118.
- Monty, Claude, ed., 1981, Phanerozoic Stromatolites: Springer-Verlag, New York.
- Monty, C. L. V., 1976, The Origin and Development of Cryptalgal Facies: in Walter, M. R., ed., Developments in Sedimentology 20: Elsevier Scientific Publ. Co., New York.
- Nelson, H. F., Brown, C. W., and Brineman, J. H., 1962, Skeletal Limestone Classification: Classification of Carbonate Rocks—A Symposium, AAPG Memoir 1, pp. 224-252.
- Park, Robert, 1976, A Note on the Significance of Lamination in Stromatolites: Sedimentology, Vol. 23, pp. 379-393.
- Park, Robert, 1977, The Preservation Potential of Some Recent Stromatolites: Sedimentology, Vol. 24, pp. 485-506.
- Peterson, M. N. A., and von der Borch, C. C., 1965, Chert: Modern Inorganic Deposition in a Carbonate-Precipitating Locality: Science, Vol. 149, pp. 1501-1503.
- Pettijohn, F. J., 1975, Sedimentary Rocks: Harper and Row, Publ., New York.
- Pettijohn, F. J., Potter, Paul E., and Siever, Raymond, 1972, Sand and Sandstone: Springer-Verlag, New York.

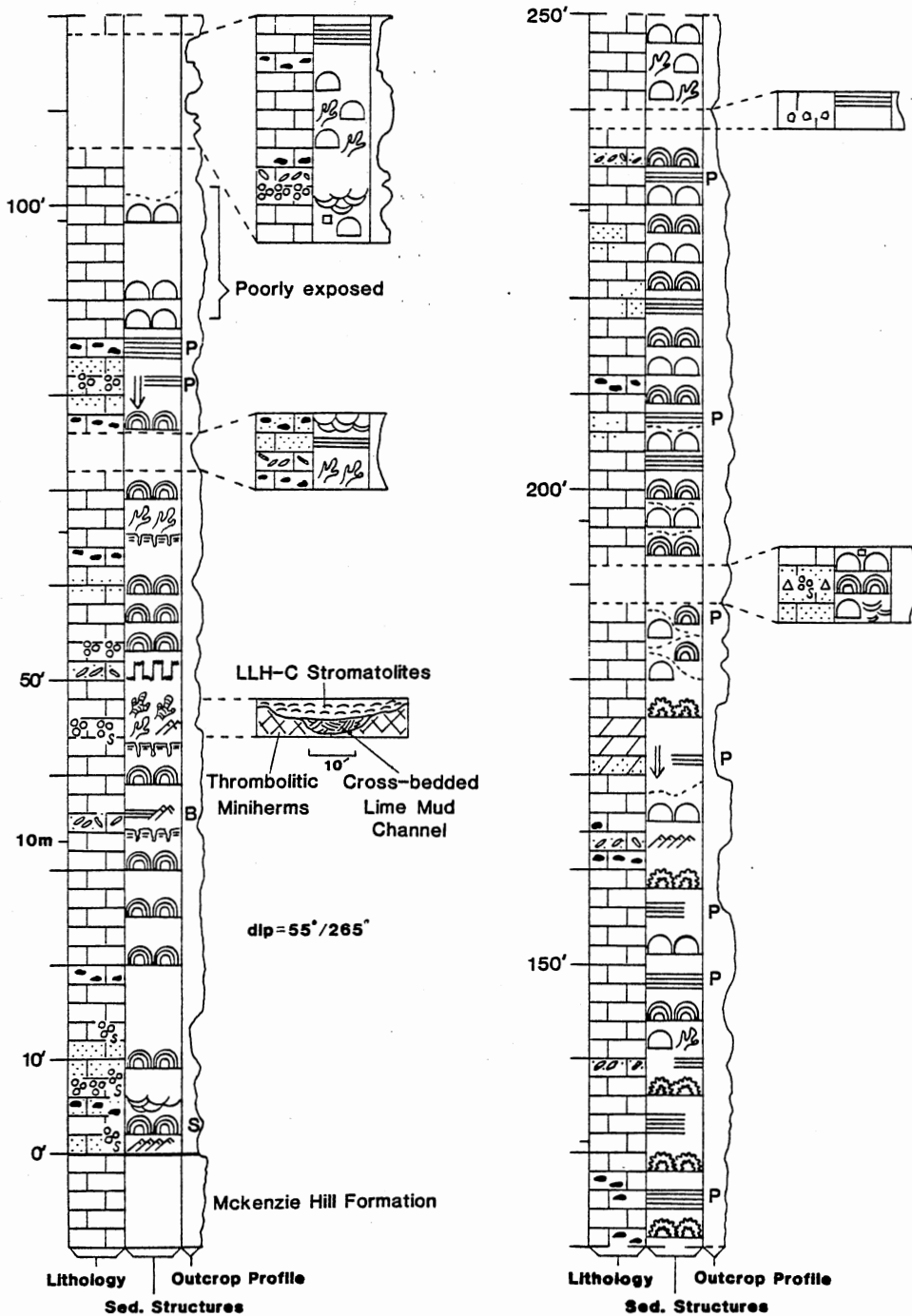
- Pratt, Brian R., 1982, Stromatolite Decline, A Reconsideration: *Geology*, Vol. 10, pp. 512-515.
- Pratt, Brian R., and James, Noel P., 1982, Cryptalgal-Metazoan Bioherms of Early Ordovician Age in the St. George Group, Western Newfoundland: *Sedimentology*, Vol. 29, pp. 543-569.
- Reading, H. G., ed., 1978, Sedimentary Environments and Facies: Elsevier, New York.
- St. John, Jack W., and Eby, David, E., 1978, Peritidal Carbonates and Evidence for Vanished Evaporites in the Lower Ordovician Cool Creek Formation, Arbuckle Mountains, Oklahoma: Transactions, Gulf Coast Assoc. of Geol. Soc. (AAPG), Vol. 28, pp. 589-599.
- Sanderson, David J., and Donovan, R. Nowell, 1974, The Vertical Packing of Shells and Stones on Some Recent Beaches: *Journ. of Sedimentary Petrology*, Vol. 44, pp. 680-688.
- Scholle, Peter A., 1978, A Color Illustrated Guide to Carbonate Rock Constituents, Texture, Cements, and Porosities: AAPG Memoir 27, Tulsa, Oklahoma.
- Scholle, Peter A., 1979, A Color Illustrated Guide to Constituents, Textures, Cements, and Porosities of Sandstones and Associated Rocks: AAPG Memoir 28, Tulsa, Oklahoma.
- Sellards, E. H., Adkins, W. S., and Plummer, F. B., 1932, The Geology of Texas: Volume I, Stratigraphy: The University of Texas Press, Austin, Texas.
- Shinn, Eugene A., 1983, Tidal Flat: in Scholle, Peter A., Bebout, Don G., and Moore, Clyde H., eds., Carbonate Depositional Environments: AAPG Memoir 33, Tulsa, Oklahoma.
- Siedlecka, Anna, 1972, Length Slow Chalcedony and Relicts of Sulphates-Evidence of Evaporitic Environments in the Upper Carboniferous and Permian Beds of Bear Island, Svalbard: *Journ. of Sedimentary Petrology*, Vol. 42, pp. 812-816.
- Toomey, Donald F., and Ham, William E., 1967, Pulchrilamina, A New Mound-Building Organism from Lower Ordovician Rocks of West Texas and Southern Oklahoma: *Journ. of Paleontology*, Vol. 41, pp. 981-987.
- Toomey, Donald F., and Nitecki, Matthew H., 1979, Organic Buildups in the Lower Ordovician (Canadian) of Texas and Oklahoma: Field Museum of Natural History, Chicago, Illinois.
- Tucker, M. E., 1981, Sedimentary Petrology: John Wiley and Sons, New York.

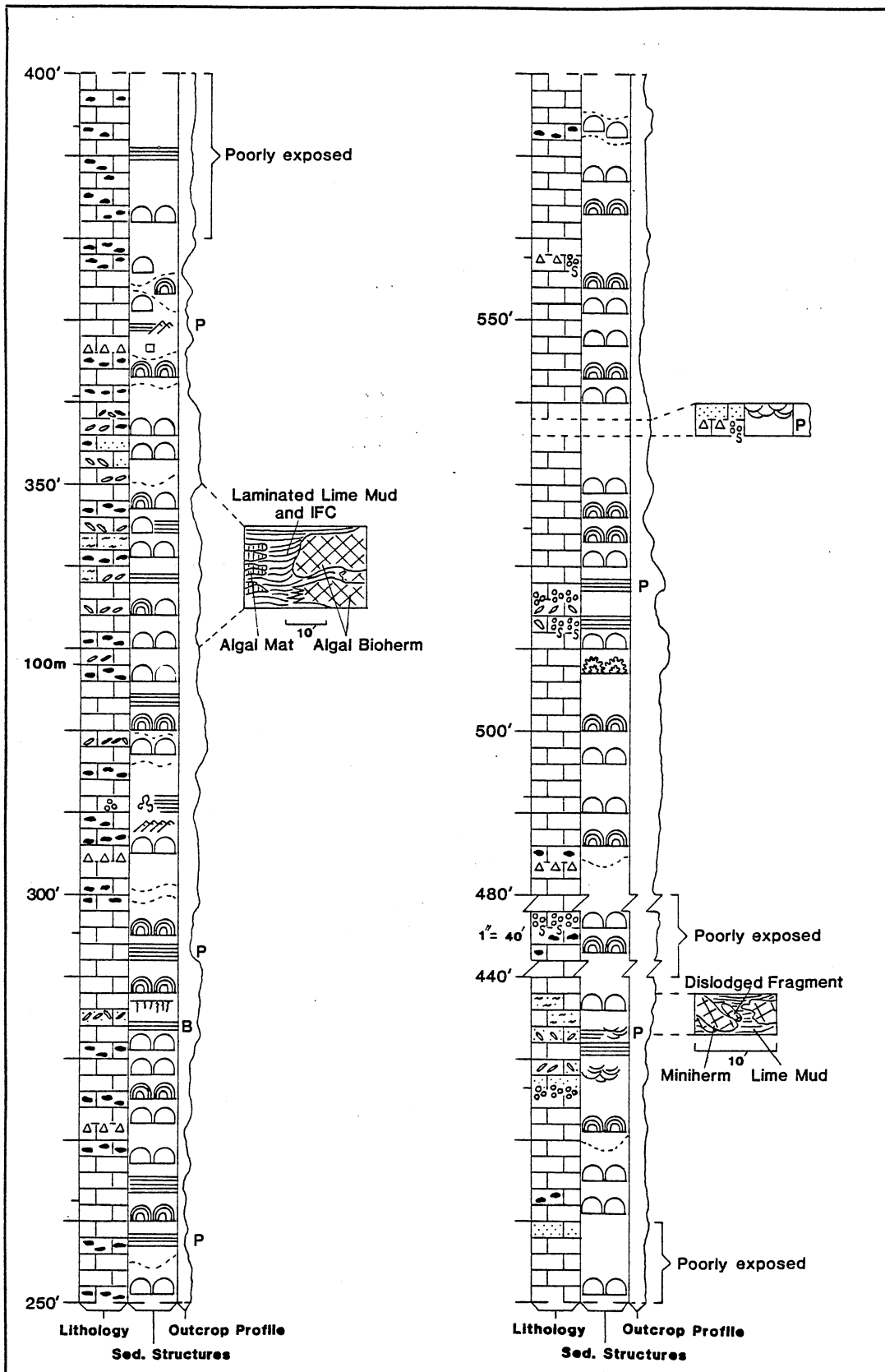
- White, J. F., and Corwin, J. F., 1961, Synthesis and Origin of Chalcedony: *American Mineralogist*, Vol. 46, pp. 112-119.
- Wilkinson, Bruce H., and Landing, Ed, 1978, Eggshell Diagenesis and Primary Radial Fabric in Calcite Ooids: *Journ. of Sedimentary Petrology*, Vol. 48, pp. 1129-1138.
- Wilson, James L., 1975, Carbonate Facies in Geologic History: Springer-Verlag, New York.
- Windley, Brian F., 1979, The Evolving Continents: John Wiley and Sons, New York.
- Wray, John L., 1977, Calcareous Algae: Elsevier Scientific Publ. Co., New York.

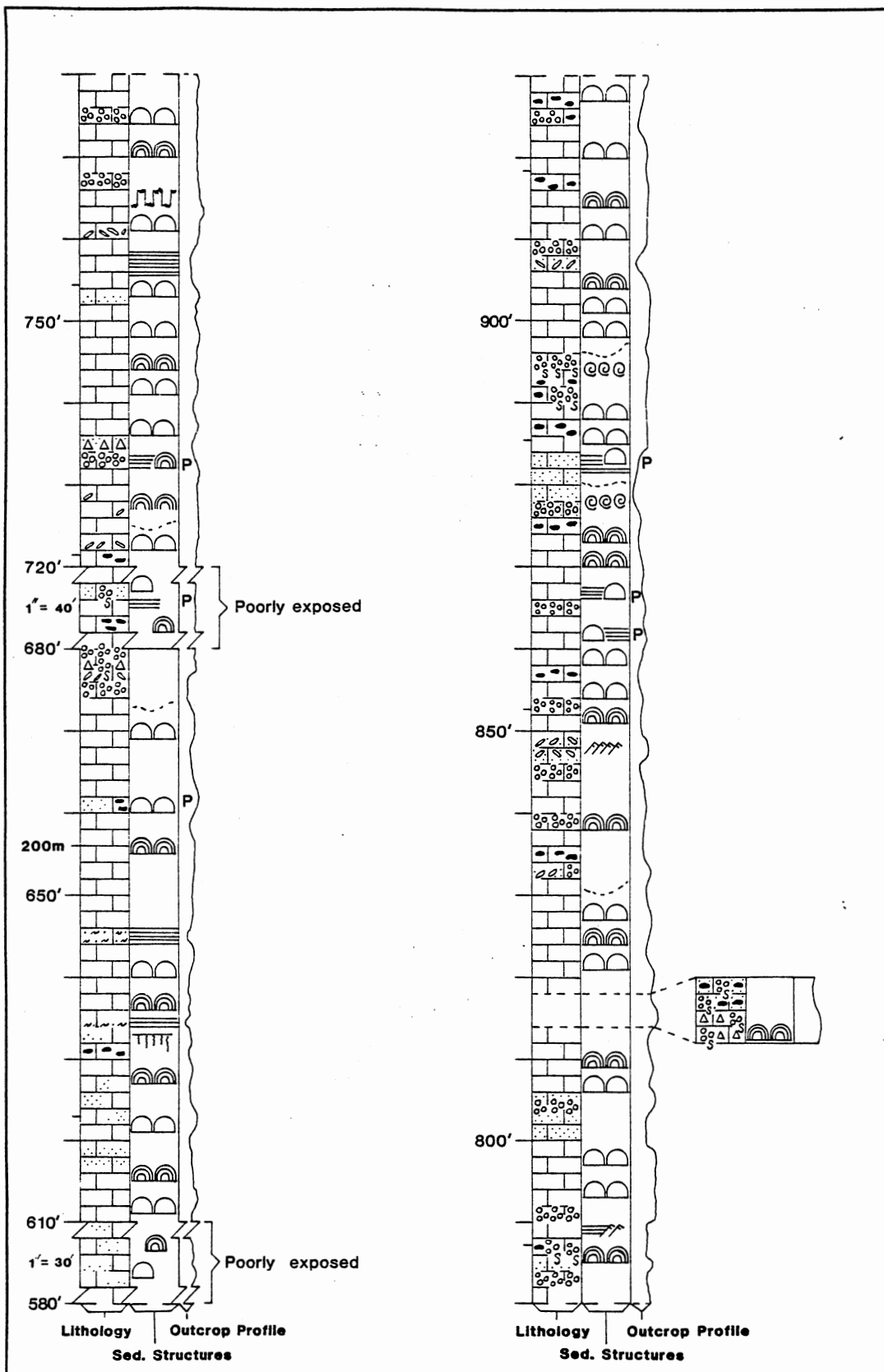
APPENDIX A

LOG OF THE COOL CREEK FORMATION AS  
EXPOSED IN BLUE CREEK CANYON

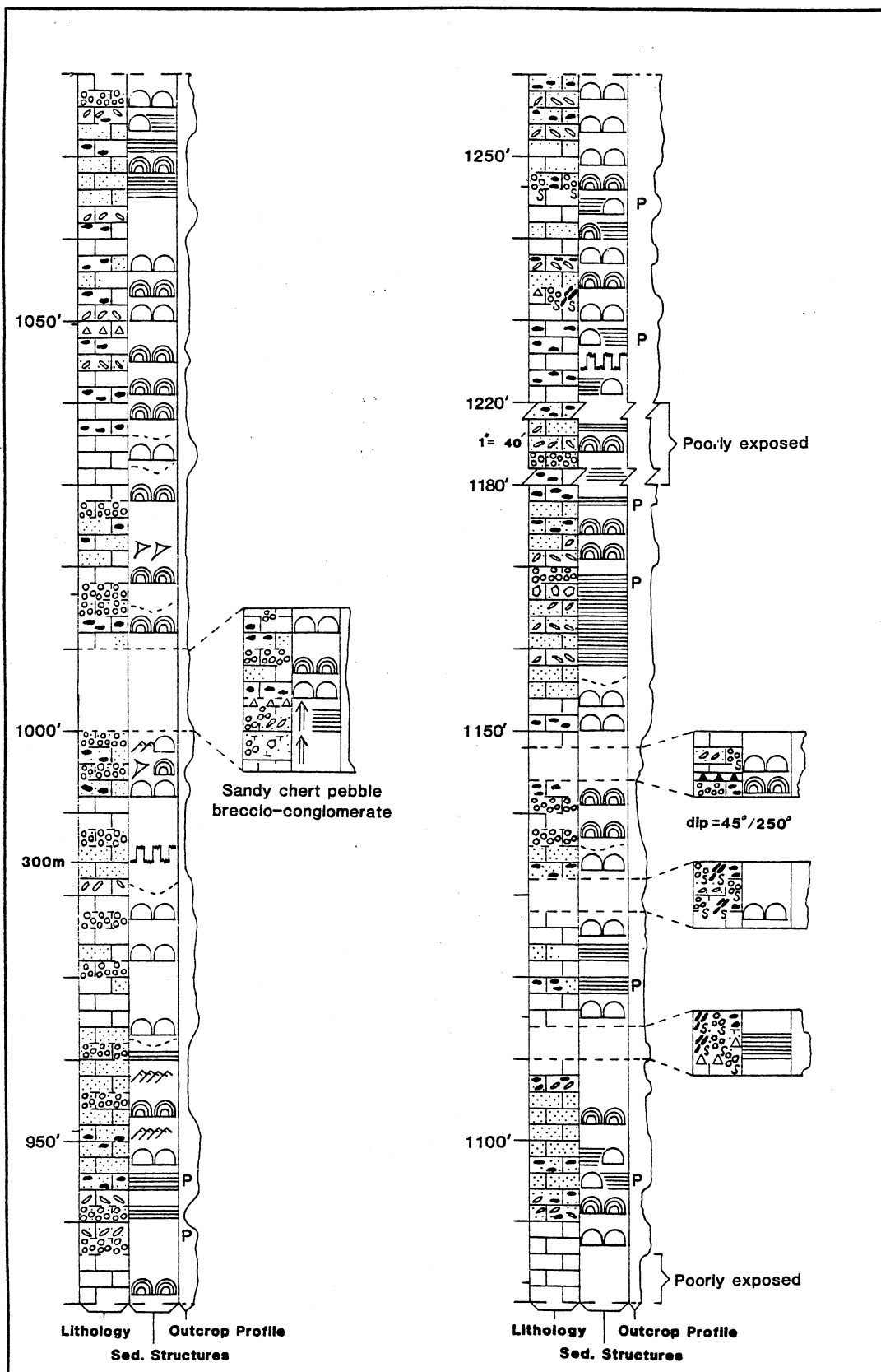
**SEDIMENTARY LOG OF THE COOL CREEK FORMATION MEASURED  
IN BLUE CREEK CANYON, SECTIONS 10 AND 11, TOWNSHIP 4  
NORTH, RANGE 13 WEST, COMANCHE COUNTY, OKLAHOMA**

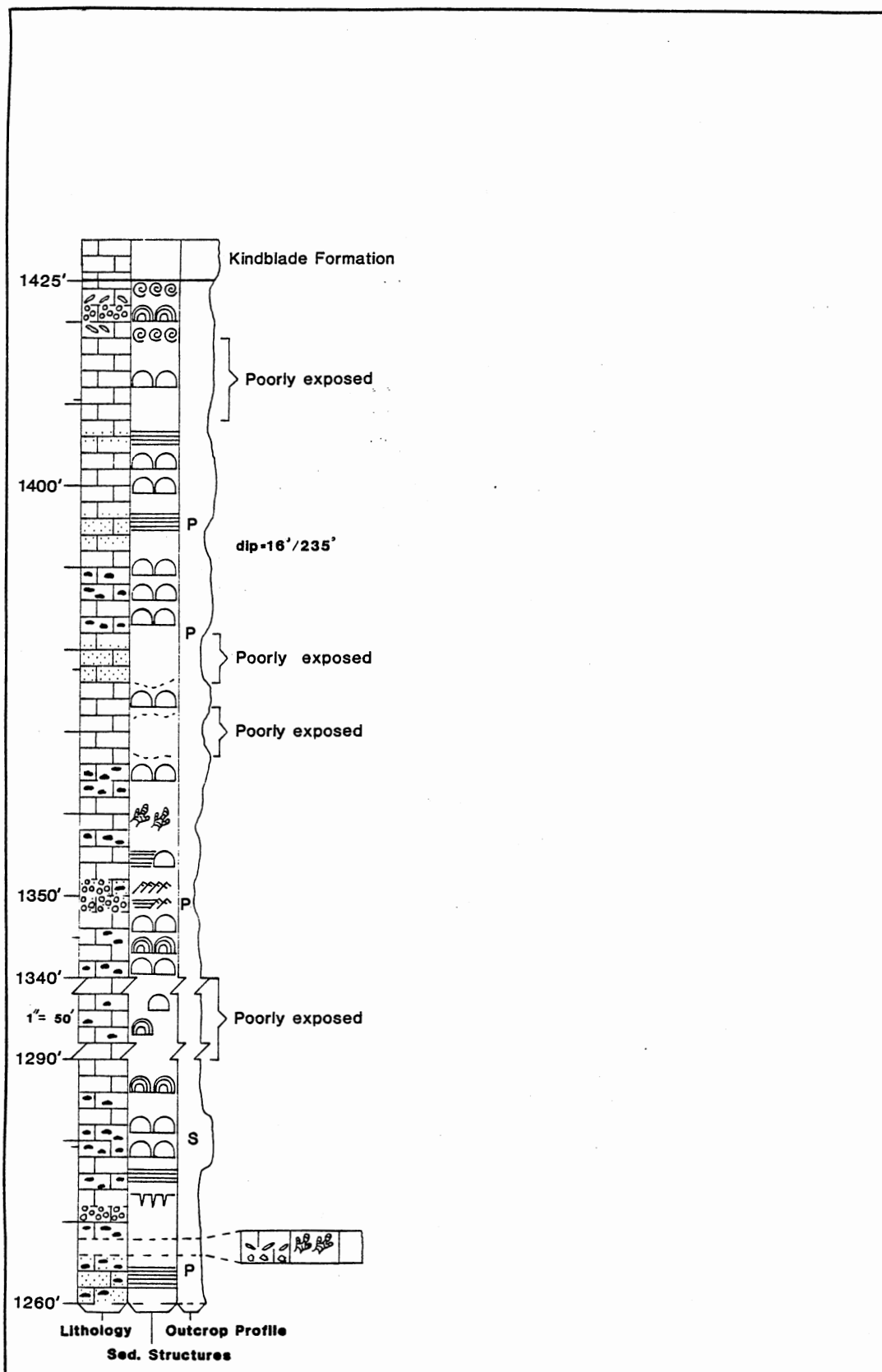




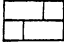
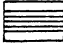
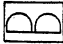

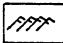
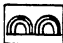


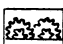

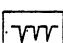
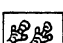
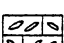
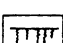
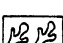
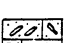
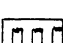
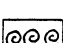
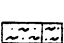
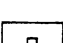
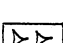
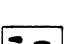
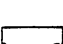
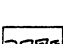
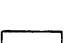
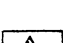
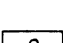
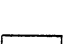
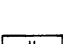
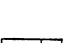
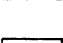
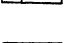
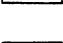
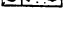
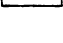
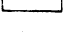
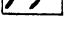
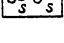








## EXPLANATION OF SYMBOLS

	Limestone		Parallel laminations		Algal mounds
	Dolomite		Small scale trough cross-bedding		Algal mat
	Sandy limestone		Medium scale trough cross-bedding		Crinkly algal mat
	Sandy dolomite		Subaerial mudcracks		Stromatolites
	Intraformational conglomerate		Subaqueous shrinkage cracks		Thrombolites
	Sandy intraformational conglomerate		Stylolites		Fossilized shelled invertebrates
	Silty, sandy limestone		Iron oxide pseudomorphs		Sponge remains
	Chert nodules		Indistinct bedding		Bioturbation
	Chert: pseudolayered		Graded bedding		Horizontal burrows
	Chert: bedded and layered		Reverse graded bedding		
	Limey chert pebble breccia		Pink		
	Sandy, limey chert pebble breccia		Buff		
	Oolitic limestone		Salt pseudomorphs		
	Peloidal limestone				
	Oolitic chert				
	Peloidal chert				

APPENDIX B

SUBSIDENCE RATES IN OKLAHOMA DURING THE PALEOZOIC

## SUBSIDENCE RATES IN OKLAHOMA DURING THE PALEOZOIC

Basin Analysis Class of '82  
Graduate Students: W. Beauchamp, T. Ferraro, C. Lojek,  
D. McConnell, M. Munsil, D. Ragland,  
B. Sweet and D. Taylor

and

R. Nowell Donovan, Associate Professor

### INTRODUCTION

Three distinct geotectonic settings can be recognized in Paleozoic Oklahoma. In the southeast of the state the Ouachitas record a history of ocean development and subsequent orogeny. In the southwest of the state a rapidly subsiding basin, the southern Oklahoma aulacogen, trapped great thicknesses of carbonate during Lower Paleozoic times. Following a major tectonic pulse, sedimentation resumed in late Mississippian times in a number of relatively modest intracratonic basins of which the Anadarko basin is the most significant. Elsewhere in Oklahoma basin development was stilted and epeiric forces controlled sediment preservation in an orthodox cratonic setting.

### THE CALCULATION OF SUBSIDENCE RATE CURVES

In Figure 1 we show sediment thickness as a function of geologic time. Dates were taken from Van Eysinga (1975) and thicknesses were compiled from sources listed below, plus our own unpublished work in

the Wichita Mountain area. From these data we have constructed the three curves shown in Figure 1. We are aware of the various inaccuracies resulting from the compilation of data in this way, but feel that these do not detract from the overall significance and value of the curves and data (Table I) presented. Specifically, there are inaccuracies in the absolute time scale itself, uncertainties in the relationship of local sequences to this time scale and variations in the estimates of thickness used (particularly as we have compiled and averaged data from more than one source).

## THE RESULTS

### Sedimentation and Subsidence Rates

The curves in Figure 1 illustrate spectacular variations in the rate of sediment entrapment (and hence subsidence) of the more mobile areas of crust in Oklahoma. In essence all three curves record relatively rapid rates of sediment entrapment in Cambro-Ordovician times, followed by a quietus in Silurian, Devonian and early Mississippian times. Subsequent sedimentation rates in both the Anadarko basin and the Ouachitas were very rapid, reaching a maximum 3,000 ft per million years in Atokan times in the Ouachitas. It is difficult to avoid the conclusion that the temporal coincidences in the three curves record a genetic relationship (perhaps best explained by the now classic plate tectonic theory for the area).

The Preservation Potential of  
Single Sedimentary Events

The data in Table I were derived from the curves of Figure 1 and serve to remind us of the fragmentary nature of the geological record even in areas and at times of rapid subsidence. It is interesting to relate these rates of sediment entrapment to specific sedimentary environments. Thus, for example, a 100-inch turbidite deposited during Pennsylvanian times in the Ouachitas is the record of the passage of about 4620 years. Such a figure may not be too far from the actual occurrence of turbidites propagated during this time span (although erosion is implicit in the basal contacts of turbidites of this size). We can at least realize that the depositional model envisaged for turbidite sequences is realistic both in recognizing the significance of erosive contacts and in limiting the resorting of clastic grain populations.

The discrepancy between actual events and their preservation in the geological record becomes greater in other depositional settings. For example, a 10-inch stromatolite in the Cool Creek Formation (Arbuckle Group) in the aulacogen is the record of c. 3800 years. On the craton a similar stromatolite records the passage of c. 17,250 years. As modern stromatolites are known to form at far faster rates than this, it is clear that only a fraction of geological time is tangibly recorded. The occurrence of numerous intraformational conglomerates (often composed of several types of intraclast, including both stromatolite fragments and chert pebbles) in this Formation attests to long periods of non-deposition, lithification and erosion.

Thus such conglomerates must be considered an integral part of the inter-supratidal carbonate sedimentation model prepared for this environment (Ragland & Donovan, in preparation). Elsewhere in the Arbuckle Group (Donovan, in preparation) the predicated hiatus are recorded by hard grounds and karst erosion surfaces.

An even more dramatic discrepancy is provided by events during the Devonian quietus where a  $\frac{1}{2}$  inch shelly hard ground records the passage of c. 10,000 to 25,000 years (depending on the area in question). Similarly we may note that a Pennsylvanian deltaic channel, eroded 10 ft into underlying sediment in the Anadarko area, removed the record of 45,500 years of sedimentation. On the craton a like channel would have removed the record of c. 180,000 years. Such figures remind us that in areas of slow subsidence "bypassing" mechanisms are not just "likely" but are predicated for the deltaic model for sedimentation.

We are aware that in our discussion much of the quantification may be suspect (for example, we have ignored the likelihood of tectonically generated unconformities due to epeiric warping). Nevertheless we feel that we are "correct" in a ballpark sense. Our general conclusion is that analyses of depositional system models must have been built into them a conceptualization of the importance of erosion surfaces, resorting and disconformities. This conclusion follows from the recognition that, even in areas of rapid subsidence, there is a profound difference between rates of sediment entrapment and rates of sediment buildup as recorded in modern environments.



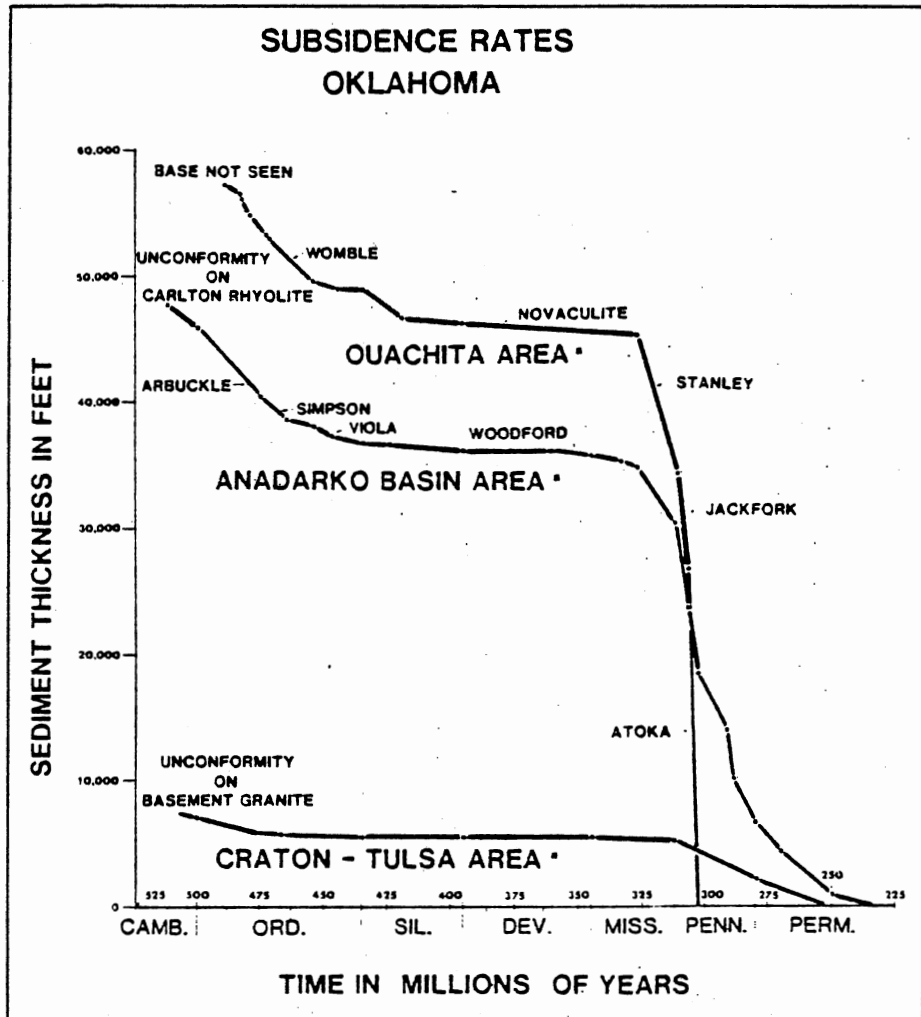


Figure 1. Sediment Thickness as a Function of Geologic Time

TABLE I

## SUBSIDENCE RATES IN OKLAHOMA DURING PALEOZOIC TIMES

Time	Area	Sediment Entrapment (Subsidence) Rate	
		ft/million years	inches/year
475-500 ma	Craton	48	0.00058
475-500 ma	Aulacogen	220	0.00264
475-500 ma	Ouachitas	212	0.00254
350-400 ma	Craton	2	0.00002
350-400 ma	Aulacogen	6	0.00007
350-400 ma	Ouachitas	20	0.00024
300-325 ma	Craton	56	0.00067
300-325 ma	Anadarko Basin	680	0.00816
300-325 ma	Ouachitas	1800	0.02160

## REFERENCES

- Adkison, W. L. and M. G. Sheldon, 1963. Well-Sample Descriptions, Anadarko Basin, Oklahoma Geological Survey Guidebook 13, 139 pp.
- Craig, L. C. and C. W. Conner, 1979. Paleotectonic investigations of the Mississippian System in the United States, Geological Survey Professional Paper 1010, 147-157.
- Ham, W. E., 1973. Regional geology of the Arbuckle Mountains, Oklahoma, Oklahoma Geological Survey.
- Harland, W. B., A. G. Smith, and B. Wilcock (eds.), 1964. The Phanerozoic Time Scale: A Symposium, Geological Society of London, 458 pp.
- McKee, E. D. and E. J. Crosby, 1975. Paleotectonic investigations of the Pennsylvanian System in the United States, Geological Survey Professional Paper 853, 177-192.
- Morris, R. C., 1974. Sedimentary and tectonic history of the Ouachita Mountains, in Tectonics and Sedimentation, W. R. Dickson (ed.), SEPM Special Publication No. 22, 120-142.
- Statler, A. T., 1965. Stratigraphy of the Simpson Group in Oklahoma, Tulsa Geological Society Digest, v. 33, 162-211.
- Van Eysing, F. W. B., 1975. Geological Time Table, Elsevier Scientific Publishing Company, Amsterdam.

APPENDIX C

ANALYSIS OF REPRESENTATIVE THIN SECTIONS  
FROM THE COOL CREEK FORMATION

Sample	Composition (%)														Comments				
	Sparite	Micrite	Fossil Frags.	Ooids	Peloids	Intraclasts	Detrital Qtz	Auth. Qtz	Chert	Chalcedony	Feldspars	Dolomite	Rock Frags.	Pyrite		Hematite	Organics	Porosity	
Occ 2	2	42	10		1		3				2	38			1				
Occ 4	16			66			8	10											
Occ 9	10	87															3	Laminated micrite of algal origin	
Occ 10	5	86					1				3						5		
Occ 13		86			10												1	3	Algal mat
Occ 16	5	83			3		1	3							5				Stromatolite; megaquartz infills tubules
Occ 17								5	80	10		5							Evaporite Pseudomorphs; quartzine
Occ 19	15	55	T		25		1	T							2	1	1		
Occ 20	2	27			15		3										3		Trace muscovite
Occ 21		93					1								5		1		
Occ 22	48	3		40		5	2	1										1	Multiple quartz overgrowths
Occ 23	25		2	56	3	15	1	1											Some reworked and composite ooids
Occ 25								5	95										
Occ 27		40					20	10			30								
Occ 30	5			50		5		40											Silicified ooids
Occ 33	15			44		20		18	2					1					20% of ooids silicified
Occ 37	10				30	59								1					Pelmicrite clasts

Sample	Composition (%)														Comments			
	Sparite	Micrite	Fossil Frags.	Ooids	Peloids	Intraclasts	Detrital Qtz	Auth. Qtz	Chert	Chalcedony	Feldspars	Dolomite	Rock Frags.	Pyrite		Hematite	Organics	Porosity
0cc 38	20		50					30										Isopachous calcite rims; late quartz cement
0cc 41	25		2		65	6	T	T			2							
0cc 42	5		80			10					5							
0cc 43	10	43				40					5		1	1				
0cc 45	8	45	15	25	2	3										1	1	
0cc 46	17		10		40	27	3			1		1		1				
0cc 54		85									15							Disrupted agal mound
0cc 57		40						60										Layered chert/micrite
0cc 58	30	23	2		40						1			2			2	
0cc 59		15	5		5	40	15				5	10	1	1	3			Authigenic feldspars
0cc 61	33				31	1		30	2		T			2			1	
0cc 63								100										Evaporite pseudomorphs
0cc 66	3	77				8				8				3			1	Authigenic Feldspars
0cc 72	10	64	2	10		10	2							2				
0cc 74	10	78			10		1							1				Laminated micrite of algal origin
0cc 75	5	83	10														2	Micrite appears to be peloidal
0cc 87								95	5									Silicified ooids and peloids; spherulites
0cc 91		85						5			9			1				Salt pseudomorphs; algal mound

Sample	Composition (%)													Comments					
	Sparite	Micrite	Fossil Frags.	Ooids	Peloids	Intraclasts	Detrital Qtz	Auth. Qtz	Chert	Chalcedony	Feldspars	Dolomite	Rock Frags.		Pyrite	Hematite	Organics	Porosity	
Occ 96	13	44	26		2	10	1			T	1	T		3					
Occ 98	23						10		7	1	55			2			2	Dolosparite	
QM	9		1	5	35	40	5		T	2	1	2							
HC 2	8	90					2											Thrombolite	
W 5		45					23		30									2	Silica pseudomorphing anhydrite nodule
W 6	5											85						10	Comprehensive dolomitization

T = Trace

VITA

Deborah Ann Ragland

Candidate for the Degree of

Master of Science

Thesis: SEDIMENTARY GEOLOGY OF THE ORDOVICIAN COOL CREEK FORMATION  
AS IT IS EXPOSED IN THE WICHITA MOUNTAINS OF SOUTHWESTERN  
OKLAHOMA

Major Field: Geology

Biographical:

Personal Data: Born in Philipsburg, Pennsylvania, March 7, 1949,  
the daughter of Mr. and Mrs. John M. Savickas; married on  
March 1, 1969, to Tommy V. Ragland; one child, Tracie Ann,  
age 13.

Education: Graduated from Dallas Senior High School, Dallas,  
Pennsylvania, June, 1967; attended University of Texas at  
Austin, Purdue University, William Rainey Harper College,  
Northern Illinois University, and Oklahoma State University;  
obtained Bachelor of Science Degree in Geology at Oklahoma  
State University in July, 1981; completed requirements for  
Master of Science degree at Oklahoma State University in  
December, 1983.

Professional Experience: Assistance in meteorite analysis,  
Harper College; teaching assistant at Oklahoma State  
University, 1981-83; teaching assistant at Oklahoma State  
University Geology Field Camp 1982 and 1983; student tech-  
nician, Oklahoma State University, 1983; Member Phi Kappa  
Phi; Member American Association of Petroleum Geologists.